Graduate Theses and Dissertations

Iowa State University Capstones, Theses and Dissertations

2009

Automated separation of bone joint structures for medical image reconstruction

Wutthigrai Boonsuk
Iowa State University

Automated separation of bone joint structures for medical image reconstruction

by

Wutthigrai Boonsuk

A dissertation submitted to the graduate faculty

in partial fulfillment of the requirements for the degree of

DOCTOR OF PHILOSOPHY

Major: Industrial Engineering

Program of Study Committee:
Matthew C. Frank, Major Professor
Douglas D. Gemmill
James H. Oliver
Frank E. Peters
Eliot H. Winer

Iowa State University

Ames, Iowa

2009

TABLE OF CONTENTS

LIST OF FIGURES

LIST OF TABLES

ABSTRACT

Automated separation of reconstructed bone joints from 3D medical images is a challenging task due to surrounding soft tissue and adjacent bones that can affect the clarity of bone boundaries. Existing approaches typically require human intervention to correct improper results of segmentation before the joint model is reconstructed. This dissertation presents a new methodology for separating bone joint models using a completely automated approach. Rather than trying to offer a solution for segmenting medical images, the proposed method first allows errors in the reconstructed model and later removes these errors without the help of a medical expert or technician. This method utilizes known anatomical information from a generic CAD model, which is a properly generated model of the anatomy of a similar human subject, with regard to age, gender, height, etc. The intent is to aid in the separation of bones in the joint areas by comparing the reconstructed model that might contain errors to the generic model which has individual bones separated properly. The human hip joint is employed as an example of algorithm implementation in this dissertation. The proposed method is a general approach that should be adequately flexible to extend to other type of joints such as knee and elbow.

CHAPTER 1. INTRODUCTION

With the development of advanced medical imaging technology, three-dimensional

(3D) models can be generated using cross sectional medical images from methods such as

computed tomography (CT) or magnetic resonance imaging (MRI). CT scanning is a widely

used medical imaging technique most suitable for capturing dense tissues (bone structures).

On the other hand, MRI is best suited for soft tissues such as brain or other objects like

ligaments. The images from both techniques use the difference of grey scale, similar to x-ray

images, in order to distinguish the object from the background. However, the images from

CT and MRI are the cross sectional slices of the body along one axis while an x-ray image is

the projection of the object onto one plane. Figure 1.1 illustrates x-ray, CT, and MRI images.

    (a) X-ray (pelvis)   (b) CT (Hip "socket")   (c) MRI (Brain)
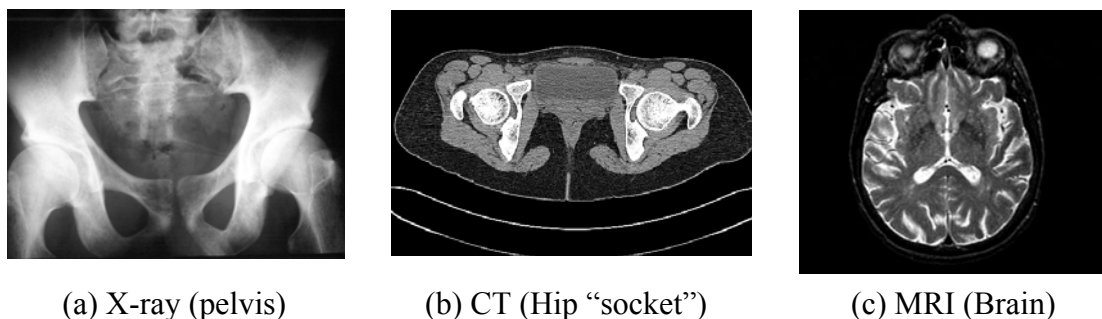
Figure 1.1. Medical images

The series of cross sectional images can be stacked in order to recreate a 3D object

(Figure 1.2). The images are used by surgeons and radiologists in clinical procedures

ranging from diagnosis to surgery planning. Other users outside the medical field include,

for example; manufacturers who design and develop prostheses or computer graphics users

who create simulations and animations. Due to the complexity of internal objects, people

outside the medical field may find it difficult to reconstruct 3D models from the images

because they lack sufficient knowledge of human anatomy. The goal of this dissertation is to investigate a new methodology to automatically create these models using robust computer algorithms rather than skill and tedious work.

(a)   (b)
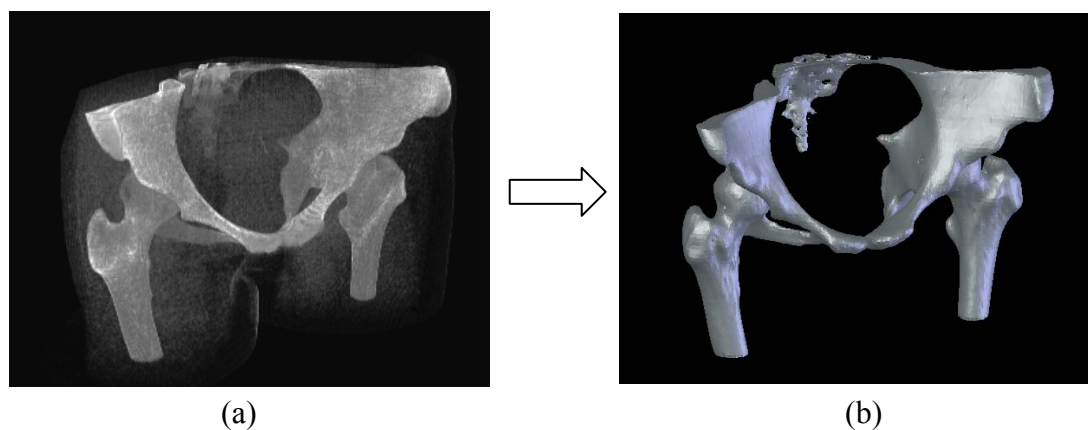
Figure 1.2 - CT images and model: (a) stack of images and (b) 3D model

An important step before reconstructing 3D models from slice images is *image segmentation*. Image segmentation is a process that distinguishes the object of interest from the image background. There are two levels of segmentation: *low-level* segmentation and *high-level* segmentation (Bohm et al., 1999). Low-level segmentation refers to a process that detects and retrieves important features from the image and translating into explicit data. For instance, the simplest low-level segmentation technique uses *thresholding* to extract objects from the image. In a thresholding operation, pixel values below the threshold values will be set to background pixels while those above the threshold values will be set to object pixels. Figure 1.3 illustrates the process to extract a 2D contour from a CT image using the thresholding method.
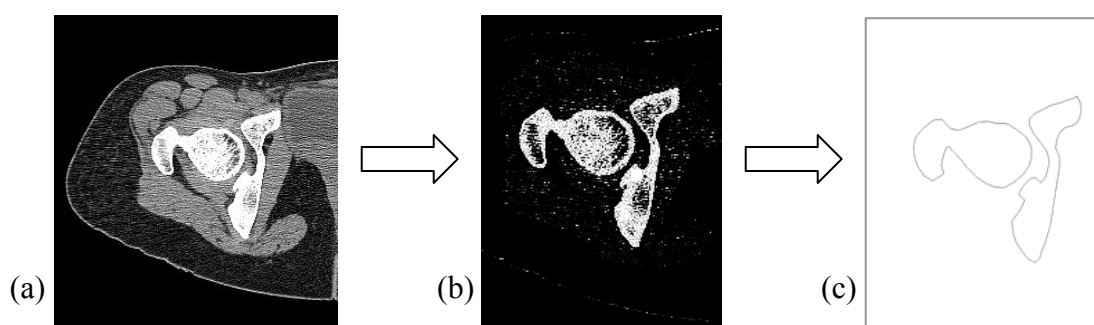
Figure 1.3. Extracting 2D contour by *thresholding*: (a) CT image, (b) thresholding result, and (c) contour extraction

High-level segmentation refers to a process that interprets the result of low-level segmentation as well as extracts and registers individual objects separately when there is more than one object in the CT images. High-level segmentation requires prior medical knowledge about the object in order to identify and separate the objects from one another. If the result from low-level segmentation is directly used for reconstructing the bone joint, bones that are too close (touching in some cases) can be mistakenly combined if the low-level segmentation fails to create a clear boundary. On the other hand, even when bone boundaries are completely separated by low-level segmentation, the relations of contours or cross-sections between image slices are not identified; one cannot tell which bone is which (e.g., the pelvis and the femur that comprise a hip joint). The problems are described as the correspondence and branching problems (Park et al., 1995, Bajaj et al.,1996, and Ryu et al., 2004). Since the reconstruction process is not intelligent enough to recognize the individual bones, each bone should be separately created. Otherwise, the resulting 3D model will have all bones combined. In this dissertation, the combined areas are called *welded regions* since they appear similar to welded joints in manufacturing processes. Figure 1.4a illustrates an example result of using only low-level segmentation to reconstruct a hip joint from CT images. The individual bones are not recognized and created separately in a reliable fashion.

The result shows the femur and pelvis are combined after low-level segmentation. Thus, high-level segmentation is used to disconnect these two bones as shown in Figure 1.4b.
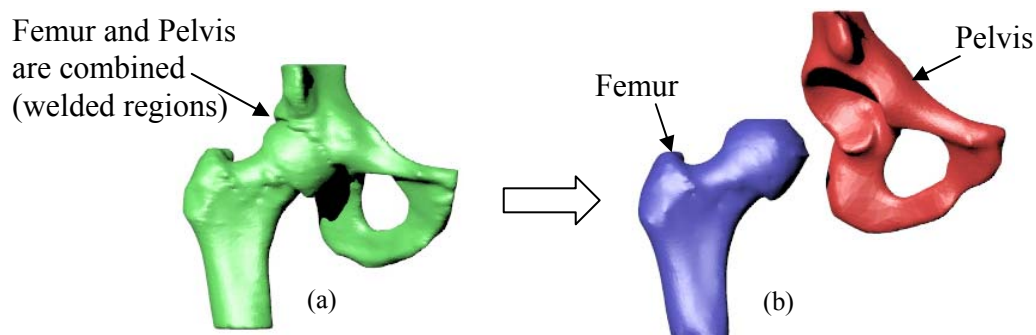
Figure 1.4. Low-level segmentation and high-level segmentation: (a) hip joint after low-level segmentation and (b) hip joint after high-level segmentation

High-level segmentation is not a simple task and is usually performed or directed by medical experts who are trained or familiar with the anatomy. The steps of high-level segmentation are illustrated in Figure 1.5. The CT image of a hip joint where the femur and pelvis are physically adjacent is shown in Figure 1.5a. As can be seen, the contours of the femur and pelvis are not separated after the low-level segmentation process (Figure 1.5b). High-level segmentation is manually performed to properly correct the results of low-level segmentation (Figure 1.5c). Finally, each contour is assigned to an individual bone as shown in Figure 1.5d. The manual approach is a time consuming and tedious task because this modification must be repeated for tens or hundreds of slice images. This dissertation assumes medical experts are not available when high-level segmentation is considered necessary. An automated system for high-level segmentation is a challenging and unsolved problem. This dissertation specifically focuses on developing an automated system to perform high-level segmentation of complex bone structures. In the current work, a human hip joint is adopted as an example of the complex structures.
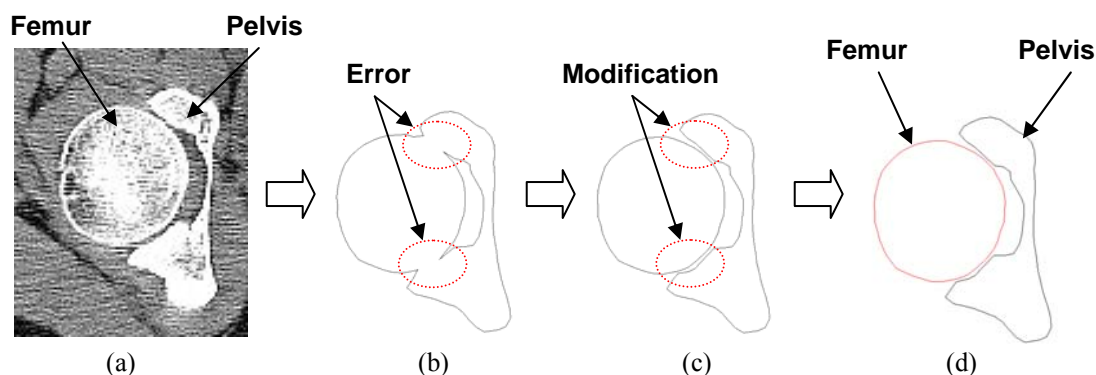
Figure 1.5. Steps of high-level segmentation: (a) CT image of hip joint, (b) contour after low-level segmentation, (c) high-level segmentation by manual modification, (d) contours after high-level segmentation

In order to substitute the required knowledge of the human anatomy in high-level segmentation, the proposed method employs a *generic* model as the prior known information. The generic model is a complete model of the bone structure without errors (bones are all separated) and with the same orientation as the CT scan images. In the proposed process, the desired model of the *object bone* joint is first reconstructed from the patient's images using only low-level segmentation. This model will be called the *object* model. In this stage of the process, the areas where the bones of the object model are inadvertently connected (welded) are not of concern; we assume welding will occur to some degree. Next, corresponding regions of the generic model are registered to those of the object model so that the generic model can be used as a reference model. Then, the object model is analyzed by comparing it to the generic model; with a goal of identifying and repairing the welded regions on the object model. Finally, the individual bones in the object model can be reconstructed as separate components of the joint.

The remainder of this dissertation is organized as follows: In Chapter 2, relevant literature from previous research is discussed. Chapter 3 presents an overview of the

proposed solution approaches. Chapter 4 presents methods for registering the generic model to the object model such that further analysis can be conducted. In Chapter 5, methods for detecting and modifying the errors of the object model using reference information from the generic model are presented. Lastly, conclusions and future research are discussed in Chapter 6.

CHAPTER 2. LITERATURE REVIEW

Traditional low-level segmentation techniques such as thresholding, edge detection, and regions growing represent the early methods in medical imaging (Pal and Pal, 1993). Thresholding is the simplest technique that classifies the image pixels into two categories, object and background, based on their threshold values (Sahoo et al., 1988). However, due to a similarity of surrounding tissue density such as cartilage and bones, adjacent bones may be combined as the result of segmentation. Edge detection refers to a technique that locates points of abrupt changes in grey level intensity of images (Davis, 1975; Marr and Hildreth, 1980). This technique often requires space closing methods to connect separated edges belonging to the same boundary. It may be straightforward to automatically connect the edges with similar levels of intensity, but it is very difficult to provide information where the edges belong to different bone boundaries. Region growing is a procedure that groups pixels into regions based on predefined criteria for growth (Zucker, 1976). The technique begins with an initial seed (a small region) and then inspects the statistical properties of neighbor regions to merge if they have similar attributes. Similar to edge detection techniques, preventing the regions from merging between different bones is complicated. In general, traditional low-level techniques can be implemented automatically (Ramesh et al., 1995; Yen et al., 1995; Bennamoun et al., 1995), or with considerably less human intervention (Adams and Bischof, 1994). Unfortunately, these techniques are not sufficient to properly separate and identify individual bones in joint areas.

Several researchers proposed additional techniques to improve traditional low-level segmentation in order to separate the adjacent bone structures. Westin introduced an

adaptive filter for enhancing structures of interest in CT images (Westin et al., 1998). The method sharpens areas around the adjacent bones. The result showed that the filter is effective to separate bones in the hip joint (pelvis and femur). However, the method works well only when the gap between adjacent bones is visible. For bones that are very close or even touch each other, the method may not improve the result of segmentation. Kang introduced a 3D segmentation method for segmenting bone structures from CT images (Kang et al., 2003). The method combines region growing techniques with some additional methods for closing the discontinuous boundaries and adjusting oriented boundaries. The results showed that the method works for segmentation of individual bones in hip joint and knee joints. The drawback is that the adjacent bone structures must be isolated before segmentation process. Yao presented estimated and corrected normal direction methods for detecting bone edges in CT images (Yao et al., 2005). The algorithm involved edge tracing and estimated normal directions of bone edges. The results showed an improvement in segmentation by decreasing the gap of contours and unrelated edges; however, the method is sensitive to noise and quality of bone edges in CT images. Overall, the methods that attempt to improve traditional low-level segmentation may suffer from poor quality of bone boundaries especially where individual bones are adjacent. The final result is still relies heavily on the result of traditional methods.

Deformable contour and *Deformable Model* are the very popular segmentation methods of the past decade. Prior knowledge or shape constraint of the object of interest is incorporated to overcome the weakness of traditional segmentation. The basic idea of deformable methods is using a shape to represent the object of interest; then this shape is iteratively deformed with some restrictions until it fits the object in the images. *Snake* (active

contour model) was the first well-known deformable contour (Kass et al., 1988). The snake is an elastic contour that is located over an image and then its shape is deformed toward the desired contour using a combination of internal and external energies. The snake method requires the initial contour to be close to the object of interest and has a limitation in changing topology. Cootes proposed a similar approach called *Active shape model* (Cootes et al., 1994). Instead of using energy constraints, the method used the statistical variation of the shape model as prior knowledge of deformation. The method begins with a generic shape and deforms it based on methods found in the training set. However, the accuracy of result depends on the alignment of the initial shape. Josephson expanded Cootes's work to segment images using 3D active shape model (Josephson et al., 2005). The active shape model is built from several sets of data using the *Iterated closest point* (ICP) algorithm, and then utilized it as prior knowledge in order to segment other CT images. The approach requires the proper initial location of the active shape model to obtain a good result of segmentation. Deformable contour or deformable model methods provide an improvement over the traditional low-level segmentation in restricting the shape to the object of interest. However, the initial shape must be located close to the object in the images to yield a good result; a step requiring skilled user with knowledge of the anatomy.

Some researchers proposed methods that could enhance deformable contour or deformable model methods. Caselles proposed the method called *Geodesic active contour* to handle a problem in the topological changing of the snake approach (Caselles et al., 1997). The method allows the contour to change topology without detecting the deformation. Lorigo combined geodesic active contour with texture information to segment a knee joint from MRI images (Lorigo et al., 1998). The method can separately detect the tibia and

femur; however, the initial contour must be placed inside the structure. Other researchers focused on improving the initial input of deformable contour or deformable model methods. Pardo presented an automated snake-based approach for CT image segmentation (Pardo et al., 2001). This work employs edge and region information from the segmentation results of a previous image slice. Although this method seems to be able to separate the adjacent bones, a solution is not presented for images that have changes in the number of contours from a previous image slice. Heo proposed segmentation of the tooth from CT images using the contour and threshold value passed from a previous image slice (Heo et al., 2004). The segmentation of a tooth is analogous to bone segmentation because some teeth may also touch neighboring teeth. The method uses B-spline snakes to segment images. The method improves the segmentation of individual teeth; however, the method only works well when the object does not change between image slices. Over all, the methods that improve the deformable contour or deformable model still require proper positioning of the initial shape; although they gain more flexibility. The methods allow topological changing but they cannot recognize the individual bone structures. This problem is classified as the correspondence problem in 3D reconstruction (Park and Kim, 1995; Bajaj et al., 1996; Ryu et al., 2004).

More recently, methods for simultaneous segmentation of multiple objects were proposed. Kainmueller proposed the method to repair the overlapping surfaces of two bone models using *Shared Intensity Profiles* (Kainmueller et al., 2008). The shared profiles are used as middle borders that adjacent bone surfaces cannot come across. This method can prevent intersection of adjacent objects; however, the individual bones should be segmented before the method can be applied. Klinder proposed a method to simultaneously segment spine bones using shape models (Klinder et al., 2008). This proposed method deforms the

shape models to multiple bones in the image while the overlapping of shape models is prevented. However, the result is sensitive to the initial position of the shape models. Manual correction is still required during the segmentation process. Simultaneous segmentation of multiple objects could be an effective approach for bone joint segmentation and separation if the proper initiation of shape models is obtained.

Other researchers proposed methods that may be used for specific types of joints or specific applications. Zoroofi et al (2003) proposed the method for automated segmentation of hip joint from CT images. The first step is to roughly estimate the joint space between the pelvis and femur; then, a technique named moving disk technique (Zoroofi et al., 2000) is used to refine the preliminary contour of the joint space. Moving disk technique refers to a method that searches for the boundary of the bone by moving a circle close to the boundary and adjusting the circle to the boundary point. Although the method was shown to be effective for segmentation and separation of hip joints, it required the center of the femoral head to be placed in its initial position; yet it was not addressed if this position was automatically obtained or manually chosen. Liu presented rigid model-based 3D segmentation for bone joints (Liu et al., 2005). The purpose of this work is to create a model for joint analysis. The method focuses on using the model, created from the first set of CT images, to subsequently segment the same bone which has different position and orientation in all other sets of images. The regional relative intensity pattern is used in matching process. The result showed high success rates; however, the method was only applied to sets of CT images from the same person. The variation of the bone among each person may cause different results. Shen presented a method to segment complex bone structures using *high-level prior knowledge* (Shen et al., 2005). This knowledge consists of *mean shape* and *high-*

level features of bone structures. The mean shape is created from several shapes obtained by manual segmentation. The high-level features such as abrupt edges or ridges are recorded and used to prevent leakage in segmentation. The drawback of this method is that the mean shape and high-level features must be developed for each type of joints. Moreover, it can be complicated to obtain the proper alignment of mean shape and features to the image slices.

Many methods have been proposed to improve segmentation and separation of bone joints in CT images. Some approaches that attempted to improve low-level segmentation are still not sufficient to guarantee the proper result since there are many variations in CT images. The approaches that employed the shape models still require proper initiation of the models. Often, manual intervention is required in the post processing of the results. This dissertation proposes a new method for the separation of bone joints by focusing on the idea of high-level segmentation. The method employs a generic shape model as anatomical knowledge and utilizes this model to compare and fix the result model from low-level segmentation. A key difference in this new method is that we allow or assume that low level segmentation will probably have errors. Instead of fixing the errors a-priori, we move forward with at least an initial 3D model where it is easier to detect problems. Then, we can fix the 3D model directly, fix the 2D slices directly, or provide feedback to the low level segmentation and then iterate until the problem areas are avoided altogether, automatically. The following chapter begins a discussion of the current approach by presenting a general problem framework and solution approach.

CHAPTER 3. PROBLEM FRAMEWORK AND SOLUTION APPROACHES

This chapter provides an overview of the research for this dissertation. It begins by presenting details on the problem with reconstructing 3D models from medical images. Next, description of problem framework and solution approaches is presented. It will be shown that the contribution of the proposed method can be divided into two important processes: 1) model registration and 2) welded removal. These two processes will then be discussed in detail in proceeding chapters.

3.1. Introduction

Reconstructed 3D models of bones are not only used in clinical applications, but also widely used in other non-medical applications such as computer graphics, simulation, and animation. Usually, medical expertise is required in order to properly separate individual bones before 3D model is reconstructed. It is often difficult and/or costly to have a medically trained person available, or when one is, they may not be skilled in 3D systems/geometry to effectively execute the task. Moreover, the task to separate bone structures is very laborious and prone to errors. Thus, the goal of this research is focused on reconstructing bone joints when it is assumed that a skilled person is not available. The focus of this research is to provide an automated system for high-level segmentation, assuming that low-level segmentation has already been done to the CT images. The method inputs a model that may or may not contain welded regions from low-level segmentation and outputs a modified model where the bones have had welded regions removed and all bones are distinct. In the next section, problem framework of this research will be presented.

3.2. Problem Framework

Since this research proposes an automated system for high-level segmentation of bone joints, two major problems must be answered before building the system. The first problem is how to substitute medical expertise with computer algorithms. The second problem is how to implement the system in a completely automated fashion. To answer the first problem, the method replaces anatomical knowledge using a *generic* model of what the bone joint should look like. This model is a complete, error free, and disassembled bone joint represented as a 3D CAD model. The basic idea is to use the generic model as a "*known*" good pattern and compare it with the reconstructed bone joint from CT images (patient's model) which will be referred to as the *object* model. Then, this object model is disassembled based on the information from the generic model such as number of bones, location, etc. In order to provide better representation of the object model, there may be a need for several versions of the generic model; a library based on age, gender, ethnicity, etc. Since this issue is outside the scope of the current research, it is assumed that a proper generic model is obtained at the beginning stage. The second problem is answered by using an automated process to repair the welded regions of object model that are created from the results of low-level segmentation. Instead of manually segmenting the bone boundaries from CT images, the proposed method accepts an object model directly from low-level segmentation whether these methods were completely effective or not. If the low-level segmentation is better, then the welded regions should be smaller; regardless, the method will detect the welded regions, and remove them.

The framework of the proposed solution methodology is illustrated in Figure 3.1. Two automated processes are proposed to build the system in high-level segmentation: 1) a

process that registers the generic model to the object model, and 2) a process that repairs the welded regions by using reference data from the generic model. These two processed will be the main focus of this research and they will be described in more details in the following two chapters.
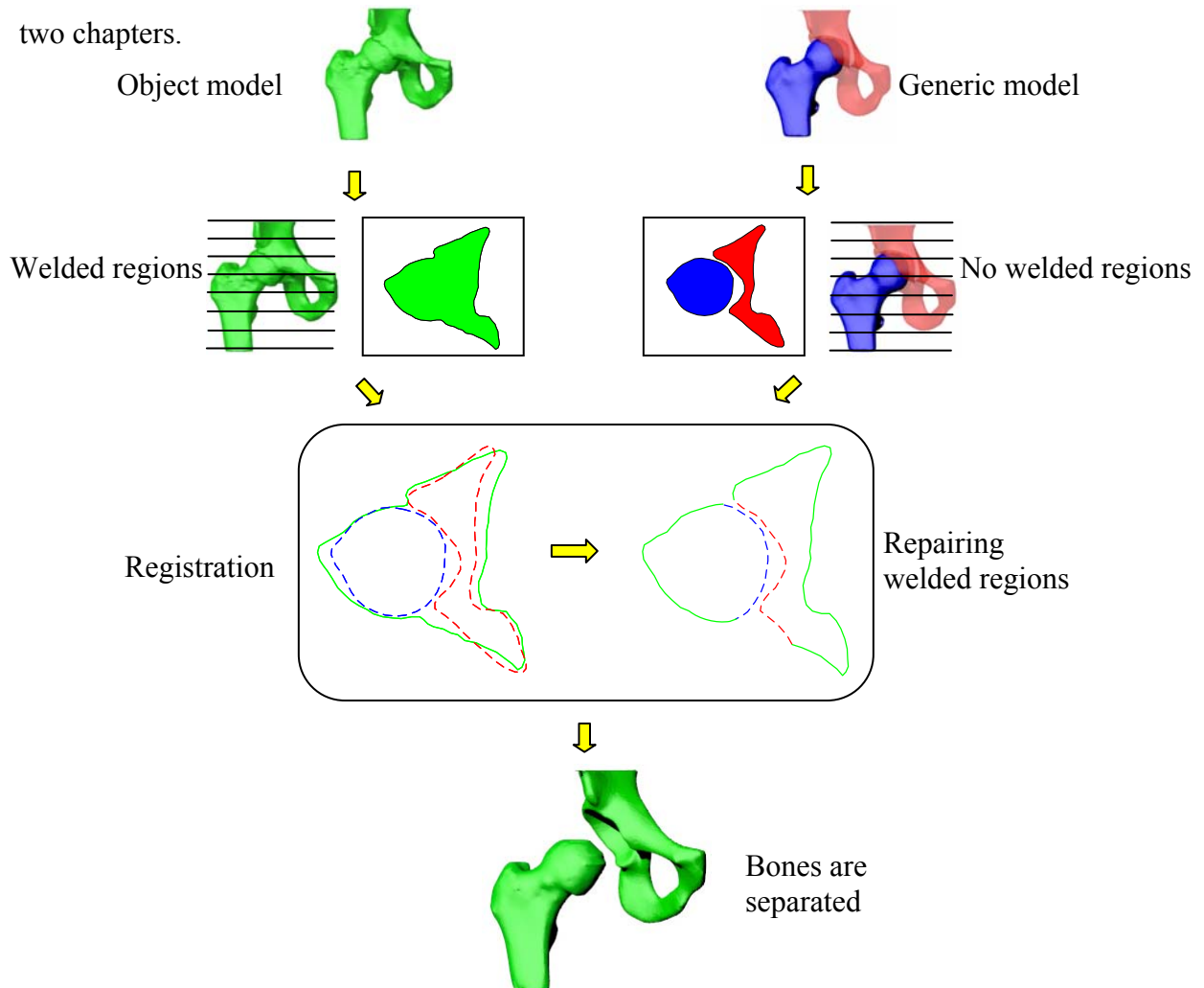
Figure 3.1. Framework to substitute anatomical knowledge in high-level segmentation

3.3. Overview of Solution Approaches

The proposed solution begins preliminarily reconstructing the 3D model (Object model), using any form of low-level segmentation. The generic model is selected from a database using several characteristics of object model to be the criteria (e.g. age, gender,

height, and ethnicity). It is assumed that the database selection process is a straightforward

step and that the generic models in the set are given the same orientation as the bones in CT

images (assuming some standard procedures are used to image the joints).
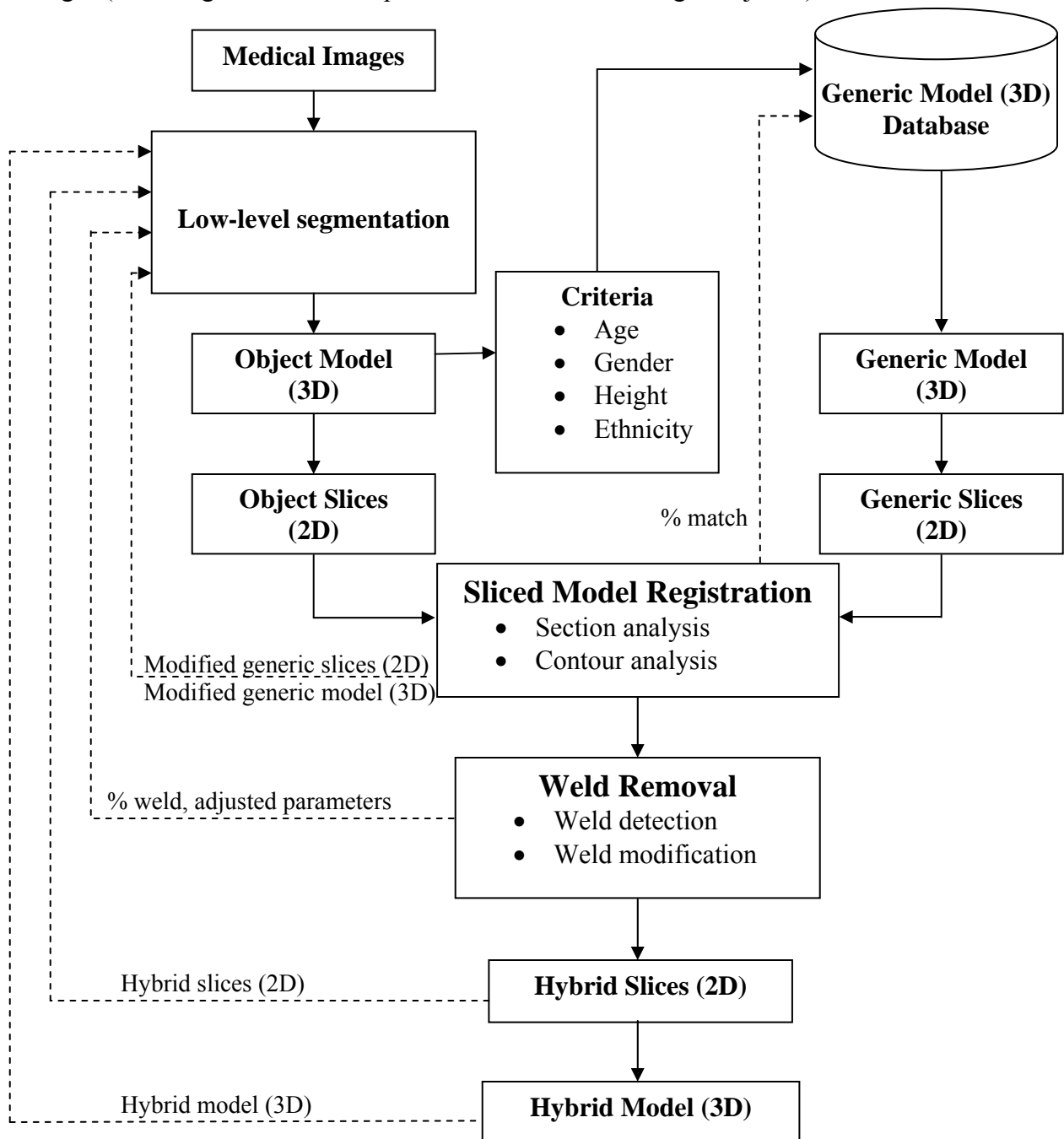
Figure 3.2. Process steps for automated system in high-level segmentation

The overall process steps for automated system in high-level segmentation are illustrated in Figure 3.2. In order to separate the object model which contains the welded regions, the method compares the object model to the generic model. Several approaches to compare 3D models were previously proposed (Suzuki et al., 2001; Zhang and Chen, 2001). The common method in previous work was using a combination of 3D features including tensors, volumes, vertices, faces, etc. However, since bone joints are complex structures, a large variety of 3D features are required for sufficiently representing the model; thus, huge computations are required. The difficulty is also how to distinguish the welded regions from regular surfaces. Instead of using 3D features, the proposed method in this research employs a *slice model* where the model is cut into a series of slices along a direction. This approach is commonly used in methods such as *rapid prototyping* processes to simplify the geometric complexity of 3D models (Pham and Gault, 1998). In a slice model, the surface of a model is replaced by a stack of 2D contours representing the cross sections of the object. From the fact that the object model are reconstructed from image slices such as CT slices, if the object model is sliced equally or smaller than the thickness of the imaging process, the set of slices can provide a close approximation of the bone joint in CT images. Thus, the proposed method cuts 3D *polyhedral* models of the object model and the generic model into a series of slices with 2D *polygonal* contours.

The slice model simplifies the process of comparing between complex 3D surfaces of the two models. For example the welded regions where the surfaces of two bones are combined in 3D space are transformed into the merging of two or more simple contours in 2D space. Figure 3.3a illustrates the slice model of a hip joint (object model). The welded regions are located where the contours of the femur and pelvis are combined (Figure 3.3b).
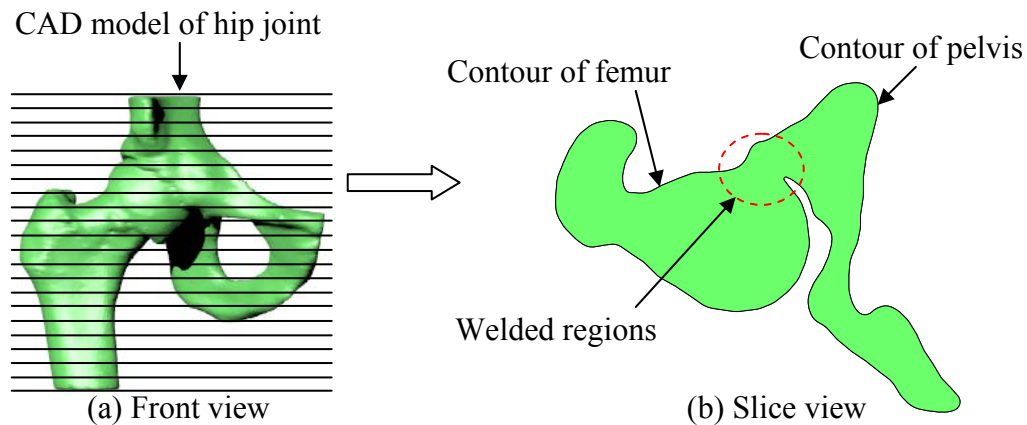
Figure 3.3. Slice of object model of hip joint

In this research, two new processes are proposed in order to compare the object to generic model and repair the welded regions. The first process called *sliced model registration* is a process to align the set of object slices with the set of generic slices (Figure 3.2). The purpose of this process is to find the generic slices that most closely represent the object slices. These generic slices will used to identify and repair the welded regions on the object slices. Two analyses are proposed for the sliced model registration process: 1) section analysis, and 2) contour analysis. Section analysis provides a coarse registration by dividing the object and generic slice models into several small sections. Then, each section of object slice model finds its corresponding section from the sections of the generic slice model. Contour analysis serves as a fine registration that compares the shape of contours on the object and generic slice within the corresponding sections. Then, the best match of generic slice is identified for each object slice. Sliced model registration outputs the object slices with their matching generic slices.

There are two feedbacks that can be generated from the sliced model registration process: 1) *match percentage*, and 2) *modified generic slices* or a *modified generic model*.

Match percentage is the measurement of similarity between the object slice model and the generic slice model. If there are several generic models that fall under chosen categories from the database, the match percentage can lead to a more optimal model from the database. Modified generic slices are the set of generic slices that corresponds to the object slice model. A modified generic model is a reconstructed model using modified generic slices. The main advantage of these modified slices or model is that they can be automatically translated and scaled to fit the object from CT images. Several techniques in low-level segmentation such as *active shape contour*, *active shape model*, and *deformable model* (Kass et al., 1988; Cootes et al., 1994; McInerney et al., 1996; Josephson et al., 2005) usually require manual alignment to position their initial contours or model before segmenting images. By using modified generic slices or model as initial contours or model, these manual steps can be eliminated.

The second proposed method called *weld removal* is a process that attempts to remove the welded regions and separate the individual bones in object model (Figure 3.2). Weld removal utilizes the output from sliced model registration in two steps: 1) *weld detection*, and 2) *weld modification*. The simple idea in weld detection is that if one contour of object slice is represented by two or more contours of the matching generic slice, this object slice contains welded regions. When a weld is detected on an object slice, there are two possible approaches to repair the weld. The first approach is sending the matching generic slice back through the low-level segmentation process as a guide to what the contour *should* have look like. The second approach is to use the matching generic slice to separate and restore the shape of the object slice that contains the welded regions. The new contribution of this work lies more in the second approach, where welds are fixed after they

are created. In the weld modification step, the welded regions are removed and then repaired by some portions of generic slice. This repaired slice is referred as *hybrid slice* since it is a combination of mostly the object slice and portions of the generic slice used to replace the welded region.

The weld removal process generates the *weld percentage* which can be used as a metric to determine the effectiveness of the low-level segmentation process and determine better parameters for their processing such as thresholding values, image filtering parameters or morphological parameters (Pitas 2000; Nikolaidis and Pitas, 2001). The parameters can be adjusted iteratively until the welded regions are minimized. The parameters could be globally or locally changed, for the entire model, or only for the specific slices that contains welded regions. The output of weld removal process, *hybrid slices* or *hybrid model*, is similar to the output of sliced model registration process; *modified object slices* or a *modified object model* (Figure 3.2). The output from the weld removal process can yield the same benefits as the output of sliced model registration in the improvement of low-level segmentation or it can also be used as a final approximated model if desired.

This section has provided a general overview of the solution methods while some details of sliced model registration and weld removal will be presented in following sections.

3.4. Sliced Model Registration

Sliced model registration process consists of two major analyses: 1) section analysis and 2) contour analysis. This process will identify the closest match of generic slices for each slice of the object model.

3.4.1. Section analysis

Section analysis will find some particular slices that have similar characteristics on both the object and generic model, but have unique characteristics compared to surrounding slices on the model itself. These slices will be utilized as section dividers called *landmarks* in the proposed method. A simple example of a landmark may be described by using the analogy of two human faces that need to be registered. In this case the nose can be detected as an outstanding landmark that can serve as a relative location to align two faces. Other landmarks may include the eyes, mouth, etc. Several attributes including area, perimeter, and distance from centroid to a reference point are currently used for automatic landmark detection. These attributes are referred as *slice descriptors* in the proposed method. It should be noted that these slice descriptors are computed from the *convex hull* (Preparata and Shamos, 1985) of the slices because the individual contours on the object slice and matching generic slice may look different due to the welded regions (Figure 3.4). The shapes of the respective convex hulls for both slices should be unaffected by the welded regions.
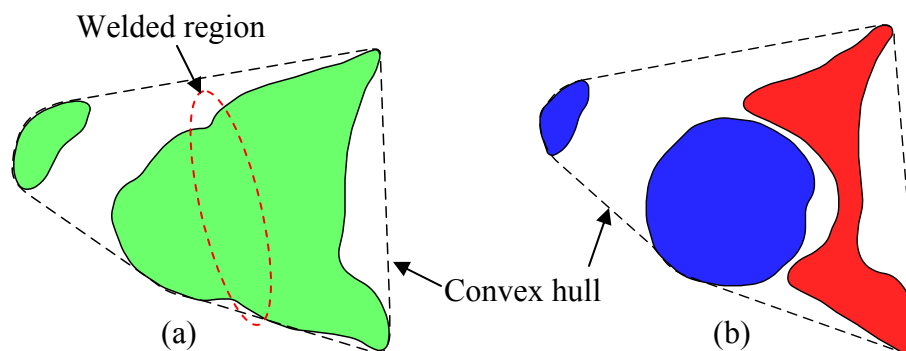
Figure 3.4. Convex hull of (a) object slice and (b) generic slice

In the proposed method, the landmarks are detected using several criteria including local minimum or maximum of slice descriptors and rate of changes of slice descriptors. Only corresponding landmarks on the object slice model and generic slice model are used for

dividing these two sets of slices into small sections. The challenge is how to identify if a selected landmark from the object slice model corresponds to any landmarks from the generic slice model. This dissertation proposes a method to identify landmarks in several levels based on the magnitude of their values. It is expected to find similar landmarks at an equivalent level. The method locates landmarks by searching through all slice descriptors and finally both slice models are divided into corresponding sections. Figure 3.5 shows example locations of landmarks on both models.
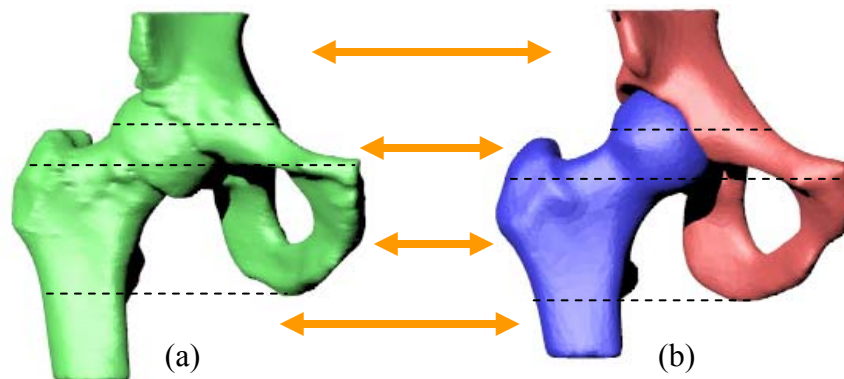
Figure 3.5. Locations of landmarks on (a) object model and (b) generic model

3.4.2. Contour analysis

Contour analysis is a process that analyzes the similarity between the slices of object and generic models, and then identifies the best matching pairs. The slices of object model are only compared to the slices of generic model within their corresponding sections. Of course, the proposed method requires 2D shape matching techniques for this analysis. Although shape matching techniques were previously proposed in the literature (Loncaric, 1998; Jiantao et al., 2004; Zhang and Lu, 2004), most of them are only suitable for

comparing between single contours or equivalent numbers of contours on the slice. Contours of a bone joint may or may not have equivalent numbers between object and generic slices.

The method in this dissertation is modified from the method of Attalla (Attalla and Siy, 2005). Attalla used three centroid attributes to describe a complex shape of contour: 1) distance from centroid to boundary point, 2) angle between the line extended from the centroid and the line connecting boundary points, and 3) ration of the line connecting boundary points to the arc of the contour. However, Attalla's method was proposed for comparing single contours.

In this dissertation Attalla's method is modified in order to properly compare the contours on two bone slices which may be more than one contour and may also contain different number of contours. Also, the proposed method utilizes the centroid of the convex hull instead of the centroid of individual contour. The boundary points are obtained by uniformly incrementing an angle of line extended from the centroid to the furthest contour boundary. This method for obtaining boundary points is similar to the method proposed by Tan (Tan et al., 2003). In this dissertation, three centroid attributes are used to match the contours (Figure 3.6): 1) distance (r_i) from the centroid of convex hull to boundary points, 2) the angle between the center line and the line connecting between two boundary points (a_i), and 3) the length of the line connecting boundary points (v_i). The similarity between the contours on object slices and the contours on generic slices is measured by computing the *sum of squared differences* (SSD) of those three proposed attributes. The lowest SSD is where the generic slice matches the object slice.
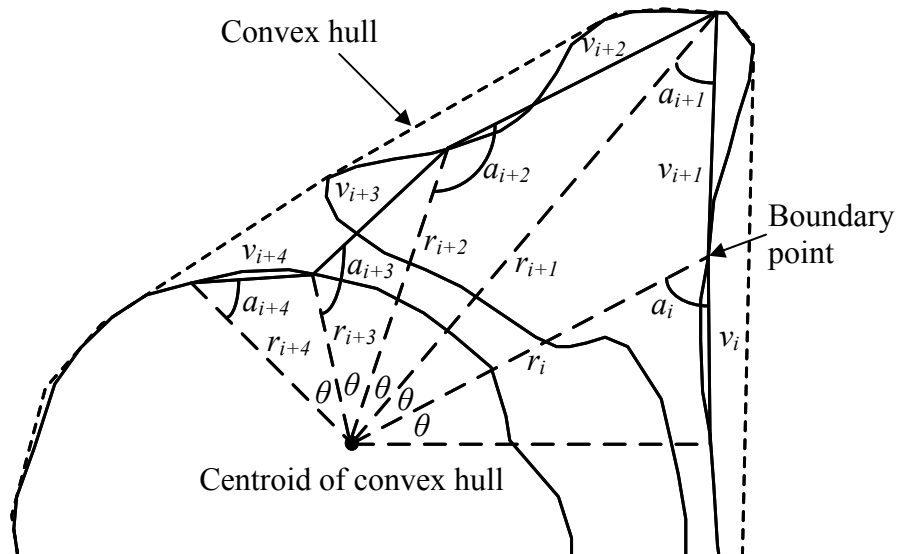
Figure 3.6. Three attributes for contour matching: r_i, a_i, and v_i

After the matching pairs between object slices and generic slices are found, the results will be further used in weld removal process.

3.5. Weld Removal

This process utilizes information from generic slices to identify and repair the welds on object slices. The proposed method involves two process steps to remove the welded regions: 1) weld detection and 2) weld modification.

3.5.1. Weld detection

Weld detection is a process that locates welded regions by comparing object slices to generic slices. Since contours on generic slice represent a good pattern of contours on object slice, if one contour of object slice matches with two or more contours of generic slice which belongs to different types of bone, this contour of object slice contains welded regions. At the beginning of weld detection, the generic slice is transformed to fit the object slice using

centroid of convex hull as a reference point. The intersection of contour is used to identify the welded regions (Figure 3.7a). If the contour of object slice does not intersect with any contours of generic slice, this contour of object slice is further identified by intersecting with a contour on the previous or next object slices that can be identified (Figure 3.7b).
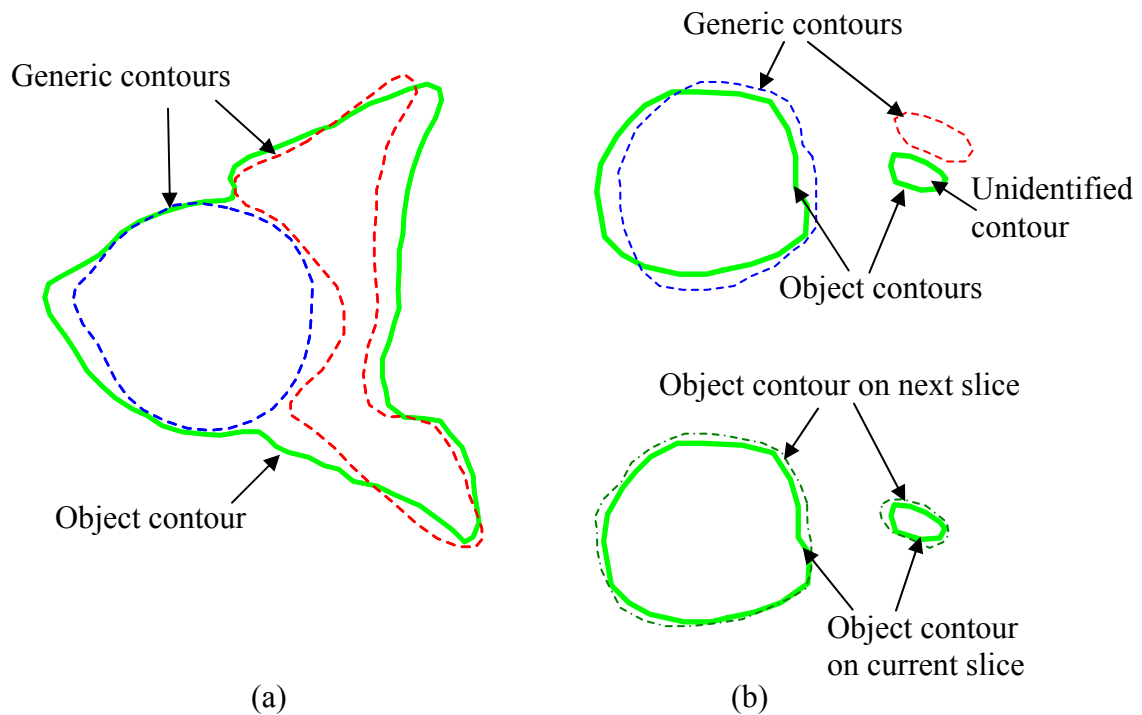
Figure 3.7. Intersection method for weld detection: (a) intersection between object contour and generic contours, (b) intersection between contours on current slice and next slice of object model when generic contours do not intersect

For the object slice that contains welded regions, the proposed method further examines the location of welds on the contour and uses this location to divide the contour into portions that belong to individual bones. The method first locates contours of generic slice on the top of relative contours of object slice. The closest generic contour is used to identify the part of object contour that relates to individual bone. Then, the object contour is taken apart into several portions corresponding to the pattern of generic contours (Figure

3.8). Next, the results from weld detection are passed to the weld modification to restore the incomplete contours of object slice.
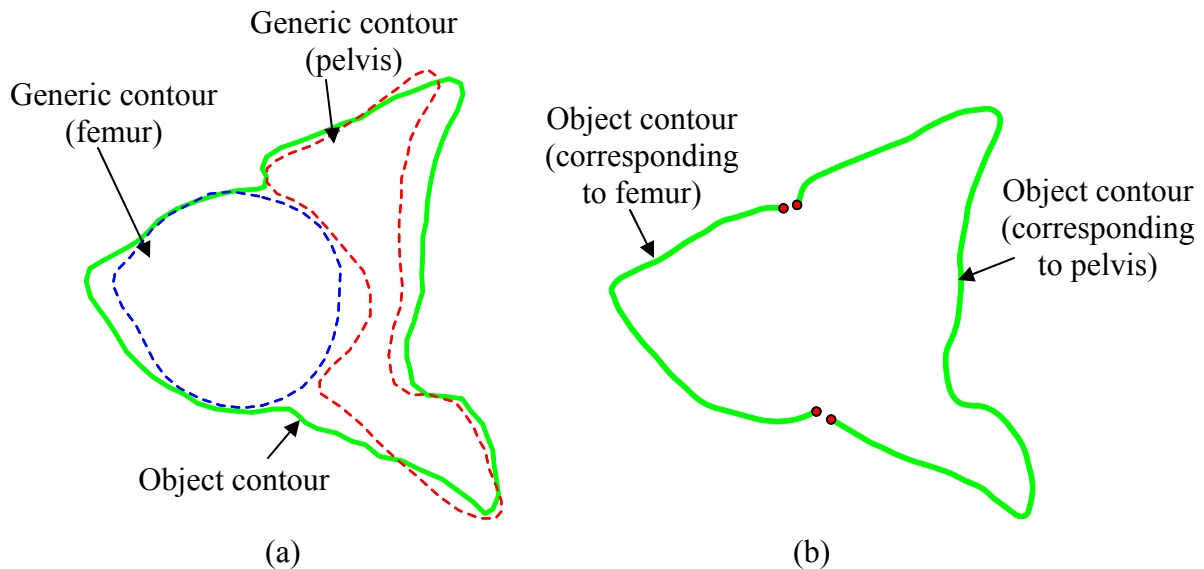
Figure 3.8. Weld detection

3.5.2. Weld modification

Weld modification refers to a process that repairs the welded regions on the object slice. From the weld detection process, the contour of the object slice that contains welded regions is divided into several portions corresponding to individual bones. The challenge is how to recreate the complete contours from these portions. A common method that utilizes *curvature* at the end points can be used to close the contour; however, it may not yield proper results when the shape of the contour is complex or the amount of data to restore is very large. Therefore, the proposed method employs parts of the generic contour to fill this missing data. Figure 3.9b shows how the portion of generic contour is created in order to fill the missing part of object contour where a weld was removed. Then, this portion of generic contour is transformed to fit the gap on object contour as shown in Figure 3.9c. The fixed

contour called *hybrid contour* is finally created by combining parts of the object contour and generic contour.
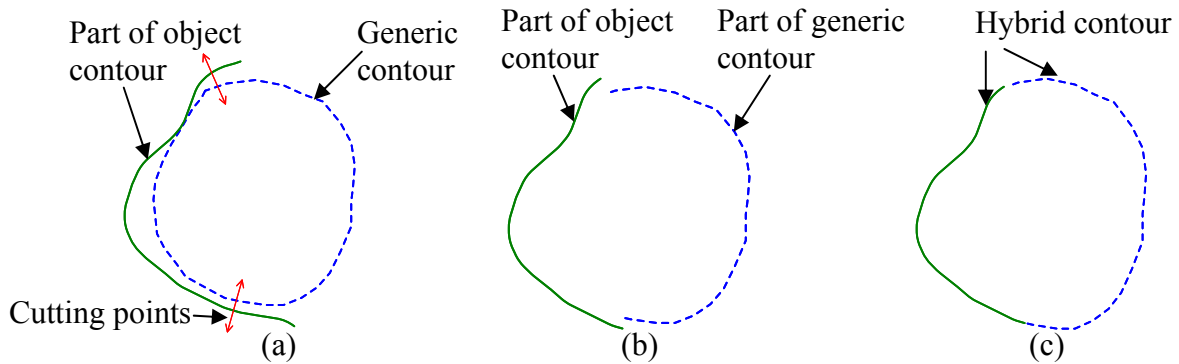
Figure 3.9. Weld modification

After the object contours are repaired, the set of *hybrid slices* are now ready for reconstructing a 3D model (*hybrid model*). These hybrid slices or entire hybrid models have their contours or models properly separated into a distinct set of bones (e.g. pelvis and femur for a hip joint). Either hybrid slices or hybrid models could be further utilized in low-level segmentation for image segmentation purpose.

3.6. Summary

In this chapter, an overview of an automated system for high level segmentation and separation of complex bone structures is proposed. This chapter briefly presents two major processes which are important to build the automated system for high-level segmentation. The first process, *sliced model registration*, registers the object model with the generic model. Then, the welded regions on object model are detected and repaired in the continuous process, *weld removal*. Chapter 4 and 5 will present both the sliced model registration and weld removal processes in more detail.

CHAPTER 4. AUTOMATED SEPARATION OF BONE JOINT STRUCTURES FOR MEDICAL IMAGE RECONSTRUCTION – PART I: A METHODOLOGY FOR REGISTRATION

Wutthigrai Boonsuk and Matthew C. Frank

4.1. Abstract

Automated segmentation and separation of bone joints is challenging since bones in joint areas are inhomogeneous structures surrounded by soft tissue such as cartilage, which makes bone boundaries unclear in the image slices. Reconstructed 3D joint models will often have bones improperly combined after traditional *low-level* segmentation methods such as *thresholding*, *edge detection*, and *region growing* techniques. These models require an extensive amount of expert intervention to manually identify and remove inadvertently combined areas, which appear as *welds* between bones. This manual task is time consuming, laborious, and inconsistent. This paper presents a methodology for automatically separating bone joint structures by utilizing known anatomical information from a *generic* CAD model. This generic CAD model is a properly generated model of the anatomy of a similar human subject, with regard to age, gender, height, etc. The intent is to aid in the separation of bones in the joint by comparing the inadvertently combined models to generic models that have individual bones separated properly. The method uses simplified representations (slices) of the CAD model; hence the two or more combined 3D surfaces are transformed to two or more merged 2D contours on a slice. *Sliced model registration* and *weld removal* are proposed as sequential processes for fixing welds on the slices. To begin, the sliced model registration process compares the two models and identifies corresponding pairs of slices.

Next, the weld removal process detects and removes welds on the slices using available information from its matched slice on the generic model. The repaired slices are then used to reconstruct 3D models with all bones in the joint properly separated.

The main contribution of this paper is a method for the sliced model registration process. In this process, two sets of model slices are first divided and registered in several bulk sections. The slices are then matched between corresponding sections of the two models, the object model under study and the generic model. The method presented is shown to be an improvement over general rigid registration and can be either used in a weld removal process or used for feedback to low-level segmentation in order to improve segmentation results and avoid welding. The human hip joint is used as an example of algorithm implementation in this paper. The proposed solution is a general approach that should be flexible enough to work with other types of joints such as the knee, elbow, etc.

4.2. Introduction

With current medical imaging technology such as computed tomography (CT) or magnetic resonance imaging (MRI), 3D CAD models can be created using the series of cross sectional images. These CAD models are used in both medical and non-medical applications ranging from clinical diagnoses, surgical planning, medical implant fabrication, or computer simulation and animation [16, 25]. Two essential processes to transform medical images into CAD models are *image segmentation* and *model reconstruction* processes. The segmentation process distinguishes the objects of interest (specific tissues like bone, cartilage, etc.) from the image background. Model reconstruction then uses the results from segmentation to create 3D models. Segmentation can be classified into two levels: *low-level* segmentation

and *high-level* segmentation [5]. Low-level segmentation refers to a process that detects and retrieves important features from the image and translates them into explicit data. This level of segmentation is commonly the first step in the segmentation process. As one example of low level segmentation, one can select threshold density values (like a band-pass filter) to separate bones from the image background. However, it is well known that low-level segmentation is not sufficient to segment bone joint structures. The boundaries of adjacent bones appear to merge after the models are reconstructed using the results from low-level segmentation. In other words, the low level segmentation can distinguish bone material from the background, but has difficulty in distinguishing one bone from another, especially when they have intimate contact, such as a joint. The primary reason is because the joint areas contain soft tissues such as cartilage which can make bone boundaries ambiguous (density is very similar at the interfaces); thus, low-level segmentation and model reconstruction may not distinguish the interface between two distinct bones. The other reason is that low-level segmentation cannot provide branching or topological information [12, 23] for properly reconstructing individual bones. In other words, even if the boundaries can be found, it is a further problem to determine which slice belongs to which bone. When these problems arise, the bones can be inadvertently joined or as we will refer to in this paper *welded* together. The research in this paper is highly motivated by solving this welding problem and to do so in an automated fashion. An example of a welded bone joint is given in Figure 4.1a, while the properly separated bones of the Femur and Pelvis are shown in Figure 4.1b.
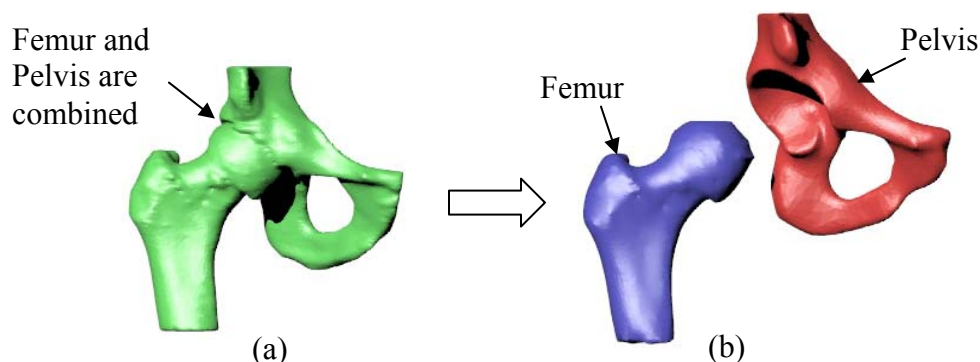
Figure 4.1. Low-level segmentation and high-level segmentation: (a) hip joint after low-level segmentation and (b) hip joint after high-level segmentation

High-level segmentation is specifically targeted at fixing the weld problem. However, this level of segmentation is usually performed by an operator who is trained or familiar with anatomical structures. The person will examine the image slices and manually repair the result of low-level segmentation where the bones are combined. Figure 4.2 illustrates steps of high-level segmentation using a CT image of hip joint where the femur and pelvis are physically adjacent. After the low-level segmentation process, the femur contour and pelvis contour were combined at the welded regions as shown in Figure 4.2b. In this case, high-level segmentation would be manually performed to repair the welded regions, and assign the contours to each individual bone (Figure 4.2c and 4.2d). The manual approach is a time consuming and tedious task because the modification might need to be repeated for tens or hundreds of image slices. The results are also prone to errors and are generally non-repeatable.
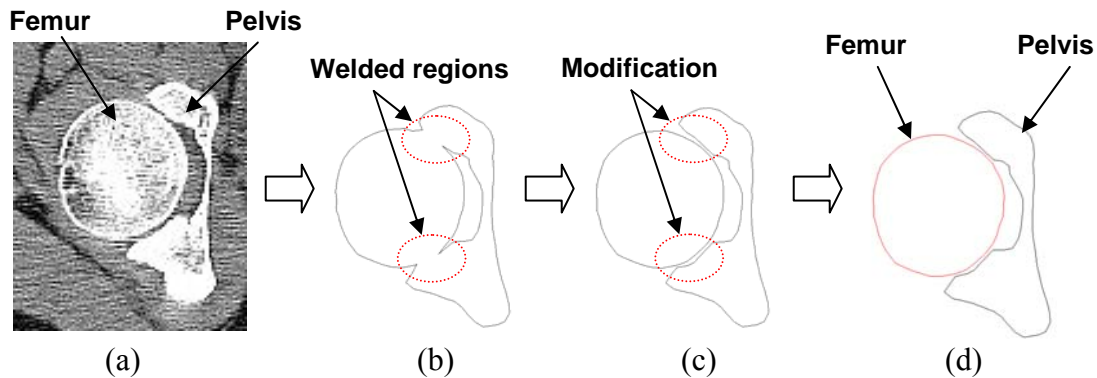
Figure 4.2. Steps of high-level segmentation: (a) CT image of hip joint, (b) contour after low-level segmentation, (c) high-level segmentation by manual modification, (d) contours after high-level segmentation

The research in this paper specifically focuses on high-level segmentation of bone joint structures with the goal of developing an automated system to perform the task. The challenge is how to provide the system with the required knowledge of anatomy and how to utilize this knowledge in the system. Figure 4.3 illustrates an overview of the approach of the proposed system. The proposed method employs a generic CAD model that represents the *known* information, properly separated bone joint model. With respect to automation of the method, using a generic model provides a flexible solution for separation of a variety of joint types. The generic model is then registered to the patient's model that has been preliminarily reconstructed from the results of low-level segmentation. The method inputs the patient's model, which may or may not contain welded regions, and outputs a *fixed* model where the welded regions are removed and all bones are distinctly separated.
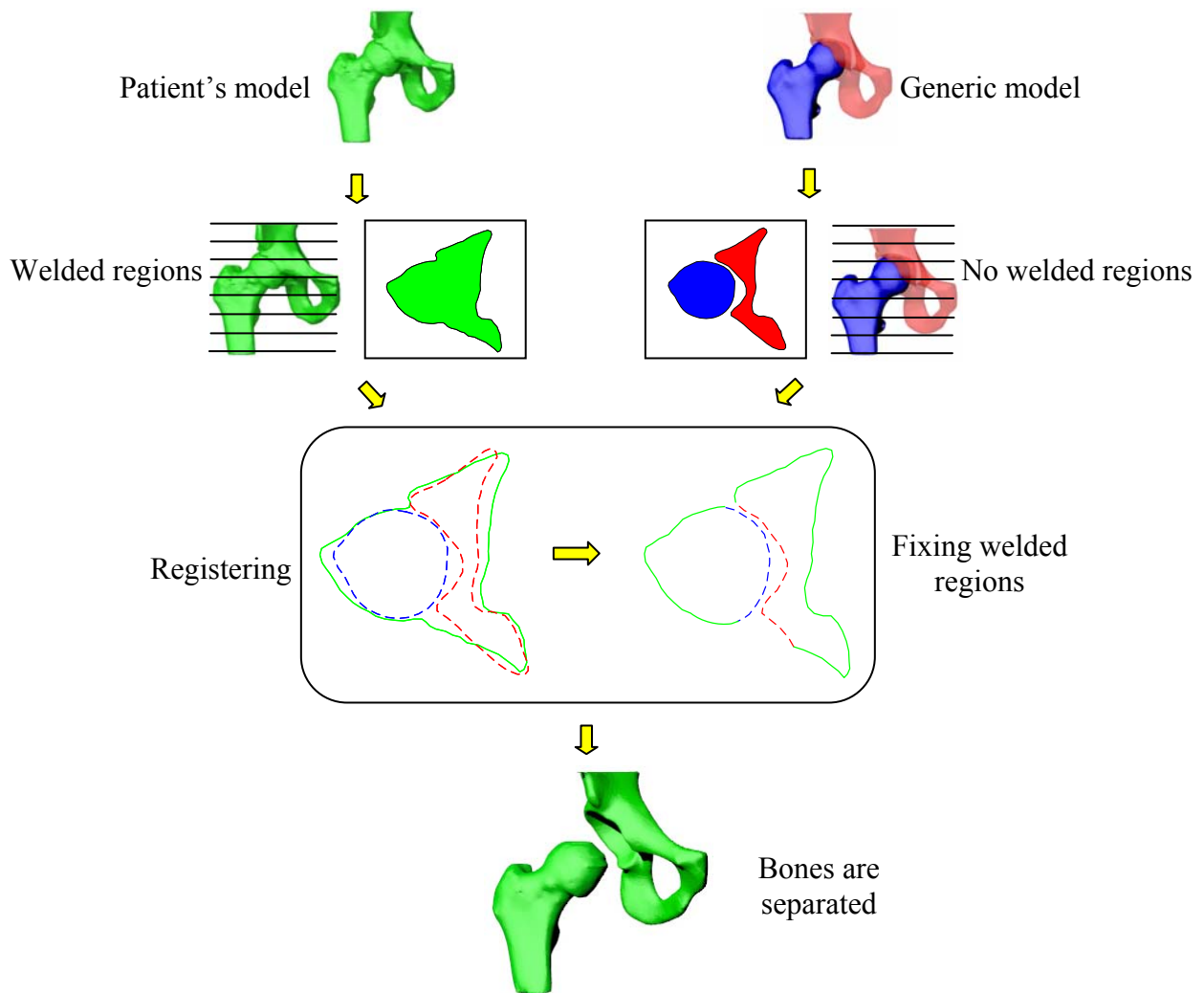
Figure 4.3. General approach for substituting anatomical knowledge in the high-level segmentation

This paper presents a method for registering the patient's model to a generic model. The registration process is critically important since the accuracy of weld detection and modification depends on how well the shape and topology of the generic model aligns to represent the patient's model. This paper is organized as follows: Previous work in segmentation techniques are reviewed in the first section followed by an overview of the solution method. Next, the methodology of the registration process and an implementation are described in Section 4.5 and 4.6. Results comparing the new method to a rigid

registration process that lacks analysis are shown in section 4.7, along with conclusions and proposed future work in section 4.8.

4.3. Related Work

Although several segmentation methods have been proposed for medical image processing, automated segmentation is an elusive solution, especially with bones in joint areas. Traditional techniques for image segmentation such as *thresholding*, *edge detection,* *region growing,* and *morphology operation* [18, 20] mainly rely on grey scale analysis of the image. These techniques can give mistaken results in regions where the grey scale is very similar between two or more adjacent objects such as bones in joint areas. CAD models of bones in these areas are often combined because one cannot distinguish the boundary of individual bones. In these cases, manual editing by medical experts is required to correct the boundaries of bones before the reconstruction process.

Knowledge-based techniques provided an improvement over traditional techniques, with example solutions such as *snake* (2D), *deformable contour* (2D), *active shape contour* (2D), *deformable model* (3D), and *active shape model* (3D) [14, 9, 15, 13]. These methods add some prior knowledge or shape constraints in order to segment the images such that the contour (2D) or model (3D) can be deformed with restriction to fit the boundary of the object of interest. However, the quality of segmentation is sensitive to the alignment of the initial contour or model. For example, the initial contour must be carefully placed at the boundary of bones since the clearance between the bones is often quite small and very difficult to see. If the contour is placed incorrectly, the segmentation results could be a combination of the adjacent bone boundary. Although some researchers [11, 17] recommended using the

contour in the previous image slice as the initial contour (2D), this does not address the problem where the number of contours differs between image slices.

The proposed method in this paper is intended to replace the manual alignment step and handle the problem of changes in the number of contours across slices. Alternatively, the proposed method could be used to augment existing techniques found in the literature by automatically generating the initial contour or model and aligning this contour or model to the object of interest in image slices. In this manner, one could aid in automating the contour selection process and perhaps avoid weld generation. In general, a major contribution of the research in this paper is a system that performs high-level segmentation without human intervention or skill required. The system will replace knowledge by an expert with an example of what the joint *should* look like. As a specific problem addressed in the work of this paper, we propose that welded bones due to poor segmentation methods can be detected and ultimately fixed if a proper example can be given.

4.4. Overview of Methodology

In the proposed method, *generic* models are employed as the "*known*" information about what the bone joint should look like. The generic model is a complete CAD model of bone structure that contains all bones in the joint area with the bones properly and distinctly separated. The generic model is given the same orientation and scale as the patient's model from CT images. A library of generic model may be necessary in order to provide a close approximated model by sorting on several criteria such as gender, age, height, and ethnicity. The makeup and structure of this library of models is outside the scope of this paper; it will be assumed that a relatively closely matched model is available as the input data.

The proposed method starts with a CAD model of the patient's joint that has been preliminarily reconstructed from CT images. In this paper, we refer to this model as the *object* model. The method first allows object model to contain combined areas or welded regions (between adjacent bones) which may occur during segmentation and reconstruction process. Later, the method identifies and removes the welded regions on the object model using known information from generic model. However, identifying welded regions by comparing the object model (3D) to the generic model (3D) becomes very complicated. Features of 3D objects such as vertices, volumes, tensors, and surfaces are commonly employed to represent models [3, 26]; however since bone joints are complex structures, a large variety and combination of 3D features are needed for representing the model in order to provide adequate information to distinguish between the object model and the generic model. Hence, computations are expensive for this approach. It should be noted that the parts of the object model will always differ at least slightly from the generic model since each human anatomy is unique.

Instead of comparing between 3D models, this paper employs a method that cuts 3D model into a series of slices along a direction. This approach is commonly used in methods such as rapid prototyping processes to simplify the geometric complexity of 3D model [19]. In the slicing approach, a CAD model is represented by a stack of 2D contours which are the cross sections of the model (Figure 4a). From the fact that the object model is created from image slices, if the object CAD model is sliced with equal or thinner slices, then one can expect a close approximation to the object. Each slice contains 2D polygonal contours (cross sections) of one or more bones. The welded regions between two model surfaces (two bones) are now represented by the merging of simple polygons (Figure 4.4b).

CAD model of hip joint

Contour of femur

Contour of pelvis

Welded regions

(a) Front view

(b) Slice view
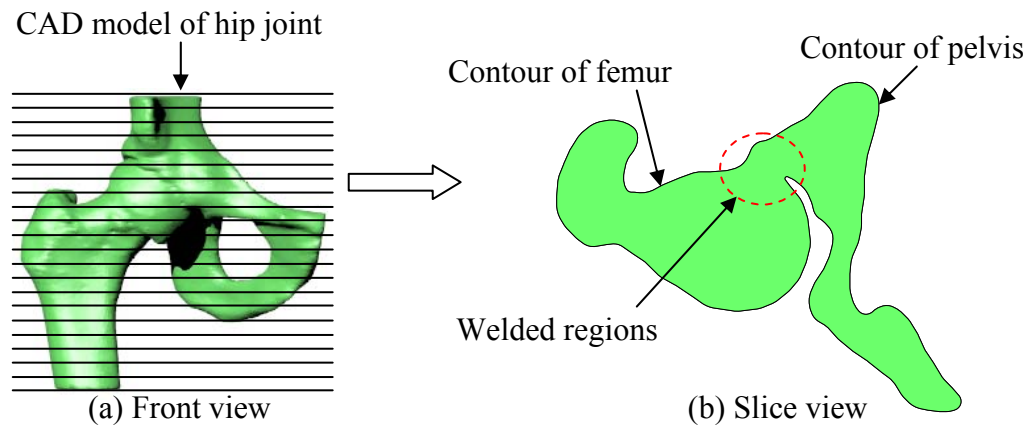
Figure 4.4. Slice of object model of hip joint

A schematic of the overall process is illustrated in Figure 4.5. Two necessary processes are proposed for comparing and fixing the slices of the object model: 1) *sliced model registration*, and 2) *weld removal*. In the sliced model registration process, slices of the object and generic models are analyzed in order to find slices of the generic model that best represent slices of the corresponding object model. Two separate steps of *section analysis* and *contour analysis* are proposed for the registration process. Section analysis divides sets of slices of object and generic models into several small sections. Ideally, the sections on the object model should correspond to the sections on the generic model. Once the corresponding sections are identified, contour analysis examines the slice contours in corresponding sections, and finds a closest pairs of slices. The output of the sliced model registration process is the initial closest pairs of slices between object model and generic model. This provides a metric of "*match percentage*" and a set of modified generic slices (2D) or a modified generic model (3D). Match percentage is a measurement of similarity between the object model and generic model. This feedback can be iteratively sent back to a generic model database to search for the closest generic model, if a library of generic models were available. The *modified generic 2D slices* or *modified generic 3D model* are the

registered slices or reconstructed model which correspond to the object model. This

feedback provides initial contours or an entire initial model for several existing techniques in

low-level segmentation found in the literature including active shape contours, active shape

models, and deformable models or for use in manual segmentation.
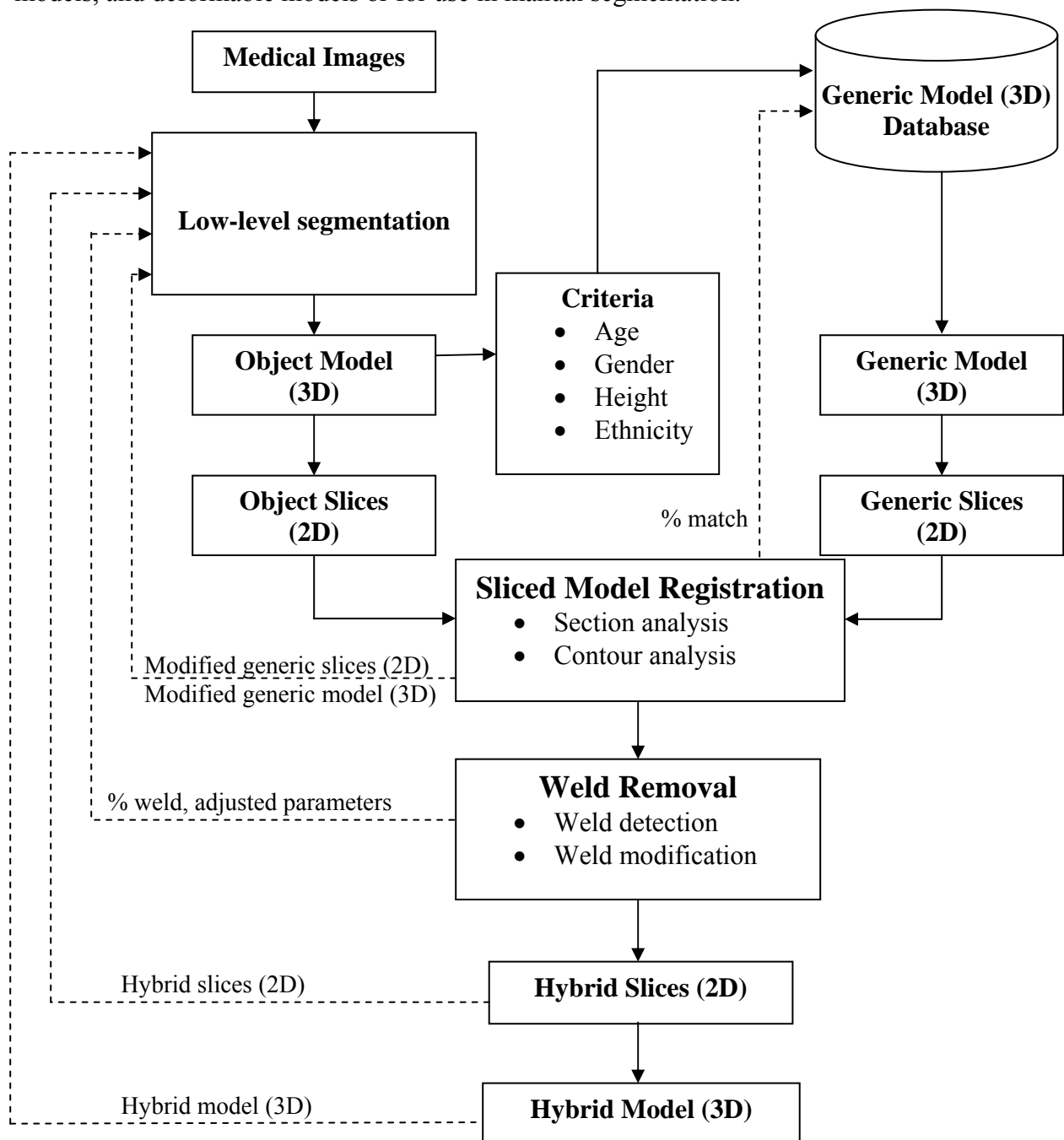
Figure 4.5. Process steps for automated system in high-level segmentation

Next, the weld removal process identifies and repairs the inadvertently joined or *welded* regions on the object model. The first step in the weld removal process is *weld detection*. This step utilizes the matched slices from the generic model to identify the welded regions on slices of the object model. If there are welds on the slice, this object slice will be passed to a weld modification step. *Weld modification* uses the contours of generic slices to repair the welds on the contours of object slices. The weld removal process can return the weld percentage along with some adjusted parameters to improve the results of low-level segmentation process. The adjusted parameters can be any given parameters that are used by low-level segmentation process such as thresholding values, filtering parameters, and morphological parameters. This feedback loop can be iterated until the welded regions on the object model are minimized. The output of weld removal process is the slices of object model that have welded regions removed and with contours on the slices assigned to individual bones (contours of the femur are correctly assigned to the femur, etc.). This output could be directly used in a reconstruction process to create an approximate 3D model which has all bones in joint separated. However, this process can also be iterated by sending back the modified 2D object slices or the modified 3D object model to a low-level segmentation process. A low-level segmentation process could use these modified slices or 3D model to directly segment the object from medical imaging, with no human intervention or skilled manual processing such as alignment of deformable models or selecting seed points. The following sections provide a detailed presentation of the sliced model registration process.

4.5. Sliced Model Registration Methodology

Sliced model registration refers to the process that finds the corresponding matches between object slices and generic slices. Two major analyses are proposed for the sliced model registration process: 1) section analysis, and 2) contour analysis. Section analysis divides slices of the object model and generic model into several sections. Then, the method identifies sections of the object model that correspond to sections of the generic model. Contour analysis continuously compares the slices of the object and generic models in corresponding sections, and identifies the comparable slices between these two sections.

4.5.1. Section analysis

Registration between slices of the object model and generic models is not simple because these models are not identical; as no two human anatomies are identical. Section analysis is a process that breaks up the slices of object model and the slices of generic model into smaller sections so that they can be generally registered for some bulk sections of slices. This analysis aims to reduce the potential of inadvertently registering slice across the two models from obviously wrong areas. The correct pair may not be located on the same numbered slice from both models, so a one-to-one match may not be appropriate. However, if we allow the system to simply find the "*best*" match in a one-to-many comparison, the best match may exist in very different sections of the bone. For example, the long bones (femur, tibia, etc.) may have numerous slices that are similar along the shaft and the best match may be far apart. Hence, the section analysis serves as a coarse registration (section-to-section registration) which will limit the fine registration (one-to-one registration) to only corresponding sections of both models.

In this paper, the locations used for dividing the model into small sections are called *landmarks*. The landmarks must be determined mathematically in order for the process to be completely automated. Moreover, landmarks on the object model must correspond to landmarks on the generic model. Simple 2D geometric attributes such as area and perimeter can be mathematically computed from a stack of contour slices. Tracing these 2D attributes can illustrate the transition in shapes of contours on the slices. However, since the contours of the object model can contain welded regions while the contours of the generic model do not, the process could return false results. To avoid this problem, the method extracts the landmarks from the convex hull of the contour slices instead, since the convex hulls cannot be affected by welded regions.

Several algorithms can be adopted for computing the convex hull including the *Gift Wrapping* [7], *Graham Scan* [10], *Divide-and-Conquer* [21], *Monotone Chain* [1], and *Quick Hull* [22] algorithms. The proposed method calculates one convex hull for all contours on the slice, which eliminates the effect of welded regions (Figure 4.6).
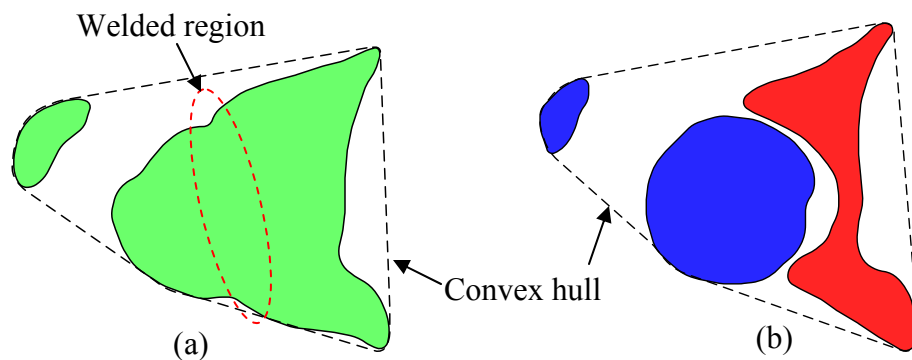
Figure 4.6. Convex hull of (a) object slice and (b) generic slice

The geometric attributes in this paper which are computed from the convex hull of contours on the slices are called *slice descriptors*. A good slice descriptor will have the ability to extract proper landmarks and is generally robust with respect to types of joints and

their orientation. Three descriptors are proposed in this paper: 1) area, 2) perimeter, and 3) distance between the centroid of the convex hull to a reference point. This reference point is the center of an enclosing cylinder for the entire model (Figure 7). Based on the geometry of bone joint structures, these three slice descriptors vary mostly along the slice direction and will be shown to be simple and robust. The slice descriptors are computed from a convex hull that has N vertices ordered counter clockwise. A vertex of the convex hull is represented by (x_i, y_i) where i is from 0 to $N-1$.

The area of a convex hull or *area descriptor* (A) is computed using a method that calculates the area of a convex polygon [6].

$$A_j = \frac{1}{2} \sum_{i=0}^{N-1} (x_i y_{i+1} - x_{i+1} y_i), \quad j = 0, 1, \ldots, m \text{ (slices)} \quad (1)$$

The perimeter of a convex hull or *perimeter descriptor* (P) is computed by the summation of the distances between two vertices of the polygon.

$$P_j = \sum_{i=0}^{N-1} \sqrt{(x_i - x_{i+1})^2 + (y_i - y_{i+1})^2}, \quad j = 0, 1, \ldots, m \text{ (slices)} \quad (2)$$

(a) Slice view   (b) Front view
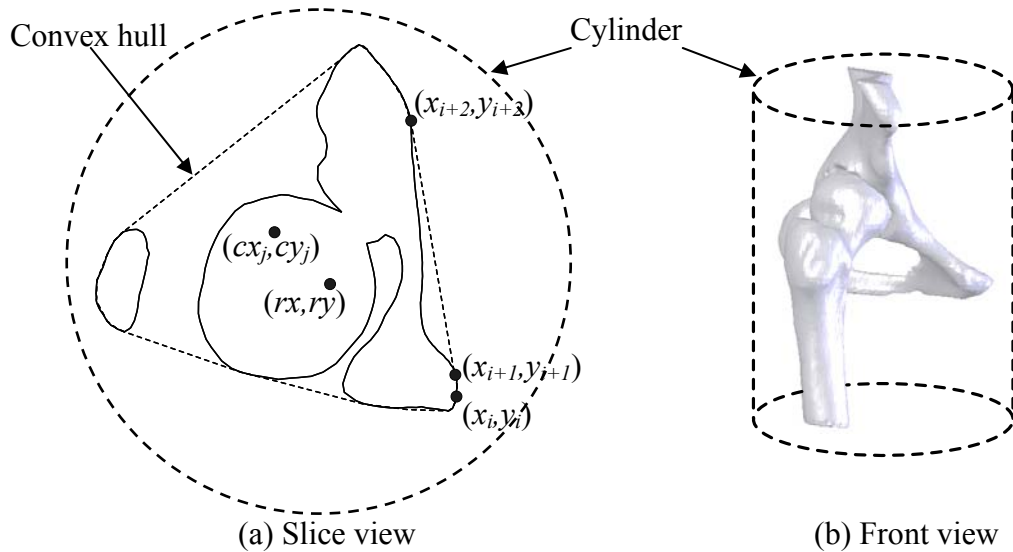
Figure 4.7. Centroid of convex hull (cx_j, cy_j), vertices of convex hull (x_i, y_i), and center of cylinder (rx, ry)

The centroid of a convex hull (cx_j, cy_j) [6] is given by:

$$cx_j = \frac{1}{6A_j} \sum_{i=0}^{N-1} (x_i + x_{i+1})(x_i y_{i+1} - x_{i+1} y_i)$$

$$cy_j = \frac{1}{6A_j} \sum_{i=0}^{N-1} (y_i + y_{i+1})(x_i y_{i+1} - x_{i+1} y_i), \quad j = 0, 1, \ldots, m \text{ (slices)} \qquad (3)$$

Lastly, the distance between the centroid of the convex hull (cx_j, cy_j) to a reference point or *centroid descriptor* (C) is a simple Euclidean distance. From Figure 4.7, if the reference point (rx, ry) is the center of the enclosing cylinder (aligned with the slice direction), the distance between the centroid to this point for each slice is computed by:

$$C_j = \sqrt{(cx_j - rx)^2 + (cy_j - ry)^2}, \quad j = 0, 1, \ldots, m \text{ (slices)} \qquad (4)$$

Once slice descriptors (A_j, P_j, C_j) are computed for the sets of slices of object model and generic model, the proposed method then extracts landmarks using these slice descriptors. Landmarks are locations where the values of slice descriptor, along the slice direction, differ from neighboring values. To reveal these landmarks, two methods are employed in this paper: 1) from maximum and minimum of descriptors and 2) from rate of change of descriptors.

Detecting maximum/minimum of descriptors can be illustrated using a plot between values of the slice descriptor and slice number. As the example shown in Figure 4.7, this figure presents a plot of the centroid descriptor by its slice number. The global maximum/minimum and local maximum/minimum along the plot are the obvious points for probable landmarks. Global maximum/minimum is the overall maximum or minimum points of the plot. Local maximum/minimum is the maximum or minimum points on the plot by comparing to values of neighboring points. It should be noted that before searching for any

landmarks from slice descriptors, the values of slice descriptors are first normalized by their

maximum value to make them scale invariant.
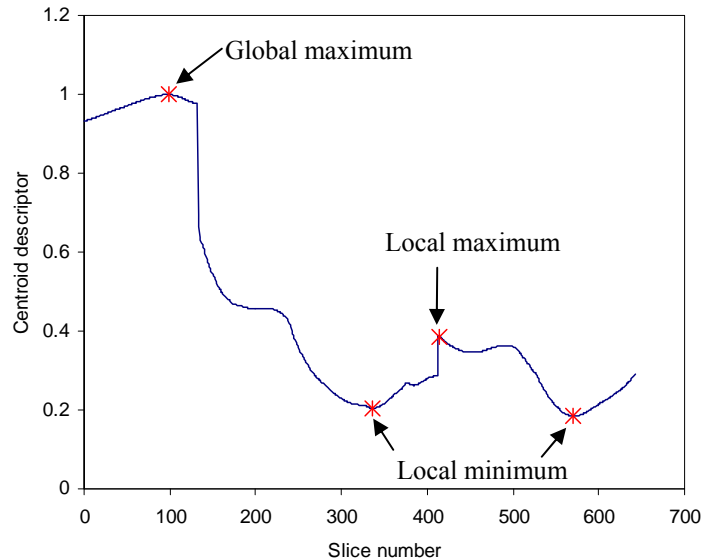
Figure 4.8. Plot of centroid descriptor

In theory, if a plot of slice descriptors is represented by $f(x)$, those maximum and

minimum points can be found using the first derivative and second derivative. However, in

practice it is too difficult to fit a curve through those slice descriptors; thus, this paper uses an

iterative method by comparing the slope between two points of descriptor with an

incremental small value (δ).

```
For ( i = 0 to N-1) {
        If (find max) {
                If (sd_{i+1} > sd_i) tempmax = sn_{i+1} ;
                Else {
                        If (Δsd_{i+1} > δ)
                        max = tempmax ;
                        tempmin = tempmax ;
                }
        }
        If (find min) {
                If (sd_{i+1} < sd_i) tempmin = sn_{i+1} ;
                Else {
                        If (Δsd_{i+1} < δ)
```

```
                              min = tempmin ;
                              tempmax = tempmin ;
                  }
            }
      }
} δ++ ;
where  N     =     number of slice descriptors,
       sd    =     slice descriptor,
       Δsd   =     the slope of two consecutive slice descriptors,
       sn    =     slice number
```

At the beginning of the detection process, all the maximum (and minimum) points are detected where δ is very small. While the value of δ increases, the number of maximum (minimum) points that can be detected decreases. The method traces the change in the number of these points until it approaches zero. The hierarchy is established by the decreasing step in number of detecting points. For instance, at the point before the number of detecting points becomes zero this point can be identified as a global maximum (minimum) point since it is detected by using the largest δ. This point is called a *first-level* landmark. In general, this is the location where the bone has the largest or smallest area, perimeter, or distance from centroid to the reference point. A *second-level* landmark is the point before the number of maximum (minimum) points is changed to the first-level. It is expected to find similar landmarks between the object model and the generic model at the equivalent level of landmark. However, the first-level has the highest confidence in landmark matching while the lower-level (higher number) has less confidence.

The second method to detect landmarks from slice descriptors is using the rate of change of slice descriptors. In this method, the landmarks are detected where the rate of change of slice descriptors is large. Since the slope of the descriptors can be both positive and negative, the lower and upper bounds are set such that the landmarks are defined where the slopes fall outside the bounds. Let γ be the bounds in this case. If *sd* is the slice

descriptor from slice 0 to N, Δsd is the slope between slice i and $i+1$. The condition for the landmark is given by:

$$|\Delta sd| \quad \geq \quad \gamma \qquad\qquad (5)$$

This method is analogous to setting the upper and lower control limits in statistical quality control [4]. The mean (μ) and standard deviation (σ) are computed from the slice descriptors and the lower and upper bounds are set by:

$$\gamma \quad = \quad \mu \pm 3\sigma \qquad\qquad (6)$$

Figure 4.9 illustrates the landmarks that are detected from the rate of change of centroid descriptors and the location of landmarks on the hip joint model.
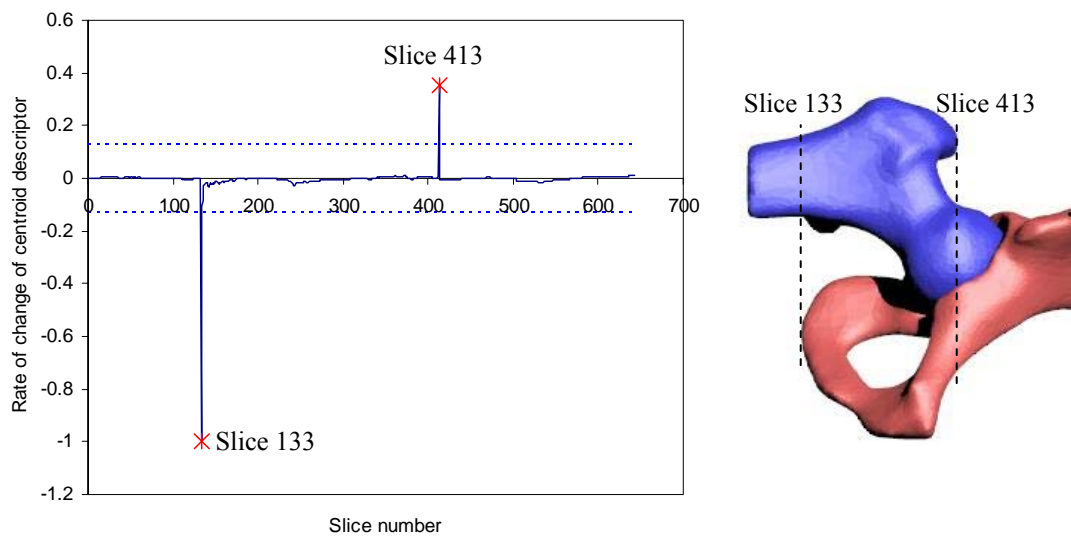
Figure 4.9. Landmarks from rate of change of centroid
descriptor and their locations on the model

The method to locate the corresponding landmarks between sets of slices of object model and generic model were presented in this section. These landmarks divide object and generic models into small sections and corresponding sections are established by related landmarks on the two models. For instance, if a section of the generic model is located

between two landmarks for the area descriptor, the equivalent landmarks on the object model will identify the corresponding section of the object model. An implementation of using this section analysis on the human hip joints is presented later in Section 4.6. In the following section, the methods for contour analysis are presented.

4.5.2. Contour analysis

After the set of slices of object and generic models are divided into several sections by the landmarks, the next task is to determine matches between the contour slices in corresponding sections. The challenge of this matching problem is that the contours on the object slice may contain welded regions which cause its shape and total number to differ from contours of the generic slice (Figure 4.10). However, the method to match the contour slices should be effective even though the welded regions do or do not exist.

(a) Object slice (one contour, due to welding)   (b) Generic slice (two contours)
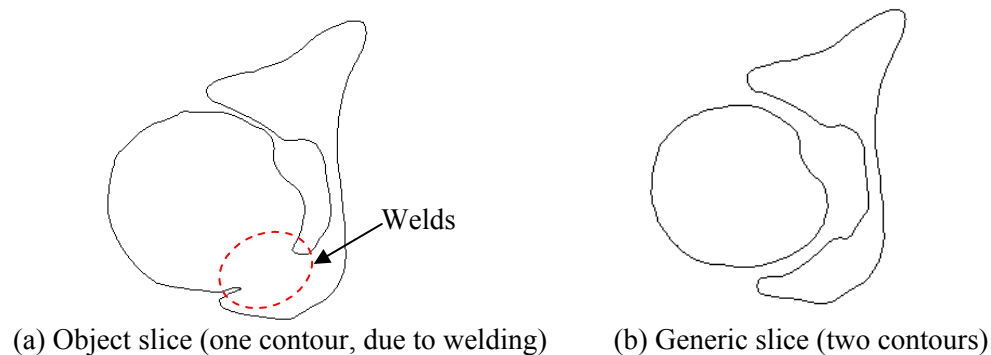
Figure 4.10. Contours between the possible matches

Many previous methods for matching 2D shape [27, 28] are not applicable for the matching problem in this paper since these methods mostly focus on comparing shapes with either a single or equivalent number of contours. The matching method in this paper employs a modification of Attala's method [2]. Generally, the method to match 2D shape

evaluates some features from a shape contour, called *shape descriptors*. Then, descriptors of one shape are compared to descriptors of another shape.

Chang [8] introduced a matching method using Euclidean distance from a center reference point, which is a centroid of the shape, to boundary points as a shape descriptor. Attala adopted a similar method with three shape descriptors: 1) distance from centroid to boundary point, 2) angle between a center line and a line that connects boundary points, and 3) ratio of a line that connects boundary points to the arc of the contour. Attala's method is intended to compare two single contours. Thus, in this paper Attala's method is modified to be suitable for comparing betweens two shapes with multiple contours. The number of contours on these two shapes can be different.
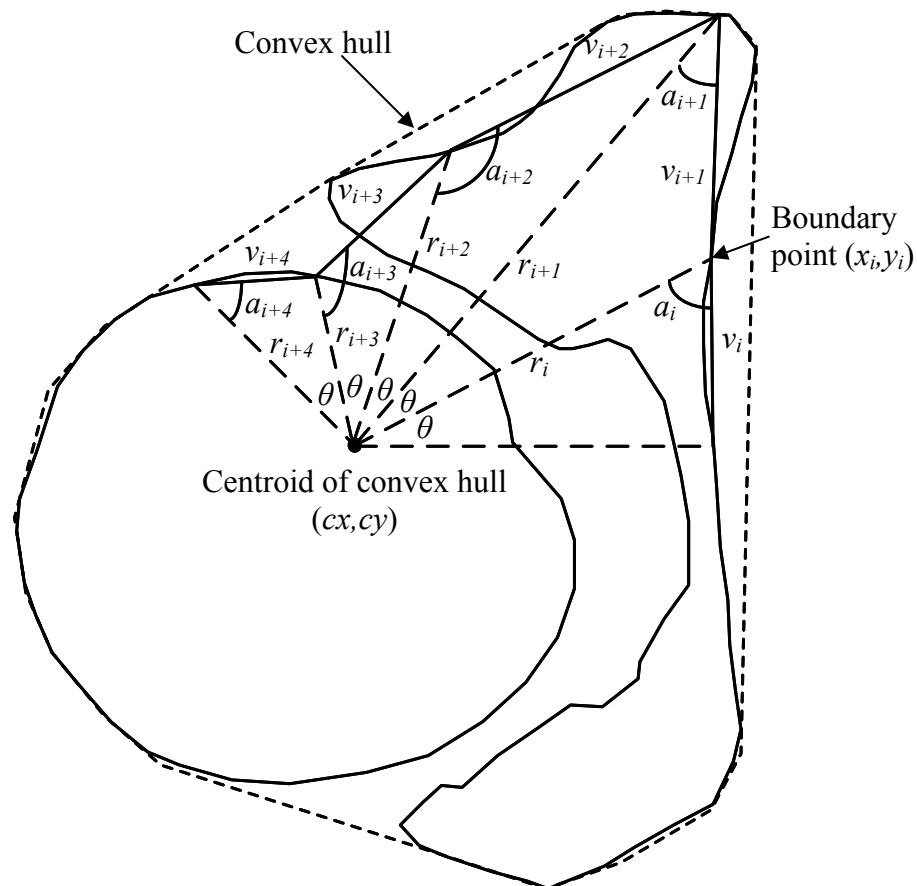
Figure 4.11. Shape descriptors for bone contours: r_i, a_i, and v_i

The matching method in this paper employs the centroid of the convex hull of the slice instead of the centroid of the shape contour. Three shape descriptors are investigated in order to compare contours of the object model to contours of the generic model: 1) distance from the centroid of convex hull to boundary points (r_i), 2) angle between center line and the line that connects boundary points (a_i), and 3) length of the line that connects boundary points (v_i). These shape descriptors are illustrated in Figure 11.

Attala's method obtains boundary points by dividing a contour with an equal space; however, the method is not applicable for multiple contours. The proposed method in this paper computes boundary points by uniformly incrementing an angle of a line extended from the centroid of convex hull to the furthest contour boundary (Figure 4.11). This method is similar to the method proposed by Tan [27]. Let θ be the uniform angle measured in degrees. Then, the number of circular angles (h) is equal to ($360/\theta$). The boundary points are denoted by (x_i, y_i) where i is from 0 to h-1. It should be noted that smaller θ results in finer describing detail of contour; however, as θ gets smaller, it becomes computationally expensive. From Figure 4.12, the shape descriptors (r_i, a_i, and v_i) are given by:
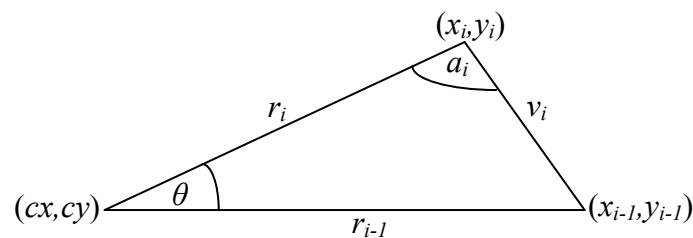
Figure 4.12. Shape descriptors: r_i, a_i, and v_i

$$r_i = \sqrt{(cx - x_i)^2 + (cy - y_i)^2}, \quad i = 0, 1, \ldots, h\text{-}1 \tag{7}$$

$$a_i = \cos^{-1}\left\{\frac{\left[(x_i - x_{i-1})^2 + (y_i - y_{i-1})^2\right] + \left[(cx - x_i)^2 + (cy - y_i)^2\right] - \left[(cx - x_{i-1})^2 + (cy - y_{i-1})^2\right]}{2\sqrt{(x_i - x_{i-1})^2 + (y_i - y_{i-1})^2}\sqrt{(cx - x_i)^2 + (cy - y_i)^2}}\right\}$$

$$a_i = \cos^{-1}\left\{\frac{v_i^2 + r_i^2 - r_{i-1}^2}{2v_i r_i}\right\}, \quad i = 0, 1, \ldots, h\text{-}1 \tag{8}$$

$$v_i = \sqrt{(x_i - x_{i-1})^2 + (y_i - y_{i-1})^2}, \quad i = 0, 1, \ldots, h\text{-}1 \tag{9}$$

Before comparing shape descriptors of the object to generic model contours, the shape descriptors are normalized with respect to their maximum values (to provide a scale-invariant property).

Measurement of similarity in this paper is a way to determine how each shape descriptor of the object model contours differs from the shape descriptor of generic model contours. The sum of squared difference (*SSD*) is employed. A lower *SSD* value indicates more similarity; therefore, if a contour is compared to itself, *SSD* is equal to 0. Let p be the slice number of the object model (for slices 0 to n), and q is the slice number of the generic model (for slices 0 to m). Let h be the total number of circular angles and i is a number from 0 to h-1. Each shape descriptor (r_i, a_i, v_i) is normalized by its maximum values. The normalized shape descriptors of the object model are denoted by ($Nr_{p,i}$, $Na_{p,i}$, $Nv_{p,i}$) while the normalized shape descriptors of the generic model are denoted by ($Nr_{q,i}$, $Na_{q,i}$, $Nv_{q,i}$). The sum of squared difference for each boundary point ($SSD_{p,q,i}$) is computed by:

$$SSD_{p,q,i} = \left\{(Nr_{p,i} - Nr_{q,i})^2 + (Na_{p,i} - Na_{q,i})^2 + (Nv_{p,i} - Nv_{q,i})^2\right\}$$

$$p = 0, 1, \ldots, m \text{ (slices)}, \quad q = 0, 1, \ldots, n \text{ (slices)} \tag{10}$$

The sum of squared difference between the contours on slices of the object model and the contours on slices of the generic model ($SSD_{p,q}$) is given by:

$$SSD_{p,q} = \sum_{i=0}^{h-1} \left\{ (Nr_{p,i} - Nr_{q,i})^2 + (Na_{p,i} - Na_{q,i})^2 + (Nv_{p,i} - Nv_{q,i})^2 \right\}$$

$$\text{or} \qquad SSD_{p,q} = \sum_{i=0}^{h-1} \left(SSD_{p,q,i} \right),$$

$$p = 0, 1, \ldots, m \text{ (slices)}, \quad q = 0, 1, \ldots, n \text{ (slices)} \tag{11}$$

In this paper, finding a match for each slice not only computes *SSD* between compared slices but also considers *SSD* of the neighboring slices. In other words, the proposed method finds the *SSD* between small sections of slices such that not only the shape of contours on the current slice is considered, but also the shape of contours on neighboring slices (Figure 4.13).

——— Current slices being compared
·········· Neighboring slices

(a) Object model   (b) Generic model
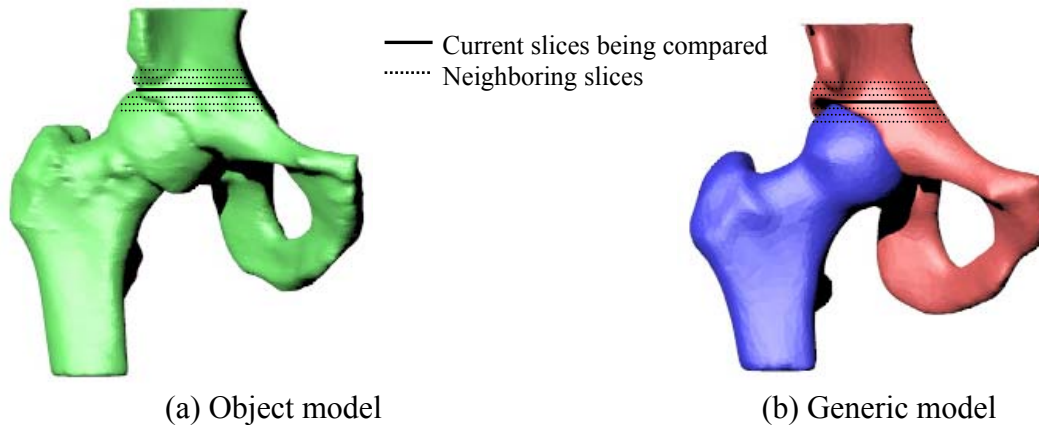
Figure 4.13. Comparing portion of slices ($\beta = 3$)

Let β be the number of neighboring slices that is considered in this comparison. An average *SSD* for the current compared section is denoted by $Avg(SSD_{p,q})$. A match for slice p of object model is defined where $Avg(SSD_{p,q})$ is minimized.

$$Avg(SSD_{p,q}) = \frac{\sum_{p-\beta}^{p+\beta} \sum_{i=0}^{h-1} (SSD_{p,q,i})}{2\beta + 1} \tag{12}$$

This section presented an algorithm for contour analysis and the following section will provide an implementation of both section analysis and contour analysis.

4.6. Implementation

The algorithms for section analysis and contour analysis were implemented in *C++* and graphically displayed using *OpenGL*. To illustrate the implementation of these analyses, two human hip joint models created from CT scans are used. The generic model was manually segmented and reconstructed using reverse engineering software (*Mimics*). The generic model in this paper is only created for illustrating the implementation of algorithms. In practice, the generic model could be created from a *mean shape* of several hip models, a method suggested by Shen [24]. In addition, the generic model could be selected from a library under the same criteria as the object model (e.g. gender, age, height, and etc.). The object model was created directly after conversion from CT scan images. The set of images had 200 slices of 512x512 voxels and its spacing was 2.00mm. Both object model and generic model were sliced with 0.01" (0.254 mm) spacing. Slice descriptors and shape descriptors were computed for sets of slices of the object and generic model. The implementation of section analysis and contour analysis for human hip joint is presented as follows: First, the results of detecting landmarks from slice descriptors are presented. Then, the landmarks are redefined using shape descriptors from contour analysis. In the last step, the method to find the match of each object model slice to generic model slice is presented.

4.6.1. Landmark extraction

A simplified way to illustrate how the landmarks of object model and generic model are detected is by showing a plot of slice descriptors with respect to the slice location (slice

number). Figure 14 illustrate the plots of area, perimeter, and centroid descriptors. The landmarks are detected from the maximum (minimum) point, as presented in Section 4.1 whereby the incremental number (δ) is set to 0.001. The results of the detection and level of landmark are shown in Table 4.1.

Object model			Generic model		
Descriptor	Level	Slice number	Descriptor	Level	Slice number
Area	1	350	Area	1	337
	2	308, 332		2	622, 636
	3	361, 373			
	4	628, 640			
Perimeter	1	347	Perimeter	1	351
	2	608		2	601
	3	315, 332		3	526, 545
	4	645			
Centroid	1	125	Centroid	1	98
	2	394, 445		2	337, 414
	3	590		3	570
	4	427		4	449, 488

Table 4.1. Landmarks from maximum (minimum) descriptors

The plots of rate of change of three slice descriptors are illustrated in Figure 15. The result of landmark detection from this method is shown in Table 2.

Object model		Generic model	
Descriptor	Slice number	Descriptor	Slice number
Area	144, 444	Area	133, 413
Perimeter	144, 444	Perimeter	133, 413
Centroid	144, 444	Centroid	133, 413

Table 4.2. Landmarks from rate of change of descriptors

This implementation only employs landmarks from the first-level since they are the most significant points. Although higher level landmarks were suggested, in practice, they have diminishing returns proportional to level and are not used in the hip model case. As a case for future work, second and higher level landmarks may prove more practical in other joints, for other cases such as patients with deformities, etc. The landmarks that will be used in the next steps are summarized in Table 4.3. The locations of these landmarks on the object and generic models are also illustrated in Figure 4.16.
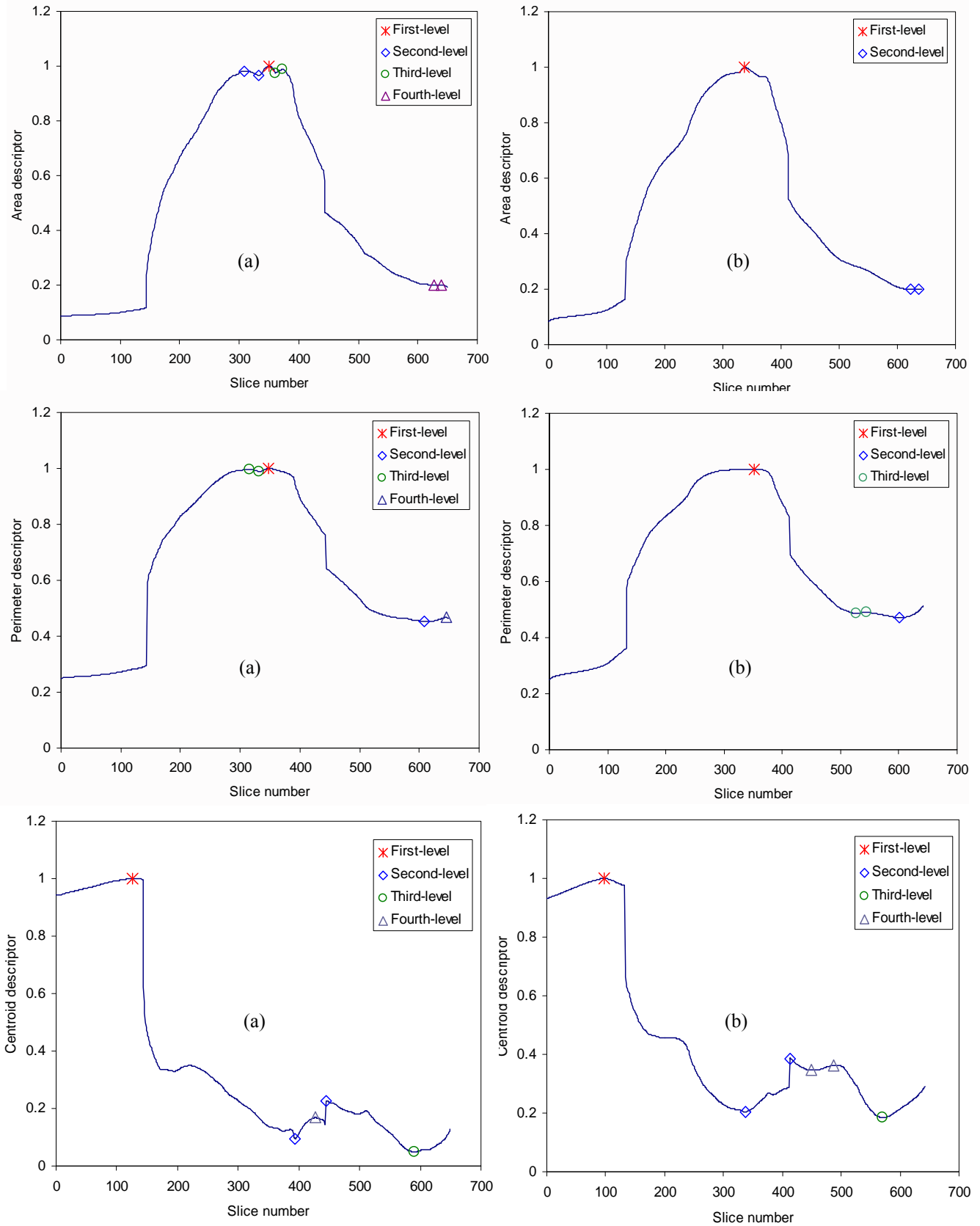
Figure 4.14. Landmarks from slice descriptors: (a) object model, (b) generic model
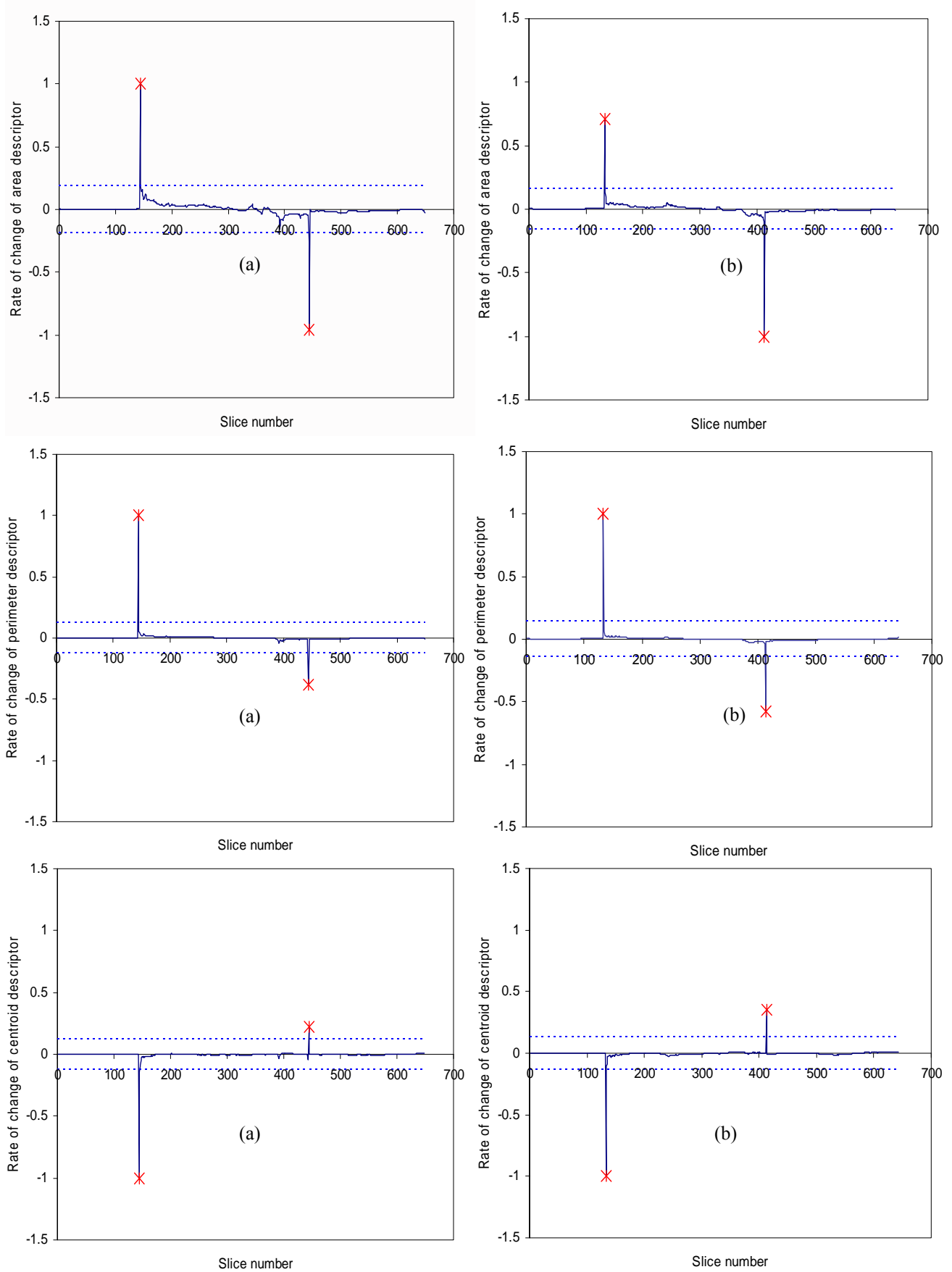
Figure 4.15. Landmarks from rate of change of slice descriptors: (a) Object model, (b) Generic model

Object model		Generic model	
Descriptor	Slice number	Descriptor	Slice number
Centroid	125	Centroid	98
ROC	144	ROC	133
Area	347	Perimeter	337
Perimeter	350	Area	351
ROC	444	ROC	413

ROC = rate of change of descriptors

Table 4.3. Landmarks from section analysis
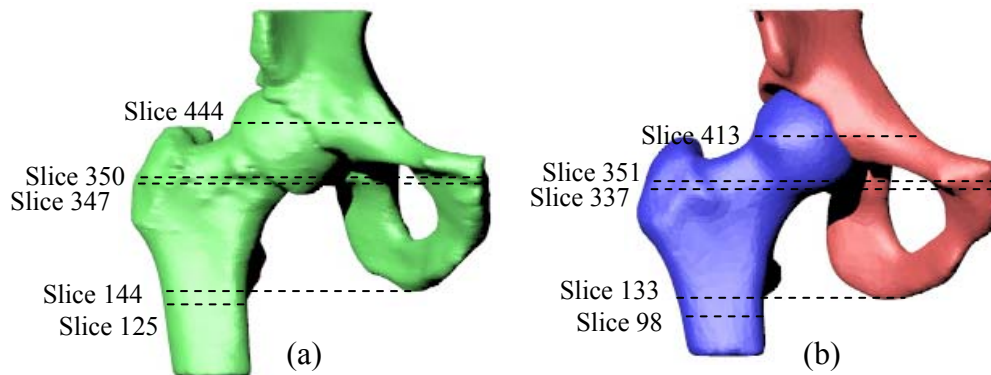
Figure 4.16. Landmark locations on (a) object model and (b) generic model

In this step, one may notice the order of landmarks on the object model differ from the order of landmarks on generic model. The locations of landmarks on the object model will be relocated in the next step.

4.6.2. Redefined landmark

The locations of landmarks in Table 4.3 are not finalized but do serve as the initial landmark locations on both the object model and generic model. To improve these landmark locations, additional methods to match contours in contour analysis are employed. Only locations of landmarks on the object model are adjusted because the contour slices of object model contain welded regions which can be a source of uncertainty of the locations of landmarks. On the other hand, the generic model has contour slices which are deemed error-

free; thus landmarks on the generic model will serve as "*good*" reference locations. It should be noted that landmarks from rate of change of slice descriptors are not redefined since these landmarks locate where the slice descriptors of both models are at the extreme points. The landmarks of the object model after they were redefined are shown in Table 4.4 while the locations of these landmarks are illustrated in Figure 4.17.

Object model		Generic model	
Descriptor	Slice number	Descriptor	Slice number
Centroid	139	Centroid	98
ROC	144	ROC	133
Area	370	Area	337
Perimeter	377	Perimeter	351
ROC	444	ROC	413

ROC = rate of change of descriptors

Table 4.4. Landmarks after adjustment
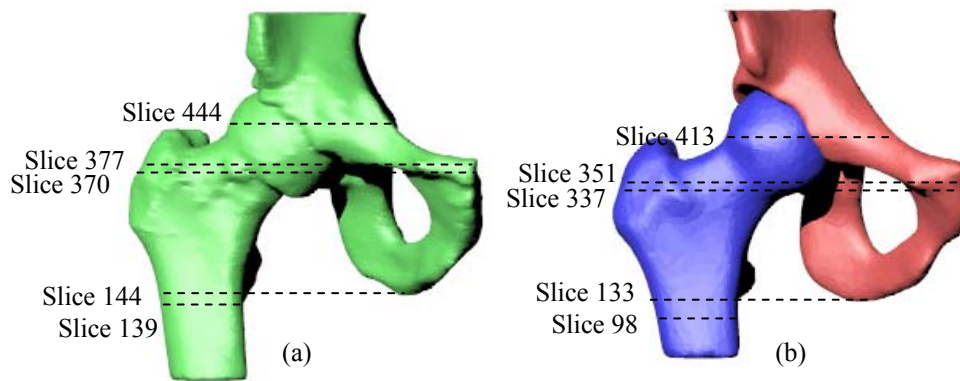
Figure 4.17. Landmark locations after adjustment on (a) object model and
(b) generic model

4.6.3. Contour slice matching

From figure 4.17**,** the landmarks are automatically arranged in correct order after the redefinition process. However, boundaries of the first section and the last section are not defined. For instance, it is obvious that the first section of generic model is much shorter than the first section of object model. The slice contours of the generic model may get

mistaken matches to slice contours of object model in this section. To remove unrelated contours in this section, a similar process as the redefined landmark process is employed. The longer section is first identified by measuring the distance from the first landmark to the first slice of the section. In this case, the section of object model is longer. Then, the slice on the object model that has the same relative distance from the first landmark to the first slice of the generic model is marked as the initial location. The best matches are searched between the first slice of generic model and the slices of object model around the initial location. The same procedure is also applied to the last sections of both models. In this step, the final sections of object model and generic model are obtained. The results are shown in Table 4.5.

Section	Object model	Generic model
1	57-139	0-98
2	140-144	99-133
3	145-370	134-337
4	371-377	338-351
5	378-444	352-413
6	445-649	414-642

Table 4.5. Sections of object model and generic model

The next step is to locate the best matches of slices between the object model and the generic model in corresponding sections. However, these matches need to be in sequential order. For example, in corresponding sections, the first slice of the generic model should not be matched to the slice near the end of section of the object model while the second slice of generic model is matched to the slice near the beginning of the section of the object model. To force the matching in logical order, the method in this paper first finds the middle slice in the corresponding section of object model and generic model (Figure 4.18a). Then, a match of the middle slices is located. Next, this first match is then used as new boundary to divide

each section of two models into smaller sections (Figure 4.18b). The same process is continued until the match for each slice of object model is found (Figure 4.18c).

(a)   (b)   (c)

------- Compared slices
———— Matched slices (borders)
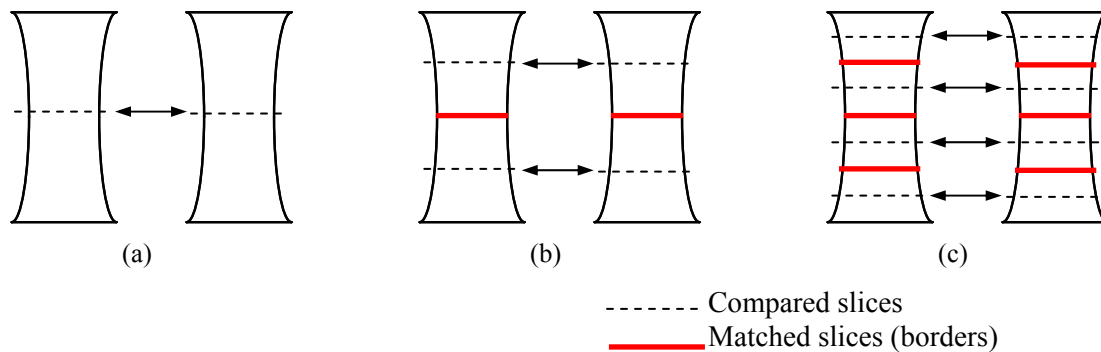
Figure 4.18. Middle slice matching

Figure 4.19 presents a plot of matching slices between slices of object model and slices of generic model. This plot shows a good result of consecutive correspondence.
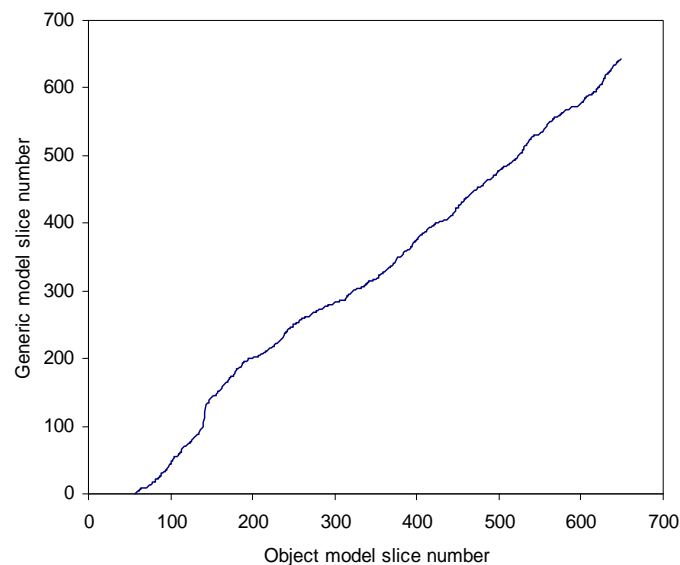
Figure 4.19. Matching results of object model and generic model slices

4.7. Results and Discussion

In order to illustrate the improvement of using section analysis and contour analysis for registering the two sets of slices three registration methods are compared: 1) naive proportion registration, 2) landmark proportion registration, and 3) landmark and contour

registration. Naive proportion registers two set of slices without using section analysis and

contour analysis. The generic model only uses rigid transformation (translation and scale) for

comparing the object model. The naive method linearly divides and matches the slices based

on their locations. Landmark proportion employs only section analysis in the registration

method. This method searches for landmarks between object and generic models and then

uses those landmarks to divide both models into several corresponding sections. However,

only linear matching method is used within the corresponding sections. In the final case, both

landmark and contour registration is completely implemented for both section analysis and

contour analysis. The result of these three registration methods are compared using the

measurement of similarity as described in Section 4.5.2. The results from Table 4.6 show

that using only section analysis can improve average of overall *SSD* from naive registration

while using both section analysis and contour analysis improve both average of overall *SSD*

and also average of *SSD* in the sections.

Section	Naive Registration (SSD)	Landmark registration (SSD)	Landmark and contour registration (SSD)
1	-	5.04	4.66
2	-	69.39	69.12
3	-	40.62	32.59
4	-	11.21	11.16
5	-	15.70	14.58
6	-	15.42	13.58
Total average	31.25	24.01	20.13

Table 4.6. SSD of three registration methods

The sliced model registration process arranges an order of generic slices based on the

corresponding slices between object model and generic model. Some slices of the generic

model may be repeated and some slices may be skipped. The pairs of generic slices and

object slices can be passed to the weld removal process as mentioned in Section 3 in order to fix the welded regions on object slices. The details of this process will be presented in a subsequent paper. Alternatively, the output of sliced model registration process can be sent as feedback to a low-level segmentation process. For 2D segmentation methods such as *active shape contour* and *snake*, the contours of generic slices can be directly used as initial contours for segmenting scan images (CT or MRI images). The centroid of the convex hull of the slice can be a reference location for mapping the contours of generic slices to the image (Figure 4.20).

(a) CT image of hip joint   (b) Modified generic slices over the image
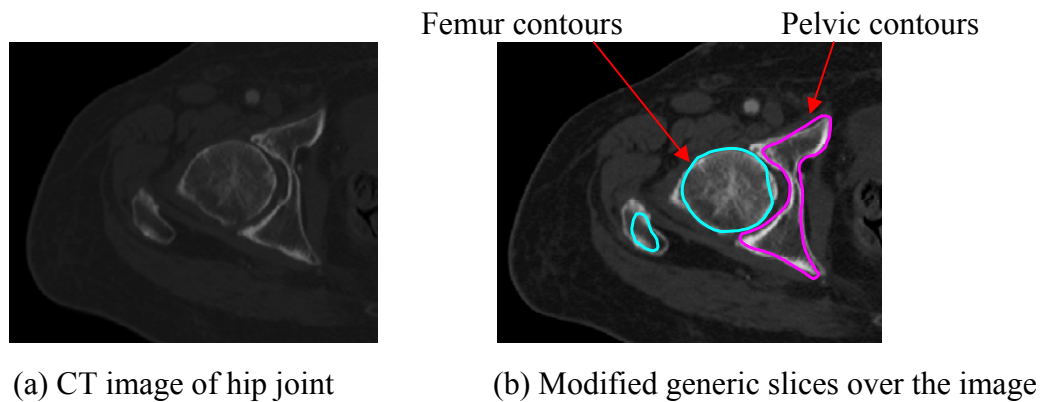
Figure 4.20. Modified generic slices for low-level segmentation

If 3D segmentation is employed such as *active shape model* and *deformable model*, 3D models of individual bones are reconstructed from the set of matching generic slices. Figure 4.21 illustrates a modified generic model that is reconstructed from the set of matching generic slices. A smoothing function could be applied for improving the transition between slices before surface reconstruction. Then, the modified generic model can be used as initial models for segmenting CT images in 3D space.

(a) Object model   (b) Generic model   (c) Modified generic model
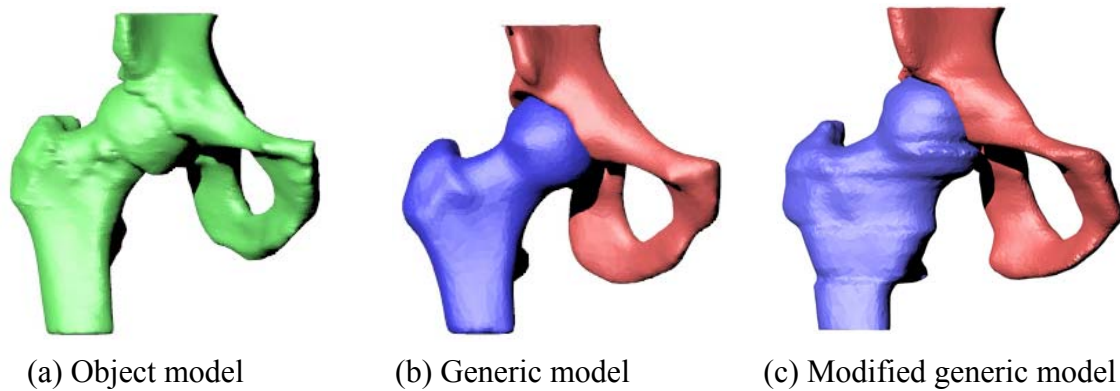
Figure 4.21. Modified generic model for low-level segmentation

4.8. Conclusions and Future work

This paper presented a sliced model registration process which is an important step in developing an automated separation of bone joints for medical images. The proposed method automatically registers the patient's CAD model (object model) to the known CAD model (generic model). The method divides both models into small sections. It first finds the corresponding sections of both models, and then redefines the results by matching slices in related sections. As the implementation showed, the proposed method is more robust than a rigid registration that only uses translation and scale. Output obtained from this registration process can be utilized in a weld removal process which is a process to repair and remove the welds on object model. This output could also be used in low-level segmentation to improve segmentation result of objects in slice images. In addition to registering medical entities, the proposed method might also be applied to measure the similarities of models that lack feature recognition. For instance, it could compare a model from reverse engineering using 3D scanning to its original CAD model, or compare a manufactured component against its known CAD model design.

This paper presents a functional method for dividing the bones of the joint; however, there are several opportunities for future directions. Although the orientation of bones is assumed to be fixed based on the standard medical procedures to obtain the images, performance of the proposed method could be reduced if the angles between the bones in the joint of the object model are different from those of the generic model. Another improvement would be to expand the number of geometric attributes or slice descriptors for other type of joints including knee, elbow, and ankle; as each type of joint may respond to different slice descriptors.

4.9. References

[1] Andrew, A.M., "Another Efficient Algorithm for Convex Hulls in Two Dimensions", Information Processing Letters, Vol. 9, pp. 216-219, 1979

[2] Attalla, E., and Siy, P., "Robust shape similarity retrieval based on contour segmentation polygonal multiresolution and elastic matching", Pattern Recognition Society, Vol. 38, pp. 2229-2241, 2005

[3] Audette, M.A., Ferrie F.P., and Peters T.M., "An algorithmic overview of surface registration techniques for medical imaging", Medical Image Analysis, Vol. 4, pp. 201-217, 2000

[4] Barnes, J.W., "Statistical Analysis for Engineers and Scientists: A Computer-Based Approach", McGraw-Hill, 1994

[5] Bohm, G., Knoll, C., Colomer, V.G., Alcaniz-Raya, M., and Albalat, S., "Three-dimensional segmentation of bone structures in CT images", SPIE Conference on Image Processing, Vol. 3661, pp. 277-286, 1999

[6] Bourke, P.D., WASP, M024, University of Western Australia, 35 Stirling Hwy, Crawley, WA 6009, Australia, 1988, Available at: http://local.wasp.uwa.edu.au/~pbourke/geometry, Access: November, 2008

[7] Chand, B.M., and Kapur, S.S., "An algorithm for convex polytopes, Journal of the ACM, Vol 17, pp. 78-86, 1970

[8] Chang, C.C., Hwang, M.S., and Bueher, D.J., "A Shape Recognition Scheme Based on Relative Distance of Feature Points from the Centroid", Pattern Recognition, Vol. 24, no. 11, pp. 1053-1063, 1991

[9] Cootes, T.F., Hill, A., Taylor, C.J., and Haslam, J., "The Use of Active Shape Models For Locating Structures in Medical Images", Image and Vision Computing, Vol. 12, no. 6, pp. 355-366, 1994

[10] Graham, R.L., "An Efficient Algorithm for Determining the Convex Hull of a Finite Planar Set", Information Processing Letters, Vol. 1, no. 4, pp. 132-133, 1972

[11] Heo, H., and Chae, O.S., "Segmentation of tooth in CT images for the 3D reconstruction of teeth", Proc. of SPIE, Vol. 5298, pp. 455-466, 2004

[12] Jeong, J., Kim, K., Park, H., and Jung, M., "A New Method for Solving Branching Problems in Surface Reconstruction", International Journal of Advanced Manufacturing Technology, Vol. 16, pp. 259-264, 2000

[13] Josephson, K., Ericsson, A., and Karlsson, J., "Segmentation of Medical Images Using Three-Dimensional Active Shape Models", Lecture Notes in Computer Science, Vol. 3540, pp. 719-728, 2005

[14] Kass, M., Witkin, A., and Terzopoulos, D., "Snakes: Active contour models", International Journal of Computer Vision, Vol. 1, pp. 321-331, 1988

[15] McInerney T., and Terzopoulos D., "Deformable Models in Medical Image Analysis", Proceedings of MMBIA'1996, Toronto, Canada, pp. 171-180, 1996

[16] Minns, R.J., Bibb, R., Banks, R., and Sutton, R.A., "The use of a reconstructed three-dimensional solid model from CT to aid the surgical management of a total knee arthroplasty: a case study", Medical Engineering & Physics, Vol. 25, pp. 523-526, 2003

[17] Pardo, X.M., Carreira, M.J., Mosquera, A., and Cabello, D., "A snake for CT image segmentation integrating region and edge information", Image and Vision Computing, Vol. 19, pp. 461-475, 2001

[18] Parker, J.R., "Algorithms for image processing and computer vision", John Wiley & Sons, Inc., New York, 1997

[19] Pham, D.T., and Gault, R.S., "A comparison of rapid prototyping technologies", International Journal of Machine Tools & Manufacture, Vol. 38, pp. 1257-1287, 1998

[20] Pitas, I., "Digital Image Processing Algorithms and Applications", John Wiley & Sons, Inc., New York, 2000

[21] Preparata, D.F., and Hong, S.J., "Convex Hulls of Finite Sets of Points in Two and Three Dimensions", Comm. ACM, Vol. 20, pp. 87-93, 1977

[22] Preparata, D.F., and Shamos, M., "Computational Geometry: An Introduction", Springer Verlag, New York, 1985

[23] Ryu, J.H., Kim, H.S., and Lee, K.H., "Contour-based algorithms for generating 3D CAD models from medical images", International Journal of Advanced Manufacturing Technology, Vol. 24, pp. 112-119, 2004

[24] Shen, H., Shi, Y., and Peng, Z., "Applying Prior Knowledge in the Segmentation of 3D Complex Anatomic Structures, Lecture Notes in Computer Science, Vol. 3765, pp. 189-199, 2005

[25] Sun, W., Starly, B., Nam, J. and Darling, A., "Bio-CAD Modeling and Its Applications in Computer-Aided Tissue Engineering", Computer-Aided Design, Vol. 37, pp. 1097-1114, 2005

[26] Suzuki, M.T., Kato, T., and Otsu, K., "A Similarity Retrieval of 3D Polygonal Models Using Rotation Invariant Shape Descriptors", Proceedings of the IEEE International Conference on Systems, Man and Cybernetics, Vol. 4, pp. 2946-2952, 2000

[27] Tan, K.L., OOI, B.C., and Thiand, L.F., "Retrieving Similar Shapes Effectively and Efficiently", Multimedia Tools and Applications, Vol. 19, pp. 111-134, 2003

[28] Zhang, D., and Lu, G., "Review of shape representation and description techniques", Pattern Recognition, Vol. 37, pp. 1-19, 2004

CHAPTER 5. AUTOMATED SEPARATION OF BONE JOINT STRUCTURES FOR MEDICAL IMAGE RECONSTRUCTION – PART II: A METHODOLOGY FOR MODEL SEPARATION

Wutthigrai Boonsuk and Matthew C. Frank

5.1. Abstract

The separation of a reconstructed bone model in the joint area is a challenging task, due to surrounding soft tissue and adjacent bones which can make bone boundaries ambiguous. Traditional image segmentation may not provide proper bone boundaries, resulting in an inadvertently combined model that has the bones of a joint merged after the reconstruction process. To avoid this problem, manual modification from medical experts is necessary to correct improper results of segmentation before the joint model is reconstructed. However, this manual task is time consuming, laborious, and unrepeatable. This paper proposes a methodology to automatically separate bones in the joint area by incorporating a *generic* model as a surrogate for the anatomical knowledge of experts. This model represents a standard CAD model that has all bones of the joint properly separated. The *object* model is the CAD model of the joint which is directly reconstructed from the segmentation results of the patient's CT images. Initially, the model directly from the patient is allowed to be combined; as traditional segmentation methods will still be employed. When the bones of the joint are joined due to these errors, we will refer to the regions of object model where the bones are combined as *welded regions*. The method developed in this paper first registers a generic model and object model; then, welded regions are detected and removed from the object model based on comparisons from the object model to the standard generic model.

The repaired results will be called *hybrid* contours or a hybrid model since it will be a combination of the object model and selected portions of the generic model (areas that were lost on the object model due to welding). An implementation of the methods shows how the reconstructed model using hybrid results shows improvement in approximating the object automatically from CT images. Since the proposed method is rapid and robust, the hybrid results can also be used as feedback to the original low level segmentation process to avoid the occurrence of welding altogether.

5.2. Introduction

Image segmentation and surface reconstruction are the two major process steps used to generate CAD models from 3D medical images such as computed tomography (CT) or magnetic resonance imaging (MRI). The images are first segmented in order to separate the object of interest (bone) from image background (soft tissue, etc.). The results of segmentation are used in the subsequent reconstruction process to create a CAD model. Figure 5.1 illustrates the most basic steps of the process.

| Medical Images | → | Image Segmentation | → | Surface Reconstruction | → | CAD Model |
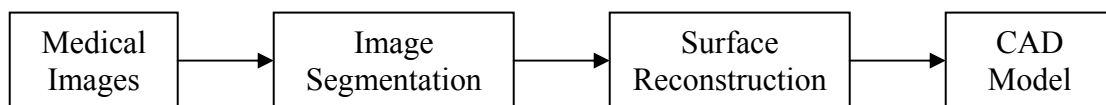
Figure 5.1. Steps for creating CAD model from medical images

CAD models from medical images are used broadly in both medical and non-medical applications, from diagnostic to surgery planning to animation and biomedical manufacturing of implants and prostheses. One major challenge in creating the CAD models is that a

skilled technician is needed when segmenting the bone joints; one must know which bones constitute the joint and where they interface. However, in this research we will assume the experts are not available in the process; hence since we wish to completely automate the process within software. To this end, computer algorithms are proposed to substitute the expert's task and generic models of the bone joint are used to substitute that expert's knowledge of the anatomy.

Segmentation can be classified into two levels: *low-level* segmentation and *high-level* segmentation [2]. Low-level segmentation refers to a process that detects and retrieves important features from the images and translates them into explicit data. This level of segmentation commonly serves as the beginning step of overall segmentation process. Selecting threshold density values, for instance, can separate bones from image background. However, the results from this level of segmentation are not adequate for properly reconstructing complex structures. For example, reconstructing bones in joint areas is not easy because the surrounding soft tissues and adjacent bones are likely to have similar grey scale. Low-level segmentation may fail to identify the proper boundaries of the bones. In addition, although the bone boundaries are well defined, the model still cannot be created correctly because the reconstruction process requires appropriate topological data to reconstruct individual bones. The problems are addressed in [1, 14, 21] as the correspondence problem and the branching problem. Many researchers attempted to solve these problems [14, 3, 6, 21] but the solution is only suitable for reconstructing one bone at a time; the remaining bones must be manually excluded before reconstruction process. Without manual operation, the finished model is a combined model of individual bones. Figure 5.2a illustrates a model of a hip joint where the femur and pelvis are combined after

the model is reconstructed from low-level segmentation results. In this paper, the area where the bones are combined will be referred as *welded regions* since it looks similar to a weld in metal joining operations.
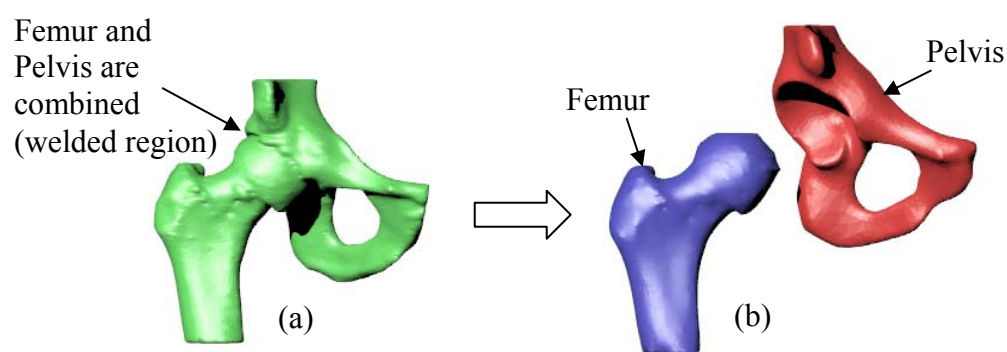
Figure 5.2. Low-level segmentation and high-level segmentation: (a) hip joint after low-level segmentation and (b) hip joint after high-level segmentation

High-level segmentation is essential to fixing this weld problem. This level of segmentation repairs faulty boundaries of individual bones and provides topological data for proper reconstruction. Usually, this high-level segmentation is conducted by experts who will inspect the slice images and manually correct the results of low-level segmentation. The steps of high-level segmentation can be illustrated in Figure 5.3. The CT image of the hip joint (Figure 5.3a) is first segmented using low-level segmentation. The results of low-level segmentation have femur and pelvis contours combined (welded regions) as shown in Figure 5.3b. High-level segmentation is manually performed to repair the welded regions, and assign the contours to individual bones (Figure 5.3c and 5.3d). This manual approach is tedious and time consuming because the modification must be repeated for hundreds of slice images. The results are also non-repeatable since they are based on user skill and judgment.
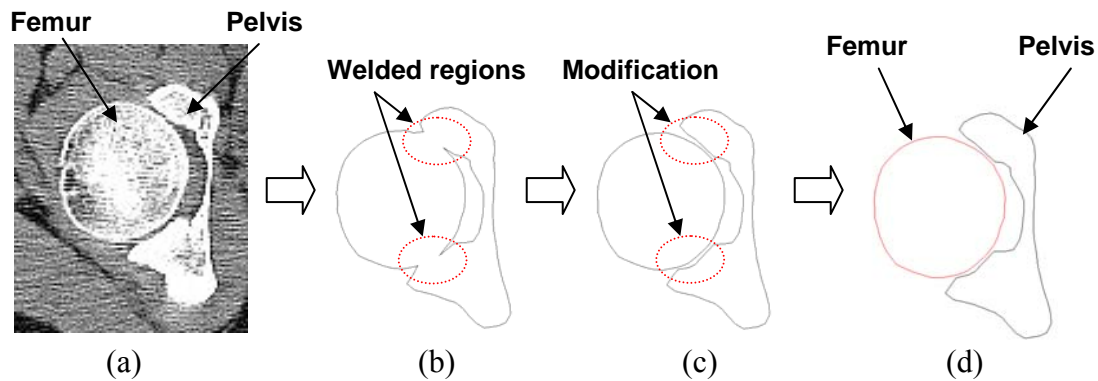
Figure 5.3. Steps of high-level segmentation: (a) CT image of hip joint, (b)
contour after low-level segmentation, (c) high-level segmentation
by manual modification, (d) contours after high-level segmentation

This paper proposes a method that employs a *generic* model as anatomical knowledge

of the expert. The generic model is a complete CAD model that has all bones separate and

closely represents the object of interest in the patient's scan data. From patient's data, the

CAD model is reconstructed using a low-level segmentation approach. This patient's model

is called the *object* model and will be utilized to compare to the generic model. The method

first allows the object model to contain welded regions, later removes the welds, providing

separated individual bones. The framework of this approach is illustrated in Figure 5.4.

For this method, registration between the object model and generic model is first

obtained so that the two models can be compared. The methods for registration had been

proposed in previous work. It is assumed that the registration process was completed and the

results of registration will be further used to repair welded regions. The goal of this paper is

to separate and repair the bone boundaries where the welded regions occur. The contents of

this paper will be organized as follows. Related literature is reviewed in the next section and

an overview of the solution methodology is presented in Section 5.4. The methods to remove

and repair welded regions are proposed in Section 5.5 and 5.6. The implementation and results are shown in Section 5.7 and finally, conclusion and future work are presented.
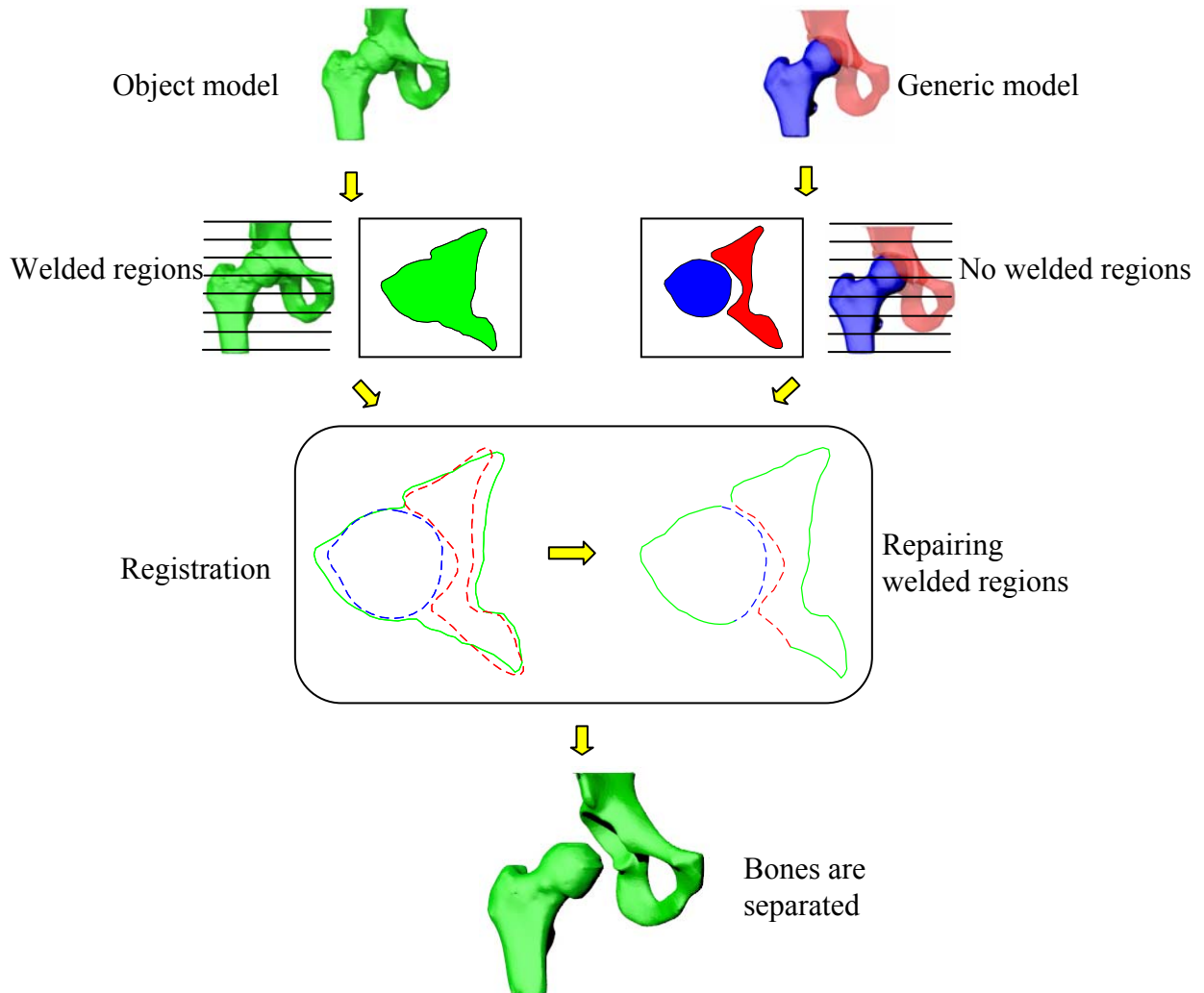
Figure 5.4. General steps in the proposed methodology

5.3. Related Work

Segmentation is intended to extract the object of interest from medical images and has been a subject of research for decades; however, the automated segmentation of bone joints has not been sufficiently developed. Traditional techniques using low-level segmentation approaches such as *thresholding*, *edge detection*, *region growing,* and

morphology operation [15, 18] usually give mistaken results where the grey scales of adjacent structures (bones and soft tissues) are similar. Westin [26] introduced an adaptive filter for enhancing boundaries of adjacent bones; however the method works well only when the gap between the bones is noticeable. Often, medical experts manually correct the boundaries of the bones; however, manual editing cannot be utilized in a truly automated system. Although adjacent bone boundaries may be detectable to human vision, replacing the perception of human vision with computer programs or mathematical processes is still challenging.

Since traditional techniques are not sufficient to identify proper edges of bones in joint areas, knowledge-based techniques have been adopted to improve the results of segmentation. These techniques include snake, *deformable contour*, *active shape contour*, *deformable model*, and *active shape model* [8, 4, 10, 7]. The methods add prior knowledge such as shape constraints in order to segment images. The constraints ranged from numerical solutions to statistical solutions in order to control the deformation of initial 2D contour or initial 3D model. The weakness of these methods is that the results of segmentation are sensitive to the initial position of the contour or model within the medical images. For bone joints, the position of the contour or model is critical since the spaces between adjacent bones are relatively small and misaligned position can cause unpredictable results. In addition, this alignment step is still manually adjusted by an expert. Heo [5] and Pardo [13] recommended using contours from previous image slices as initial contours for 2D segmentation; however, a solution for changes in topology was not addressed. In bone joints, not only the number of contours can be different, but also the type of bones can change between slices.

Several methods for bone joint segmentation have been developed for specific type of bones. Zoroofi [27] proposed the *moving disk* technique to search for boundaries of the bones. The method required the initial center location of the bone; however, automated selection of this location was not addressed. Shen [22] not only employed a 3D model as prior knowledge but also included features such as abrupt edges and ridges for segmentation. His initial shape was not easy to develop and it needed to be generated for individual types of joints. Liu [9] presented segmentation of the bone joint using a rigid 3D model as prior knowledge. This work focused on using the model created from the first set of images to subsequently segment the same bone which had different position and orientation. The variation of the bone among each person may cause an uncertainty.

In this paper, high-level segmentation is achieved by employing a CAD model of the bone joint (generic model) as prior knowledge. However, the proposed method does not utilize this model for segmenting images. This generic model is compared to a CAD model (object model) that was initially reconstructed from patient's images. The object model may contain welded regions which have two or more bones combine in joint area. This paper will focus on a method to repair these welded regions. The main idea is to utilize some parts of the generic model to fix the welded regions. This idea is analogous to fixing bad pixels of one image by good pixels of a similar image. Several researches applied this idea for repairing incomplete data, such as Pauly [16], who proposed a method to fill missing surfaces of a 3D model with surfaces of prior shapes. The results showed an advantage over interpolation of end points to fill the missing surfaces. Rakshe [19] proposed a method to reconstruct incomplete contours of an arterial centerline by using the estimated contour from several sets in a database.

In this paper, the method involves firstly removing the welded regions from the object model. Then, the removed contour sections are replaced by the shapes of the generic model.

5.4. Overview of Methodology

In this section, an overview of the general solution methodology involving generic models for high-level segmentation is presented. The generic model is given a similar orientation and scale as the object model which retains the same position of the object from its CT images. The generic model could be created by finding a mean shape from several set of CT images as the method was suggested by Shen [22]. In addition, a library of generic models may be used to provide a closer approximated model by sorting on several criteria such as gender, age, height, and ethnicity.

The purpose of using *object* model is to reduce the complexity and numerous data contained in the CT images with a 3D model that can be sliced into polygonal contours. Starly [23] describes the steps to reconstruct a CAD model from CT images and in this paper, the object model is obtained without expertise using known low-level segmentation and reconstruction tasks. Once the CAD models are created, they are sliced in order to simplify the geometric complexity. A slice representation is very common for rapid prototyping processes [17] in representing freeform objects for a similar reason; in the case of RP, it reduces the tasks involved in process planning. Both the object model and generic model are cut into this series of slices along the same oriented direction. Each slice of the models contains 2D polygonal contours (cross sections) of one or more bones. From the fact that the object model is created from image slices, if the object model is sliced at increments equal or

smaller than the thickness of image, the set of slices should be adequate in representing the objects scanned in the medical imaging process. The benefit of using a slice representation is that the complex 3D surfaces of welded regions are transformed into simple 2D polygon contours where two or more contours from different bones are inadvertently combined (Figure 5.5).
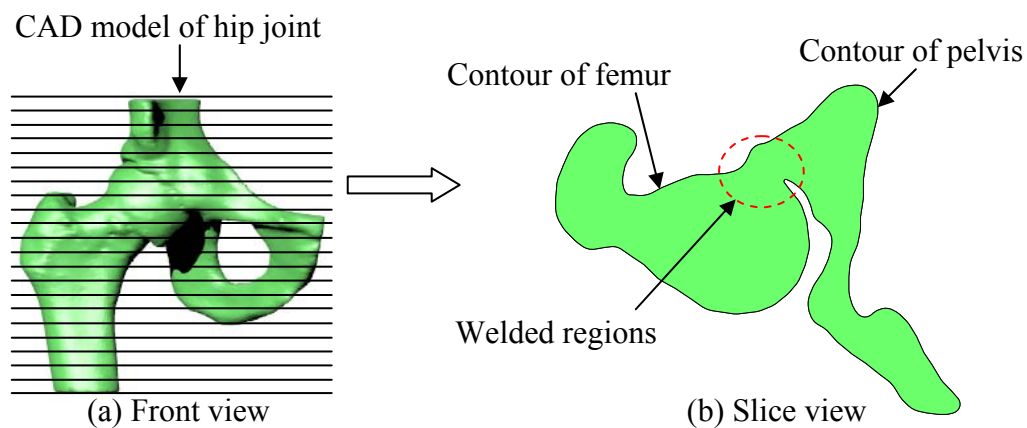
Figure 5.5. Slice of object model of hip joint

A schematic of the overall process for bone joint separation in high-level segmentation is illustrated in Figure 5.6. S*liced model registration* and *weld removal* are proposed as two automated processes for high-level segmentation. Sliced model registration is first used in order to align sets of slices between the object and generic models. Two analyses are employed within the sliced model registration process: 1) *section analysis* and 2) *contour analysis*. The purpose of these analyses is to find the slice of the generic model that most closely represents the slice of the object model.
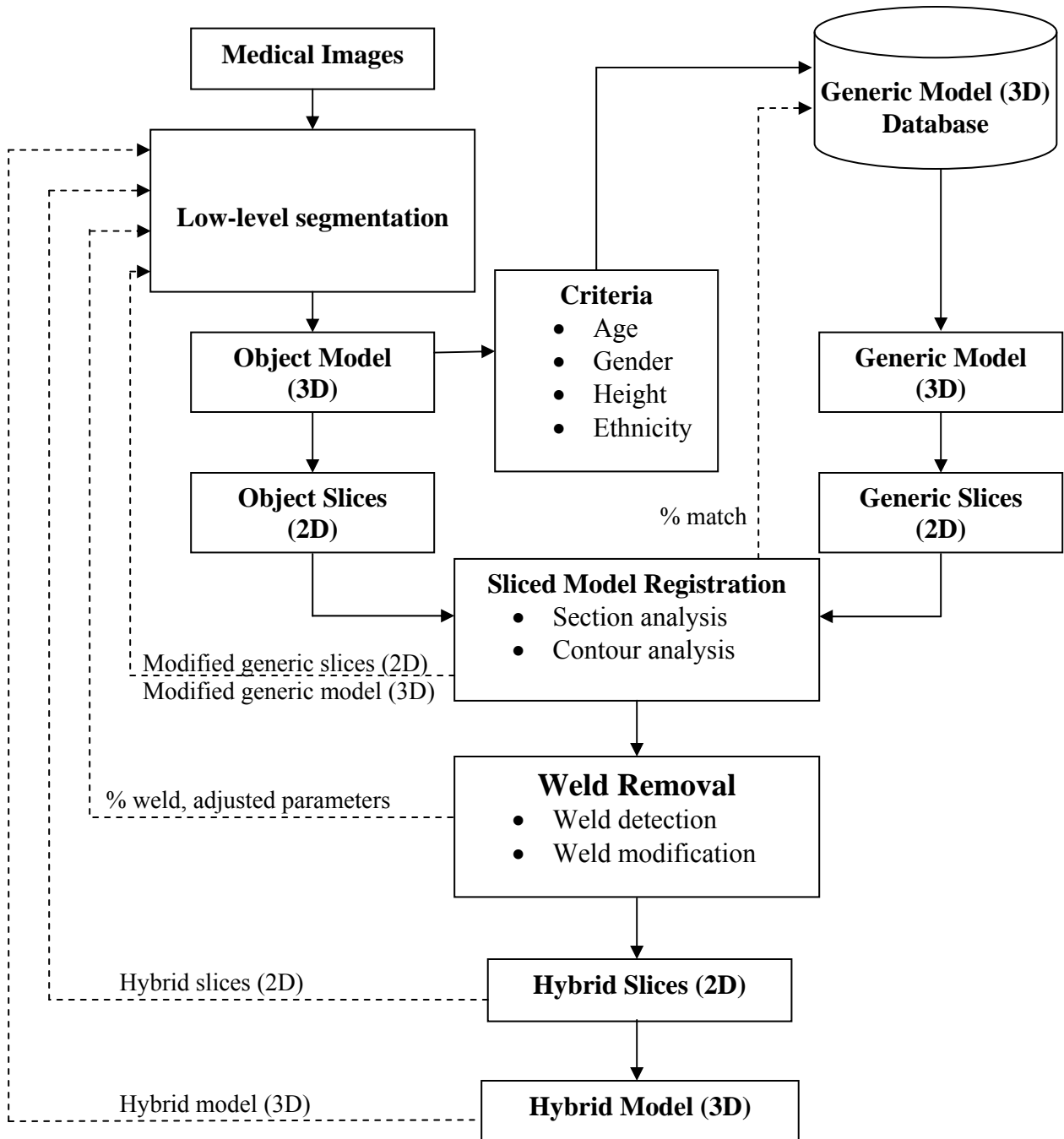
Figure 5.6. Process steps for automated system in high-level segmentation

Section analysis serves as a coarse registration process that divides the slices of the

two models into several corresponding sections. The registration results are refined within

the subsequent process, contour analysis, which identifies closest pairs of slices in corresponding sections. Two feedback items are generated from the registration process: 1) *match percentage* and 2) *modified generic slices* or a *modified generic model*. The first feedback, match percentage, is the measurement of similarity between the object and generic models. This feedback could be iterated in order to search for the best generic model from a database that closely approximates the object model. The second feedback, modified generic slices or a modified generic model, are generated from the output of sliced model registration process. This feedback can be sent to low-level segmentation in order to improve the results of segmentation in a second or subsequent iteration. The modified generic slices could be utilized as initial contours for 2D segmentation, and similarly, the 3D model can be reconstructed and used for 3D segmentation. Several existing methods found in the literature could be improved upon using this form of iterative feedback (i.e.: *active shape contour, deformable contour*, *active shape model*, *deformable model*, etc.).

In this paper, it is proposed that the registration process results can be used in the high level process of separating the bones of the joint by removing the welded sections of the object model. However, the areas where the welds are removed need to be repaired before the separated model is reconstructed. This paper proposes weld detection and weld modification as two steps in the weld removal process. Weld *detection* utilizes the results of sliced model registration to evaluate if the slices of the object model contain welded regions. Weld *modification* then uses the contours of the corresponding generic slice to restore the proper shapes of the contour on the object slice. In this manner, a hybrid contour is formed, which is actually a combination of the original object contour minus the welded region and the replacement portion from the generic contour (Figure 5.7). One feedback from the weld

removal process, a *percentage of weld* perimeters, can be indirectly used to minimize the size of the welded regions created on the object model. That is, some parameters during low-level segmentation such as thresholding values, filtering parameters, and morphological parameters could be adjusted based on the percentage of welds that is detected in this subsequent process. The output of weld removal process is the *hybrid slices* that have all contours of individual bones separated and assigned. At this point, the process could be halted and the models of the individual bones (*hybrid models*) could be reconstructed. Alternatively, the outputs (hybrid slices or hybrid models) could be used as initial contours or initial models within existing low-level segmentation processes from the literature.

(a) Object contour   (b) Generic contour   (c) Hybrid contour
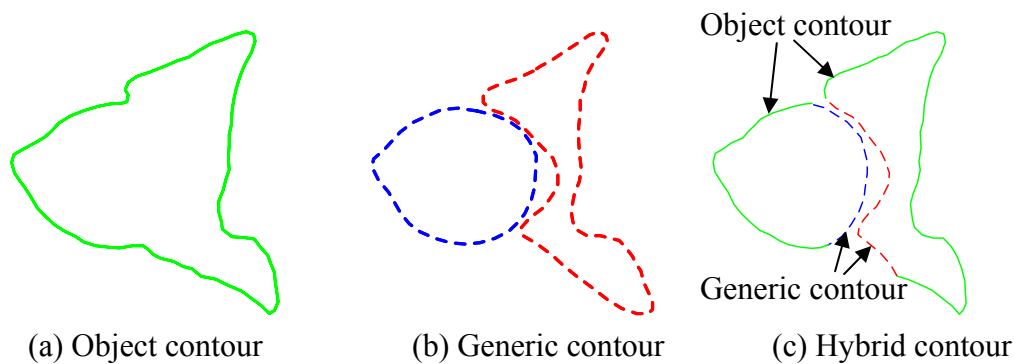
Figure 5.7. Weld modification

The scope of this paper is focused on the weld removal process; therefore, the sliced model registration process is assumed to be completed and available for use in weld removal. Next, sections 5.5 and 5.6 will present the details of the two major processes of weld removal: 1) weld detection and 2) weld modification.

5.5. Weld Detection

Weld detection refers to a process that verifies if there are welded regions on the object slice, and locates them by comparing to the corresponding generic slice. Since each contour of generic slice is already assigned to individual bones, this information can be used to recognize contours of the object slice. At the beginning of the process, a transformation is executed to align the generic and object slices. This transformation, $T(\ )$, is a translation and scale in the xy plane (2D). The generic slice (G) is transformed to $\widetilde{G}$ and is defined as:

$$\widetilde{G}(\widetilde{x}, \widetilde{y}) = T\big(G(x, y)\big) \text{ where } (x, y) \text{ and } (\widetilde{x}, \widetilde{y}) \in \mathrm{R}^2 \tag{1}$$

The point (x,y) of a generic slice is translated the distance between the centroid of the convex hull of both slices $(\Delta c_x, \Delta c_y)$. Then, this translated point is uniformly scaled relative to the centroid (c_x, c_y) by factor S.

$$\begin{bmatrix} \widetilde{x} \\ \widetilde{y} \\ 1 \end{bmatrix} = \begin{bmatrix} S & 0 & c_x(1-S) \\ 0 & S & c_y(1-S) \\ 0 & 0 & 1 \end{bmatrix} \begin{bmatrix} 1 & 0 & \Delta c_x \\ 0 & 1 & \Delta c_y \\ 0 & 0 & 1 \end{bmatrix} \begin{bmatrix} x \\ y \\ 1 \end{bmatrix} \tag{2}$$

The uniform scale S is computed by iterating a small number to minimize the difference of area between convex hull of generic slice (CH_G) and convex hull of object slice (CH_O).

$$MIN \quad \{\ |\ Area(CH_G) - Area(CH_O)|\ \} \tag{3}$$

The initial alignment step is illustrated in Figure 5.8 where a generic slice is transformed to fit the object slice. As shown in Figure 5.8, a convex hull polygon is employed in this alignment because the contours on the object slice and generic slice can be dissimilar where the welded regions appear but the convex hulls of either slices will not be affected by welding.
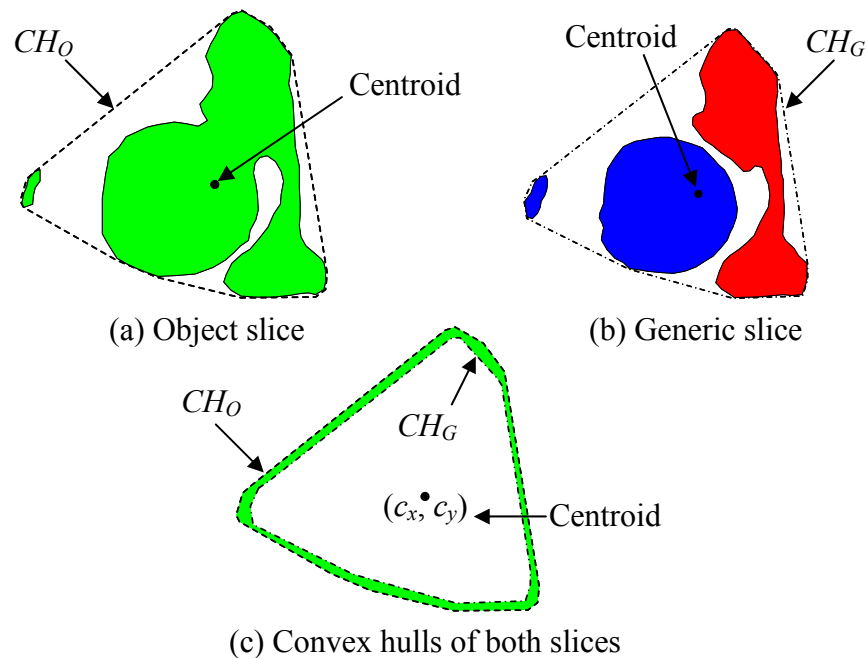
Figure 5.8. Aligning slices using convex hulls of both the generic
slice (CH_G) and object slice (CH_O)

After the alignment step, the proposed method detects the welded regions in two
levels: 1) contour level and 2) vertex level. Within the contour level, the method identifies if
any contours on the object slice contain welded regions. This level of detection serves as a
coarse evaluation step. If there are welded regions on the slice, then the locations of welded
regions are further analyzed at the vertex level.

5.5.1. Contour level

The intersections of generic contours and object contours are computed to evaluate if
there are welded regions. Since generic contours have been assigned to individual bones, if
one object contour intersects two or more generic contours that belong to different bones, this
object contour contains welded regions. Contours of the generic slice (P) and object slice (Q)
are given by:

$$P = \begin{Bmatrix} P_{11}, P_{12}, ... \\ P_{21}, P_{22}, ... \\ P_{n1}, P_{n2}, ... \end{Bmatrix} \quad \text{where different types of bones are listed in row } (1, 2, ..., n)$$

$Q = \{Q_1, Q_2, ... Q_m\}$ where m = total number of contours

The intersections of contours on P and Q are computed. The welded regions are identified when

$P_{ai} \cap Q_k$ and $P_{bj} \cap Q_k$ if $a \neq b$, then Q_k contains welded regions

(a) Object contour   (b) Generic contour   (c) Contour intersection
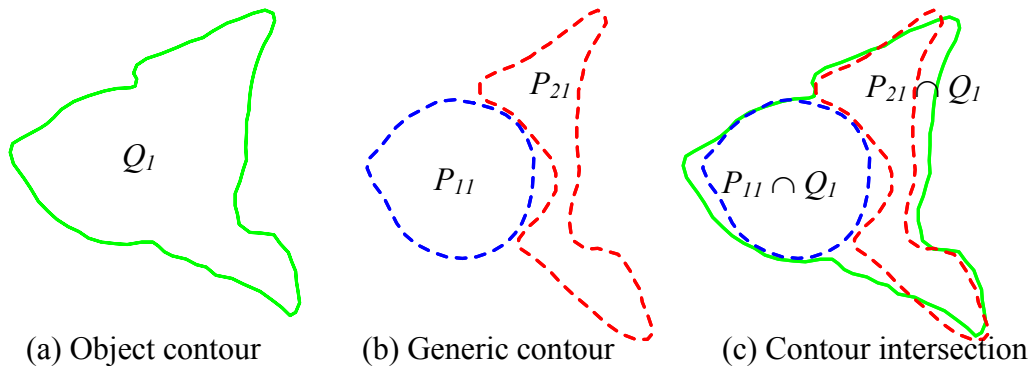
Figure 5.9. Contour intersection: Q_1 contains welded regions

Figure 5.9 illustrates the object slice that contains the welded regions. On the other hand, if Q_k intersects contours of P that are listed on the same row (same types of bones), Q_k can be classified to the bones on that row. For example

$P_{ai} \cap Q_k$ if only row a intersects, then $Q_k = Q_{ak}$

There is a possible case where a contour of the object slice does not intersect with any contours of the generic slice. This case (Figure 5.10) may occur where a bone end is reached or a new bone appears along the slice axis. From Figure 5.10a, Q_2 cannot identify with any contours of the generic slice (P_{11} and P_{21}). Since the transition of contours between object slices is generally consistent, the problem can be handled by intersecting the unidentified

contour with identified contours on a previous object slice or the next object slice (Figure 5.10b).

(a) Intersection between object contour (Q) and generic contour (P)

(b) Intersection between object contour (Q) and object contour on the next slice
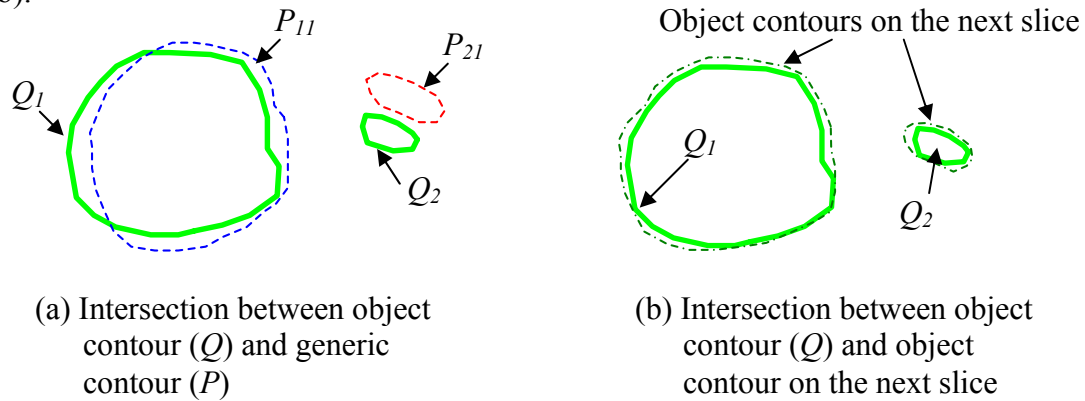
Figure 5.10. Intersection error between object contour and generic contour

Once welded regions on the object contours are identified, the location of welded regions are further analyzed at the vertex level.

5.5.2. Vertex level

At the vertex level, the method first focuses on regions of the object contour that can result in welds, and then identifies each vertex in that region for separating the contour into individual bones. The corresponding generic contours are generally used for identifying the vertices of the object contour. In theory, if two or more polygons are adjacent, the welded regions are restricted to the space between these polygons and contained inside the convex hull of the polygons. This assumption is analogous to finding the intersection between two polygons presented by Toussaint [24].

Figure 5.11, for example, illustrates when polygon P_{11} and P_{21} are adjacent. Segment s_1s_2 and s_3s_4 are the *bridges* on convex hull which connect between P_{11} and P_{21}. The welded regions in this case are enclosed in the space between s_1s_2, s_3s_4, and the middle region between P_{11} and P_{21}. Polygon P_{11} and P_{21} can be divided into two *chains* using the start and

end points of the bridges (s_1, s_2, s_3, and s_4). Parts of contours inside the closed area are called *inner chains* and those outside the closed area are called *outer chains*.
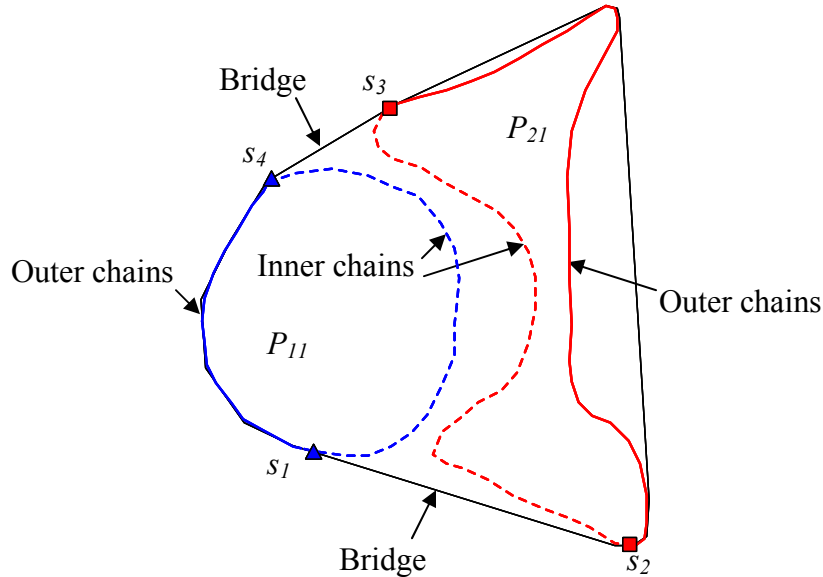
Figure 5.11. Convex hull of two polygons

If Q_1 is identified as a welding contour in the previous contour level and P_{11}, P_{21} are generic representations of Q_1, the corresponding bridge points on Q_1 can be computed by finding the closest points from Q_1 to point s_1 and s_4 of P_{11}, and from Q_1 to point s_2 and s_3 of P_{21}. These new bridge points (t_1, t_2, t_3 and t_4) on Q_1 are used as the furthest boundaries that contain the welded regions (Figure 5.12).
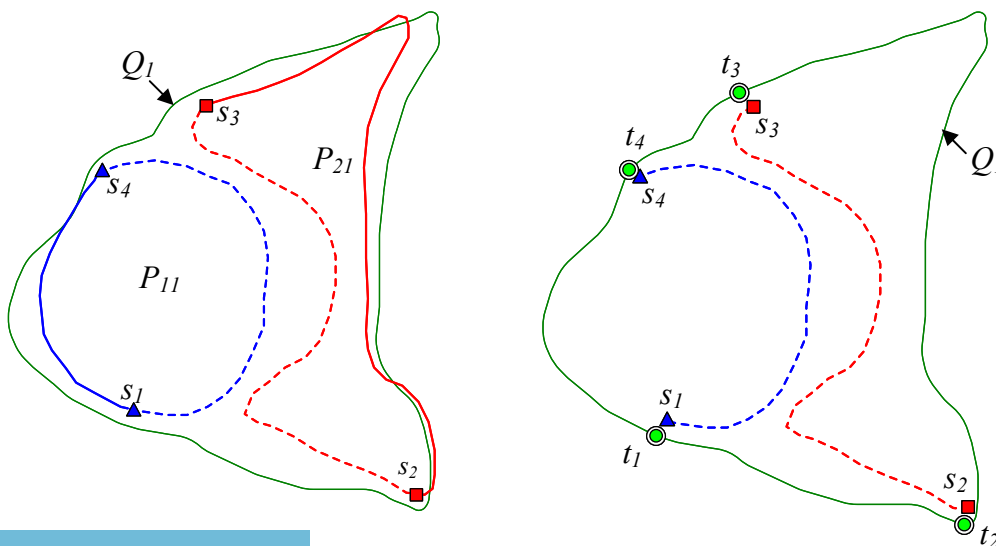
Figure 5.12. Bridge points t_1, t_2, t_3 and t_4 on object contour Q_1

Locations between the start and end of bridge points on the object contour (t_1 to t_2 and t_3 to t_4) can be where the two contours of adjacent bones are connected. In order to identify the connecting points, the vertices between the bridge points need to be recognized. In the proposed method, rays are extended from these vertices to intersect generic contours as a process of identification. The general idea is to identify the vertex to the closest generic contour that the ray intersects. The direction of the ray is computed from an average of normal vectors on its neighbor segments. Figure 5.13 illustrates how the direction of vector (Vo_i) at object vertex is computed from normal vector u_i and u_{i+1} next to the vertex.

$$Vo_i = \text{Average}(u_i, u_{i+1}) \tag{4}$$
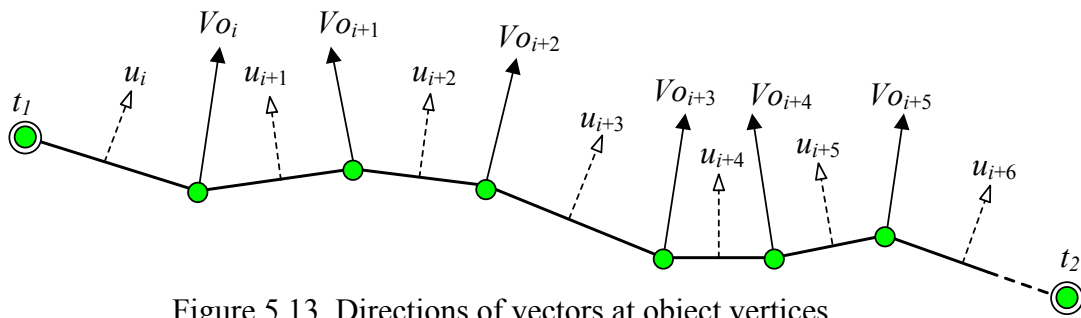
Figure 5.13. Directions of vectors at object vertices

If the ray intersects the generic contour, the vertex of the object contour may be assigned to the same bones that the generic contour is assigned to. However, the closest ray intersection can be ambiguous in the regions where generic contours become close to each other. Thus, the proposed method also compares the directions of vectors between the object and generic contours in order to assign the vertex of the object contour. Figure 5.14a illustrates how the vector direction from the vertex of the object contour (Vo_i) is compared to the vector direction of the generic contour (Vg_i) at the intersection point. It should be noted

that the vector direction on the intersection point is computed by averaging two vectors of

neighbor vertices.

(a) Ray intersection and direction of vector

(b) Assignment of vertices of object contour
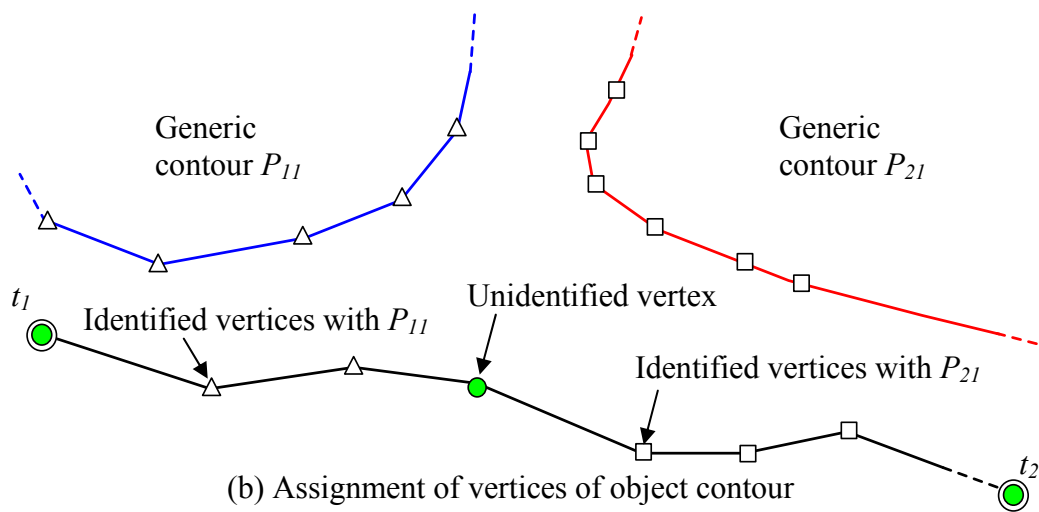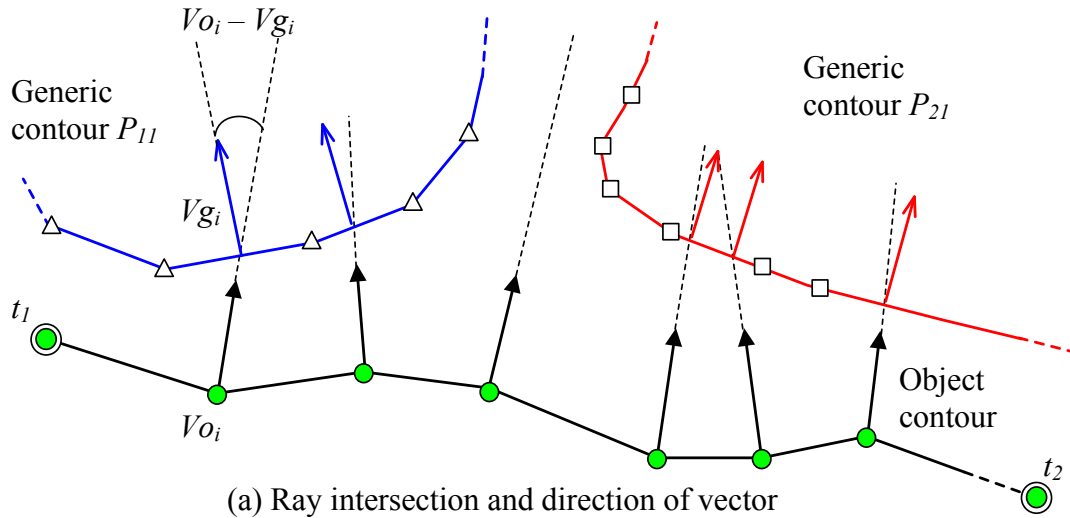
Figure 5.14. Vertex assignment at vertex level

At the closest intersection of the ray and generic contour, the difference of vector

direction between Vo_i and Vg_i is computed. The difference can range from 0 to π radians. In

order to prevent improper intersections, the allowable angle between Vo_i and Vg_i is set to a

small range of $\pi/3$. This value was derived through preliminary experimentation using

human hip joints; however it is not proposed to an optimal general value. An example of vertex assignment is illustrated in Figure 5.14b.

After the steps of ray intersection and comparing vector direction, each vertex of the object contour between the bridge points may be assigned to one of the bones that the generic contour is assigned to. The case may arise where the vertex of an object contour cannot be assigned to any bone. This occurs when the ray from the vertex of an object contour does not intersect with any generic contours or the difference of vector direction is larger than the allowable angle at intersection points. These unassigned vertices can be reassigned if they lie between vertices that are assigned to the same bone. The vertices of object contour are searched and reassigned from each bridge point to the other side. The process stops when a vertex that belongs to a different bone is found.
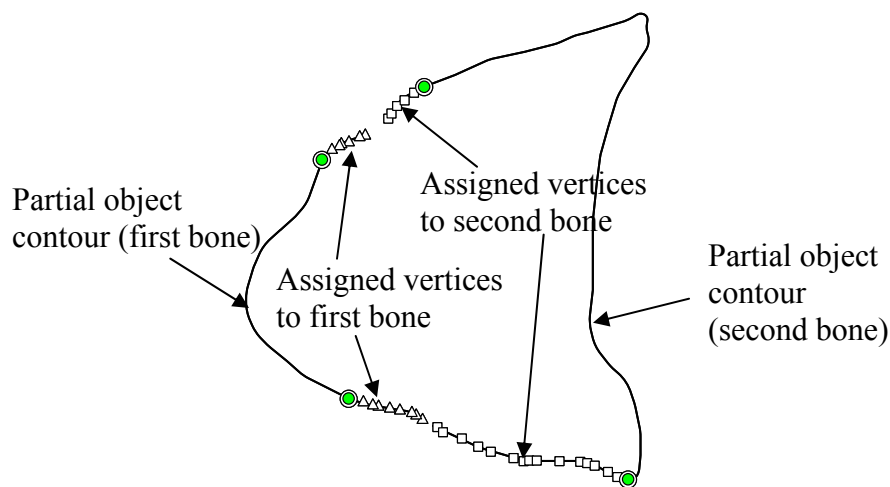
Figure 5.15. Partial object contours

At this point, the vertices of the object contour between the bridge points can be grouped into the same bones and joined with portions of contour outside the bridge points (outer chains) to form partial contours (Figure 5.15). The object contour is now divided into partial contours that belong to individual bones. The next challenge is to recreate complete

contours from these partial contours. In other words, the missing data at the ends of partial contours need to be regenerated so the loops can be closed.

5.6. Weld Modification

Weld modification is a process to repair the welded regions by modifying the partial object contours after the weld identification process. The purpose of this modification is to create complete contours from partial contours that belong to individual bones. There is a common method in the literature that utilizes *curvature* at the end points to close the partial contours. However, the result can be uncertain if the shape of the contour is complex or the amount of data to restore is very large. Instead of using the curvature at the end points, the method in this paper employs portions of generic contours to fill the missing parts of partial contours. The main reason is because generic contours represent how the object contours *should* approximately appear if the welded regions are removed. The newly formed contours called *hybrid contours* will be a combination of portions of both object and generic contours (Figure 5.16c).
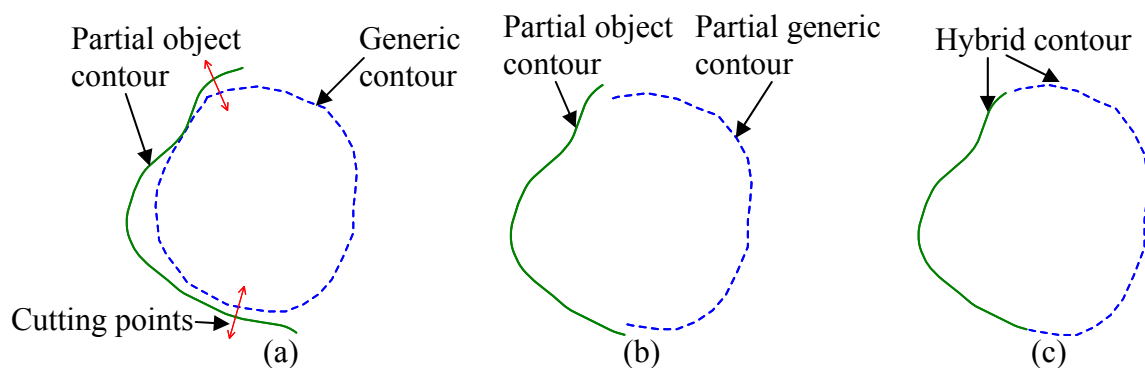
Figure 5.16. Hybrid contour

The steps of repairing the partial object contour with portions of generic contours are illustrated in Figure 5.16. To begin the weld modification process, location of *cutting* points

needs to be identified. Cutting points are where the object contour and generic contour will be connected. The cutting points should be first located near the end of the partial object contours. Then, rays are extended from these cutting points on the object contour to the generic contour. The intersections at the generic contour determine cutting points that divide the generic contours into partial contour sections (Figure 5.16a and 5.16b) that will be used to replace the missing portions of object contours. From the weld detection process described in the previous section, the bridge points on the object contour represent the boundaries that the welded regions can possibly occur; therefore the proposed method determines locations of cutting points between the bridge points and the end points of partial object contours. In order to improve continuity between partial object and partial generic contours, the method determines the cutting points by considering both minimum distance and minimum difference of vector directions. The distance is measured from the object vertex to intersection points on the generic contour (d_i). The difference of vector directions (vd_i) is the angle between the vector on a vertex of the object contour and the vector of the intersection point on the generic contour (Figure 5.17)
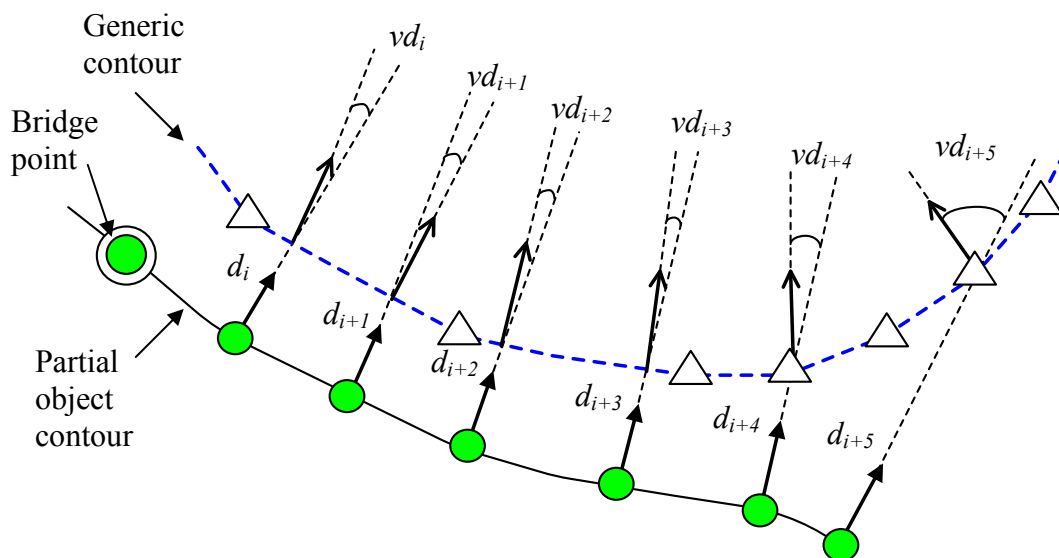
Figure 5.17. Distance from object vertex to intersection point (d_i)
and the difference of vector directions (vd_i)

Both distance and direction difference values are divided by their maximum to make them scale invariant. The cutting point is then given by:

$$\min\left\{w_1\left[\frac{d_i}{\max(d_i)}\right] + w_2\left[\frac{vd_i}{\max(vd_i)}\right]\right\}$$ (5)

where w_1 and w_2 are weights associated with each variable

Optimal settings for weights are not a subject of the current research, as these values may change for different joints, imaging methods, etc. They are included for completeness, but simply set equal for the current implementation based on preliminary testing. Once cutting points are determined, the partial generic contours are created and used for filling the gap on partial object contours. A transformation is required to initially fit these partial generic contours to partial object contours. This transformation consists of three steps: xy translation, rotation, and scaling:

Partial object contour (Q) is defined as

$Q(xq_i, yq_i)$ where $i = 0, 1, 2,\ldots, n$

and partial generic contour (P) is defined as

$P(xp_j, yp_j)$ where $j = 0, 1, 2,\ldots, m$

If the cutting points (end points) of partial object contour are given as (xq_0, yq_0) and (xq_n, yq_n) and the end points of partial generic contour are (xp_0, yp_0) and (xp_m, yp_m), the transformation is defined as the following matrixes [25]:

$$\textit{Translation:} \quad \begin{bmatrix} 1 & 0 & (xq_0 - xp_0) \\ 0 & 1 & (yq_0 - yp_0) \\ 0 & 0 & 1 \end{bmatrix}$$ (6)

$$
\textit{Rotation:} \quad
\begin{bmatrix}
\cos\theta & -\sin\theta & xq_0(1-\cos\theta) + yq_0(\sin\theta) \\
\sin\theta & \cos\theta & yq_0(1-\cos\theta) + xq_0(\sin\theta) \\
0 & 0 & 1
\end{bmatrix}
\quad (7)
$$

where θ = the angle of rotation and (xq_0, yq_0) = the point of rotation

$$
\textit{Scale:} \quad
\begin{bmatrix}
\dfrac{(xq_n - xq_0)}{(x\widetilde{p}_m - xq_0)} & 0 & xq_0\left(1 - \dfrac{(xq_n - xq_0)}{(x\widetilde{p}_m - xq_0)}\right) \\
0 & \dfrac{(yq_n - yq_0)}{(y\widetilde{p}_m - yq_0)} & yq_0\left(1 - \dfrac{(yq_n - yq_0)}{(y\widetilde{p}_m - yq_0)}\right) \\
0 & 0 & 1
\end{bmatrix}
\quad (8)
$$

where $(x\widetilde{p}_m,\ y\widetilde{p}_m)$ is end point of the partial generic contour after translation and rotation
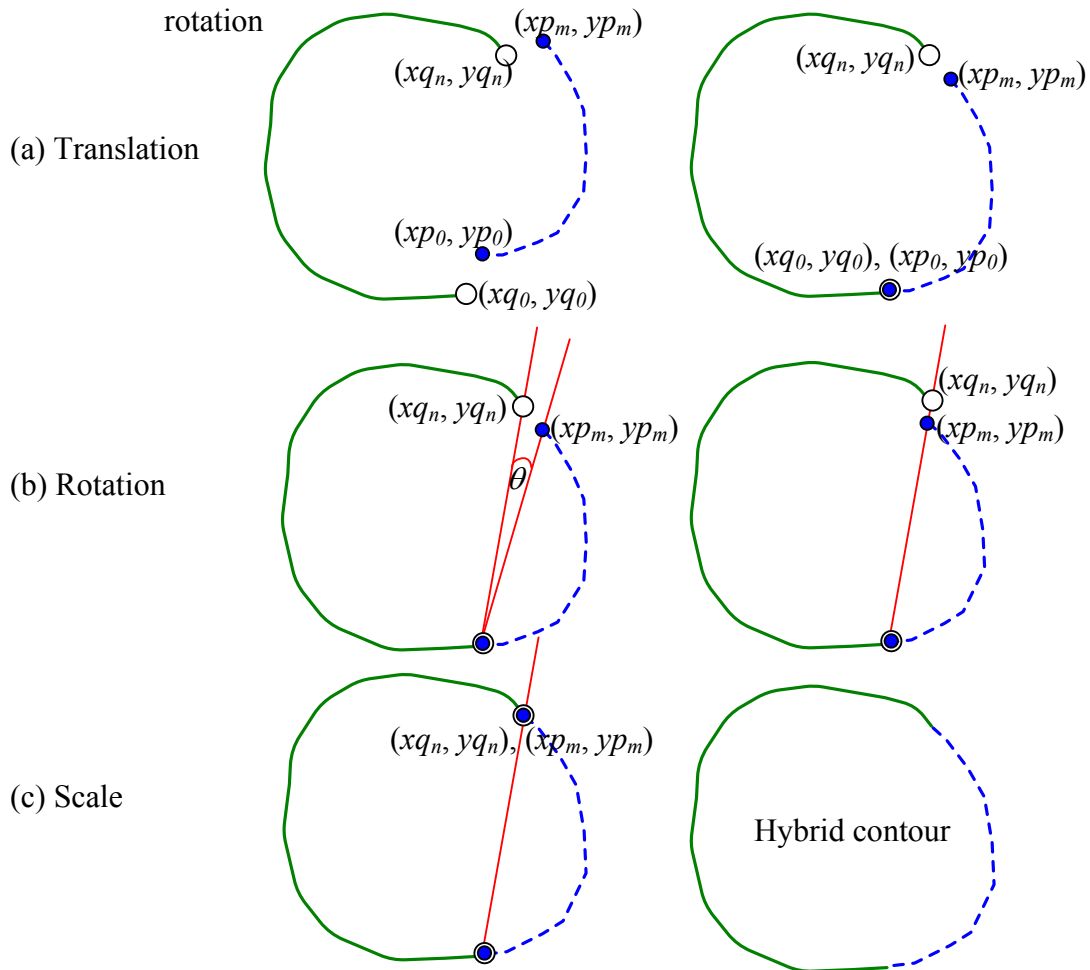
Figure 5.18. Example of transformation to create hybrid contour

Figure 5.18 illustrates the steps involved in transforming a partial generic contour to complete the missing portion of the object contour. Once the partial object contours are repaired, the newly formed hybrid contours can be assigned to each individual bone, enabling surface reconstruction.

There is a special case where the proposed method for weld detection at the vertex level and weld modification fails to find a solution. This case is when the generic contour is fully contained within the convex hull of the slice (Figure 5.19). The reason for failure is that the bridge points that connect two generic contours do not exist. The proposed solution for this case is to insert both the interior chain and contained generic contour into the partial object contour.

(a) Object contour   (b) Generic contours

(c) Cutting points   (d) Transformation   (e) Hybrid contour
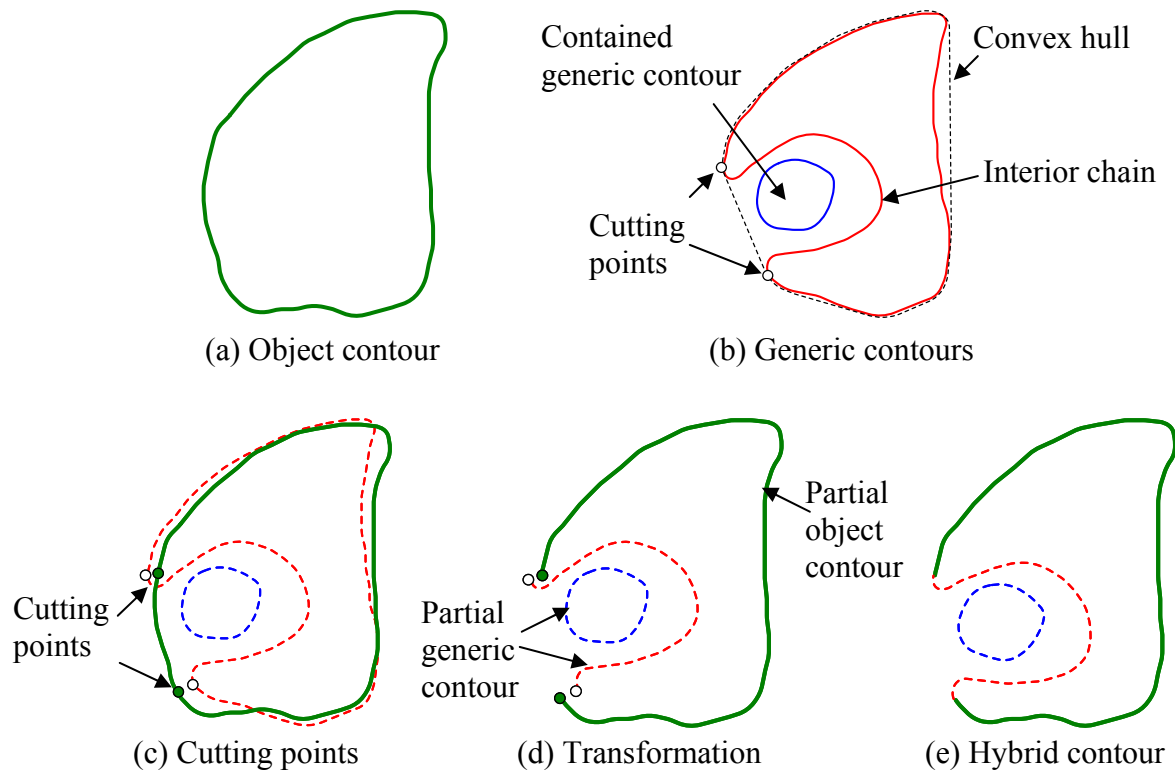
Figure 5.19. Fixing steps for fully contained generic contour

Figure 5.19 illustrates the modification steps for this special case. At the beginning, the interior chain that fully contains the generic contour is identified (Figure 5.19b). The points on the convex hull boundary where the interior chain is closed are used as cutting points on the generic contour. The cutting points on the object contour are determined by finding the closest points between cutting points on the generic and object contours (Figure 5.19c). The partial object contour and partial generic contours are created (Figure 5.19d). The partial generic contour (interior chain and contained contour) is transformed to fit the gap within the partial object contour (Figure 5.19e). The transformation matrices are computed as previously discussed.

This section presented a reliable weld detection and modification process that utilizes portions of a standard generic CAD model of the bone joint. In next section, we present an implementation of these methods with an example human hip joint model.

5.7. Implementation

The methods for weld detection and weld modification were implemented using *C++* language and the results graphically displayed using *OpenGL*. Testing was performed on an Intel Core 2 Duo (2.4 GHz, 2 GB memory) PC. Two sets of CT images of hip joints from the sample sets on the OsiriX website [12] were used in this implementation. The first hip model was manually segmented and reconstructed using standard medical imaging software called *Mimics* [11] and designated as the *generic* model (Figure 5.20a). In practice, one would choose a generic model that closely relates to the patients age, gender, height, etc. As the generic model, the tedious process of manually segmenting and assigning contours was executed to the extent that a successfully separated set of bones was created. The second hip

model was reconstructed in *Mimics* using only low-level techniques including thresholding and region growing. This model was designated as the *object* model and the welded regions expectedly occurred where the *femoral head* and *pelvis socket* (acetabulum) are adjacent (Figure 5.20b).

Both object and generic CAD models were sliced with 0.01" (0.254 mm) spacing and the two slice sets were registered using a previously proposed sliced model registration process (discussed in Section 5.4). The sliced model registration process outputs 593 slices of object model and their corresponding slices of generic model. The implementation in this section will utilize the output of this registration process for subsequent weld detection and weld modification.

(a) Generic model   (b) Object model
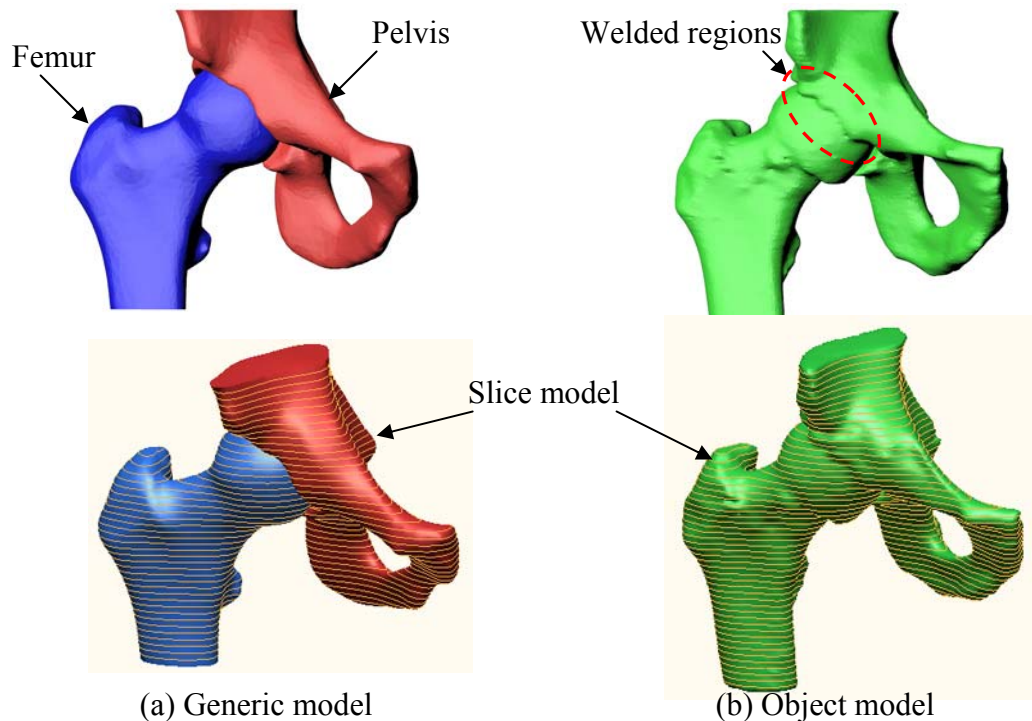
Figure 5.20. (a) Generic model and (b) Object model

5.7.1. Weld detection

The corresponding generic slices are first transformed to align with the object slices. At the *contour level*, the intersection of contours on generic slices and object slices is computed to determine if any contours on object slices contain welded regions. Figure 5.21 illustrates the result of weld detection at the contour level. For example, the contours of object slices from slice 0 to 86 are identified as femoral contours and there are no welded regions in this section. According to Figure 5.21, the welded regions between the femur and pelvis start at object slice 286 and continue until slice 466 (181 contours).
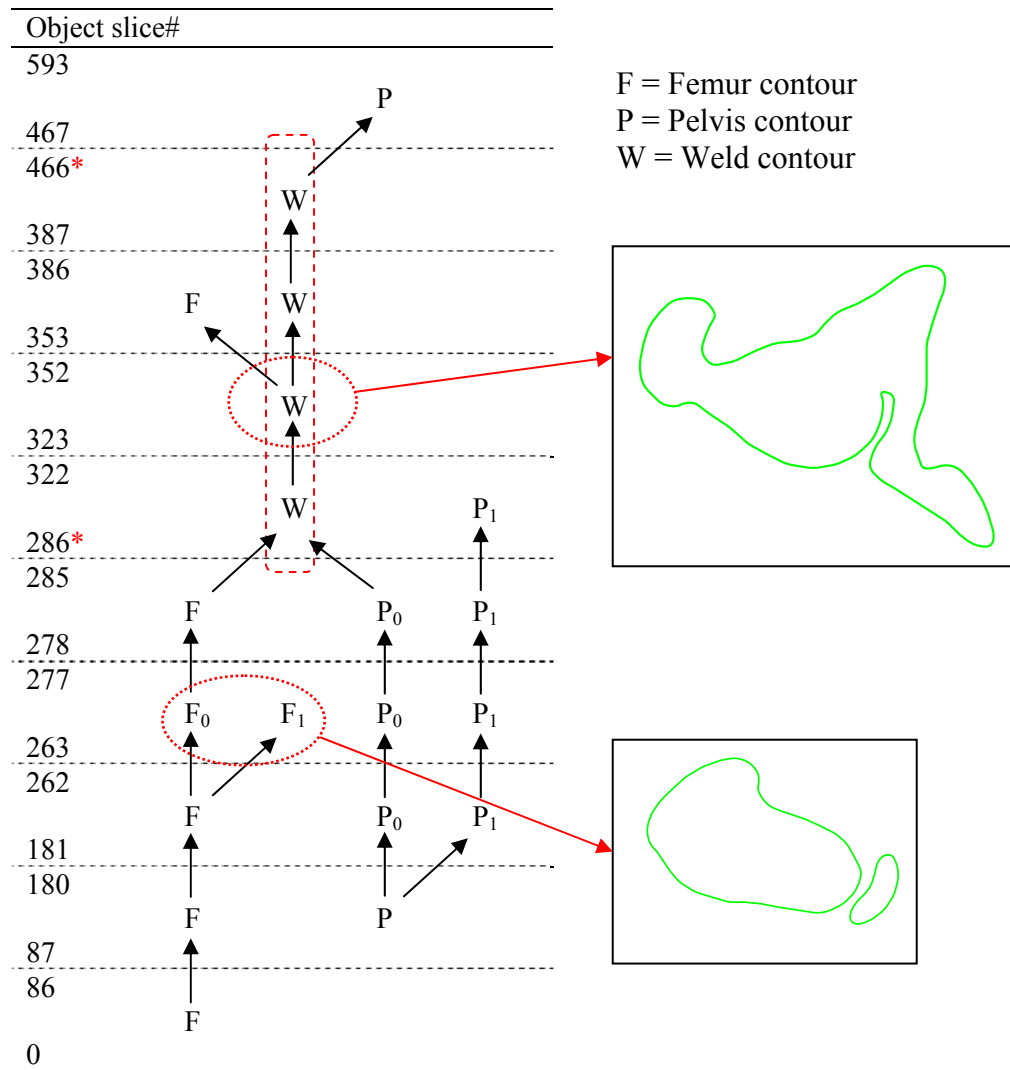
Figure 5.21. Diagram of results of weld detection in contour level

An example of weld detection at the *vertex level* is illustrated in Figure 5.22. The bridge points of the convex hull are first computed for the generic slice. The corresponding bridge points on the object contour are then identified (Figure 5.22a). Each vertex between the bridge points on the object contour is assigned to a single bone by extending rays that intersect generic contours. At this point, the object contour can be divided into partial contours that are assigned to individual bones (Figure 5.22b).
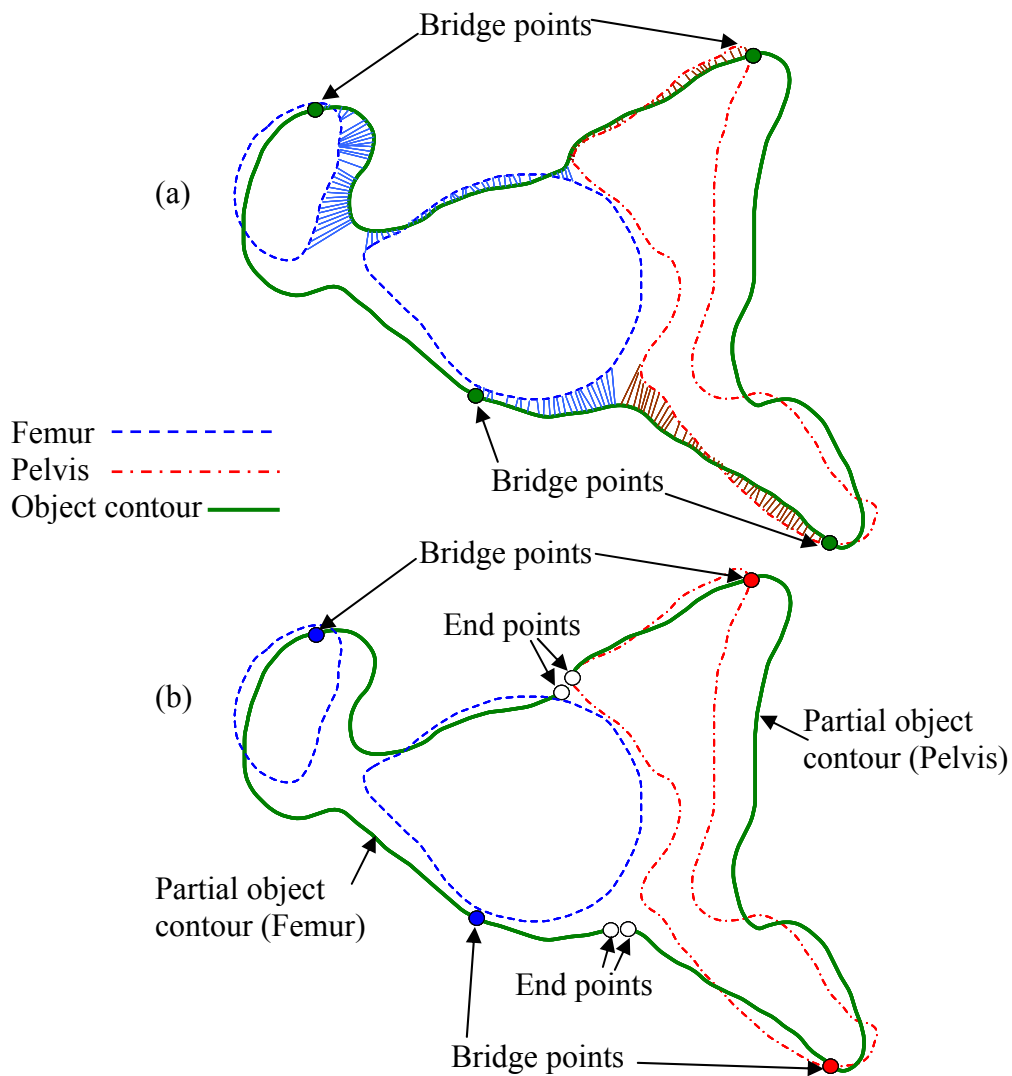
Figure 5.22. Results of weld detection at the vertex level

5.7.2. Weld modification

In the weld modification process, cutting points are first identified between the end points of partial contours and the bridge points. This is done by minimizing the summation of the nominal value of distance and nominal value of directional difference. Once the cutting points are located, partial object contours and corresponding partial generic contours are created (Figure 5.23a and 5.23b).

(a) Cutting points   (b) Transformation   (c) Hybrid contours
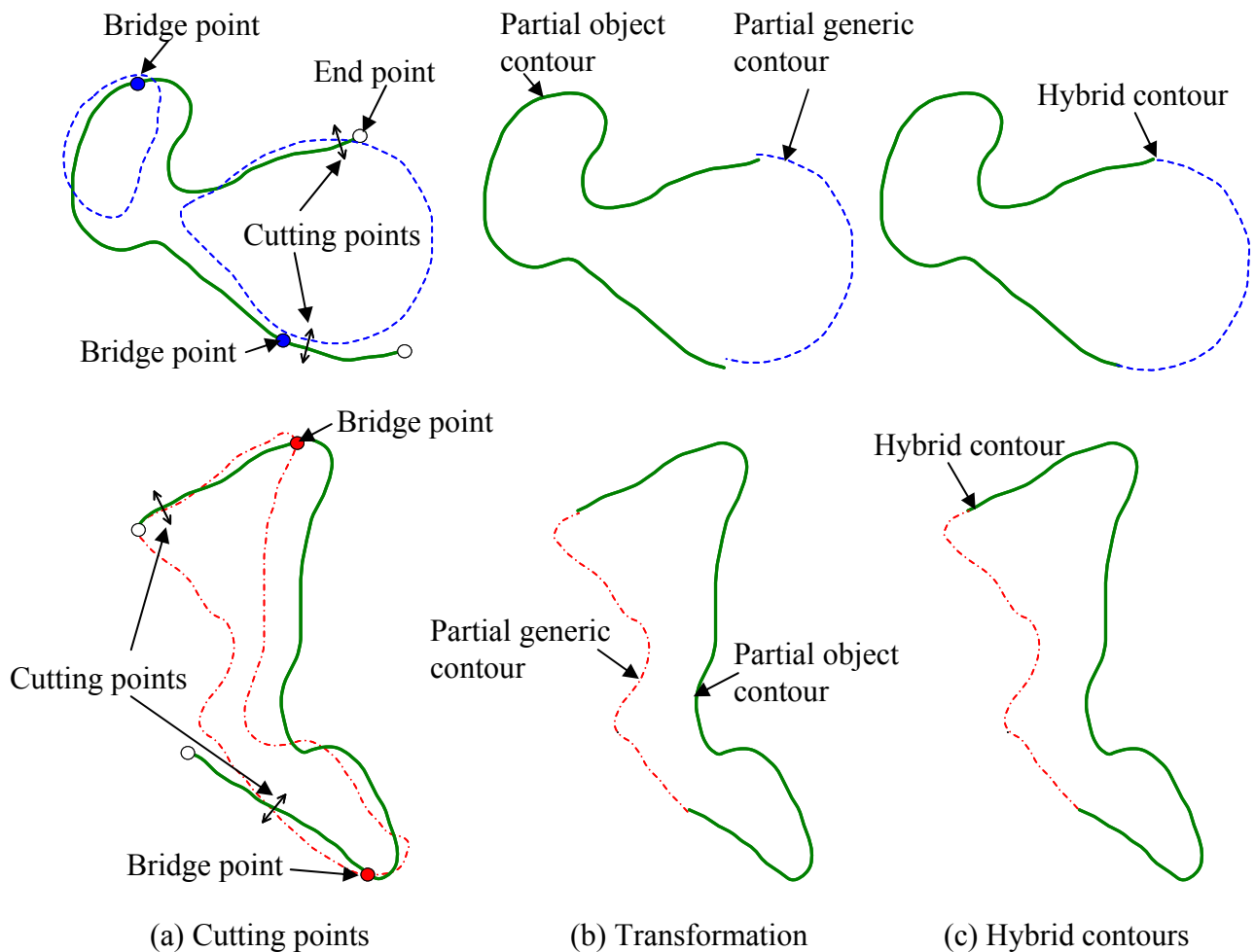
Figure 5.23. Weld modification process

The partial generic contours are then transformed to complete the partial object contours. Finally, the hybrid contours of individual bones are created (Figure 5.23c). The

special case where the generic contour is fully contained inside convex hull of the slice is detected at slices 465 and 466 of the object model. The contours on these object slices are repaired by the proposed special case method described in Section 5.6. Once the welded regions are removed from all object slices, the repaired contours of object slices (hybrid contours) are assigned to individual bones. The computation time for each process is shown in Table 5.1. The total time of weld removal process for the example joint is less than 200 seconds.

Process	Time (seconds)
Weld Detection	187
Weld Modification	less than 2

Table 5.1. Computation times for weld detection and weld modification

5.7.3. Results

3D Models of femur and pelvis were reconstructed from the *hybrid* contours of individual bones to illustrate the results of implementation. Each model (hybrid mode) is created using volume-based techniques within reverse engineering software (*Rapidform* [20]). Figure 5.24 shows the reconstructed models of femur and pelvis and regions on the models that were repaired by generic contours.
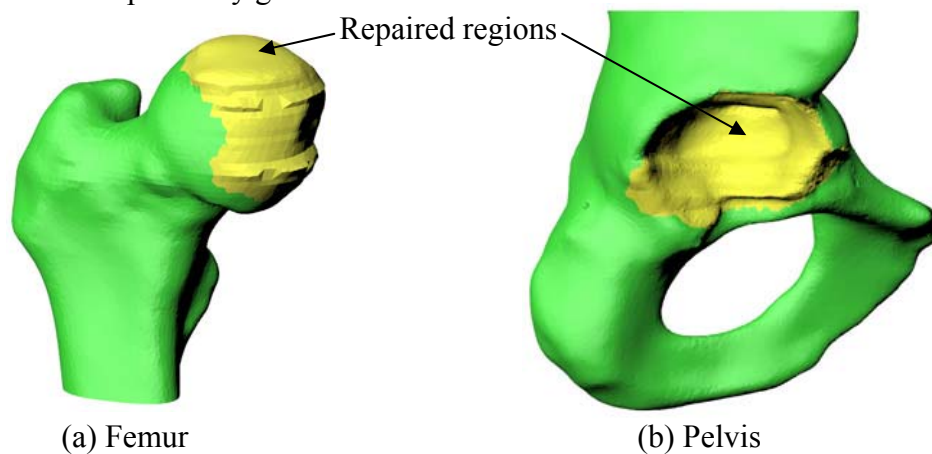
(a) Femur (b) Pelvis

Figure 5.24. Hybrid model

Table 5.2 shows the area of the fixed regions on both femur and pelvis models and the percentage of the fixed area out of total area.

Bones	Area of repaired regions	% of repaired area
Femur	6.474 in^2 (4176.996mm^2)	17.8
Pelvis	6.784 in^2 (4377.075mm^2)	12.5

Table 5.2. Repaired regions

The hybrid model may be used as an approximated model (finish model) or it may be utilized in an iterated low-level segmentation process in order to extract the object from CT images. This paper evaluates the improvement of using a hybrid over a generic model by comparing both models to a reference model from manual segmentation. Figure 5.25 illustrates a hybrid model, generic model, and the reference model from manual segmentation.

(a) Hybrid model   (b) Generic model   (c) Reference model
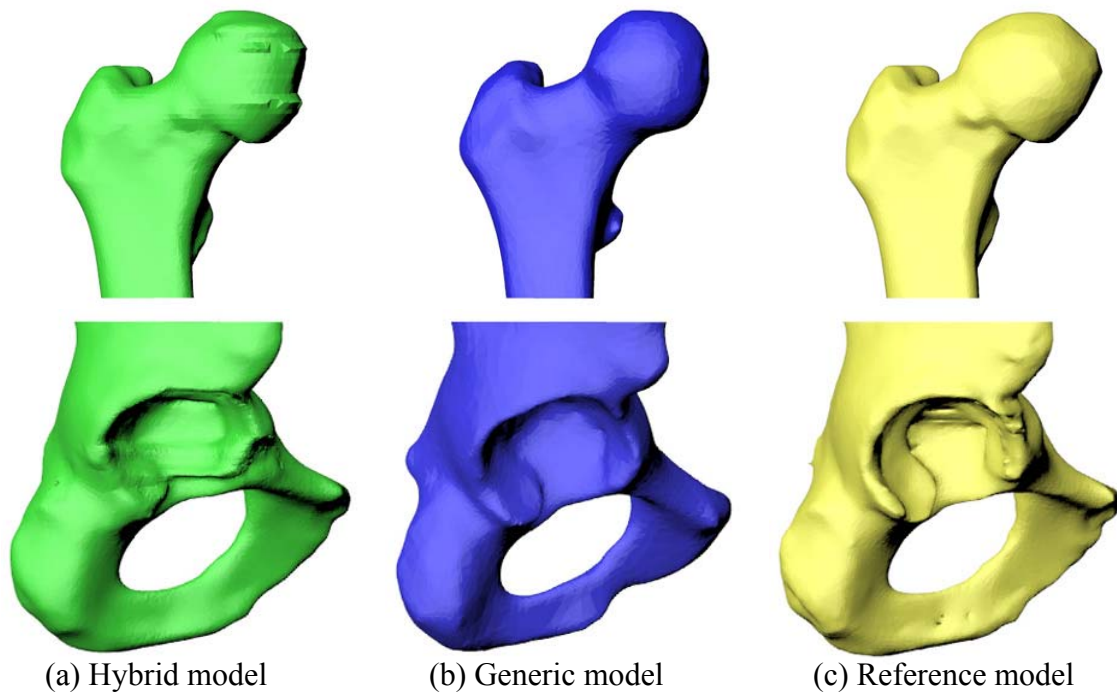
Figure 5.25. Hybrid model, generic model, and reference model

The surface-to-surface deviation model surfaces were measured using an inspection tool in Rapidform software and presented in three parts. Part I illustrates the deviation between the entire models. Part II specifically focuses on the deviation of sections that are related to the welded regions. Lastly, Part III shows the deviation results if global surface smoothing is applied to the hybrid model.

5.7.3.1. Part I

In Part I of the evaluation, the whole surfaces of hybrid and generic models are compared to the surfaces of the reference model. It should be noted that since the hybrid model is created based on objects generated from the same CT images, the hybrid model is automatically aligned with the reference models. On the contrary, the generic model requires surface registration with the reference model before comparison. Manual registration was repeated 10 times in Rapidform software to capture variability of this registration process, to avoid bias of the surface deviation from registration rather than fitting accuracy of the hybrid model. Femur and pelvis bone models are individually compared and their deviation results are illustrated in Table 5.3.

As shown in Figure 5.26, the femur and pelvis of hybrid model have lower *maximum* and *average* surface deviation than those of the registered generic models. Specifically, the maximum surface deviation of the hybrid femur is 13-34% lower than the maximum surface deviation of the generic femur, and the average surface deviation of the hybrid femur is 61-63% lower than the average surface deviation of the generic femur. For the pelvis model, the maximum surface deviation of the hybrid model is 30-40% lower than the maximum surface deviation of the generic model and the average surface deviation of hybrid model is 45-46% lower than the average deviation of the generic model. In addition, in all cases the standard

deviation and root mean square error (RMS) of the hybrid model are lower than those of generic model. Based on these results, it is clear that the hybrid model has an improvement over the generic model, an improvement over the methods found in the literature that likewise use standard/generic models.

	Femur				
Type:	Hybrid	Generic 1	Generic 2	Generic 3	Generic 4	Generic 5
Max:	0.2596	0.3207	0.2969	0.3040	0.3940	0.3370
Average:	0.0225	0.0602	0.0587	0.0582	0.0598	0.0601
Std dev:	0.0242	0.0475	0.0476	0.0475	0.0482	0.0481
RMS:	0.0330	0.0767	0.0756	0.0751	0.0768	0.0770
Type:		Generic 6	Generic 7	Generic 8	Generic 9	Generic 10
Max:		0.3444	0.3094	0.2991	0.3576	0.3075
Average:		0.0596	0.0582	0.0588	0.0594	0.0584
Std dev:		0.0481	0.0477	0.0473	0.0482	0.0477
RMS:		0.0766	0.0753	0.0755	0.0765	0.0754
	Pelvis				
Type:	Hybrid	Generic 1	Generic 2	Generic 3	Generic 4	Generic 5
Max:	0.2273	0.3413	0.3629	0.3541	0.3784	0.3780
Average:	0.0408	0.0754	0.0742	0.0743	0.0749	0.0744
Std dev:	0.0278	0.0586	0.0564	0.0575	0.0591	0.0579
RMS:	0.0494	0.0955	0.0932	0.0940	0.0954	0.0943
Type:		Generic 6	Generic 7	Generic 8	Generic 9	Generic 10
Max:		0.3614	0.3339	0.3226	0.3486	0.3737
Average:		0.0748	0.0750	0.0750	0.0749	0.0744
Std dev:		0.0589	0.0579	0.0570	0.0574	0.0578
RMS:		0.0952	0.0948	0.0942	0.0944	0.0942

Unit: inch (x 25.4 millimeter)

Table 5.3. Surface deviation of hybrid model and registered generic models

Figure 5.26. (a) Maximum surface deviation and (b) Average surface deviation of hybrid model and registered generic models

5.7.3.2 Part II

In Part II of the evaluation, the specific section of the hybrid model where welded

regions were repaired is further investigated. Although the hybrid model was shown to be

generally superior to the generic model, this may have been due to the variation of surfaces

outside the weld areas; hence, we wish to specifically target the welded regions.   Moreover,

if the hybrid model will be employed in low-level segmentation, it may be that the only

feedback necessary will be where welding occurred (assuming other errors were not present).

Only the sections of the CAD models with welded regions were studied. This was

accomplished by using 2D cutting planes at the slices where a welded region begins and

ends, as we traverse the model along the slice axis. The corresponding locations of these 2D

planes were found on both the reference model and all 10 registrations of the generic model.

Figure 5.27 illustrates the sections of hybrid, generic model, and reference models and the

respective deviation results are shown in Table 5.4.

Femur

Pelvis

(a) Hybrid   (b) Generic   (c) Reference
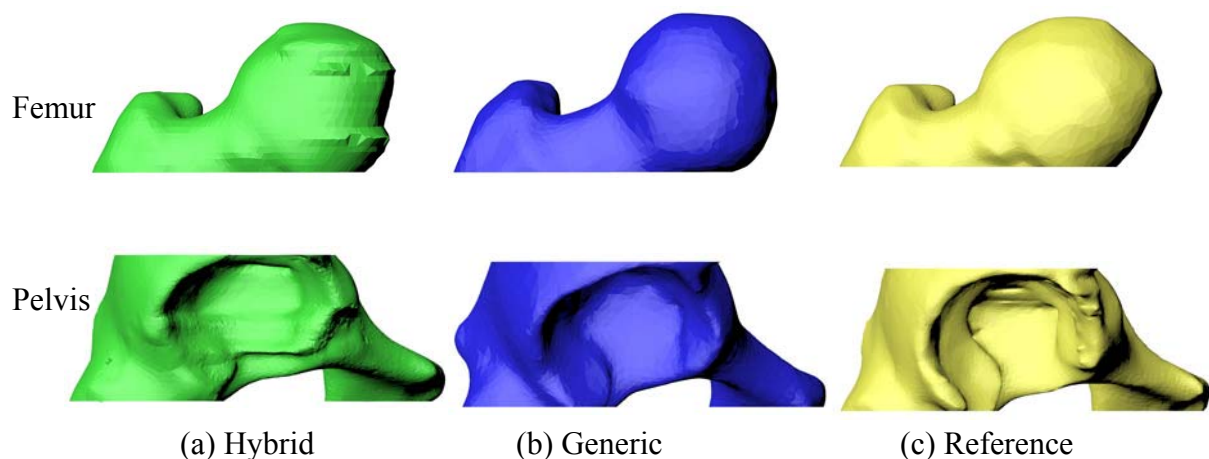
Figure 5.27. (a) Section of hybrid model, (b) Section of generic model,
and (c) Section of reference model

Femur (Section)					
Type:	Hybrid	Generic 1	Generic 2	Generic 3	Generic 4	Generic 5
Max:	0.2621	0.2887	0.2904	0.3004	0.3077	0.2890
Average:	0.0330	0.0609	0.0601	0.0596	0.0593	0.0605
Std dev:	0.0368	0.0486	0.0496	0.0492	0.0478	0.0484
RMS:	0.0494	0.0779	0.0779	0.0773	0.0762	0.0774
Type:		Generic 6	Generic 7	Generic 8	Generic 9	Generic 10
Max:		0.2901	0.3022	0.2988	0.3270	0.3075
Average:		0.0595	0.0591	0.0617	0.0594	0.0595
Std dev:		0.0484	0.0494	0.0501	0.0479	0.0494
RMS:		0.0767	0.077	0.0795	0.0763	0.0773
Pelvis (Section)					
Type:	Hybrid	Generic 1	Generic 2	Generic 3	Generic 4	Generic 5
Max:	0.2353	0.4124	0.4047	0.4071	0.3825	0.3652
Average:	0.0501	0.0787	0.0776	0.0823	0.0798	0.0746
Std dev:	0.0352	0.0603	0.0580	0.0645	0.0627	0.0567
RMS:	0.0612	0.0991	0.0969	0.1046	0.1015	0.0937
Type:		Generic 6	Generic 7	Generic 8	Generic 9	Generic 10
Max:		0.4003	0.4229	0.3614	0.3634	0.3557
Average:		0.0767	0.0753	0.0786	0.0806	0.0780
Std dev:		0.0603	0.0594	0.0601	0.0604	0.0592
RMS:		0.0976	0.0959	0.0990	0.1007	0.0980

Unit: inch (x 25.4 millimeter)

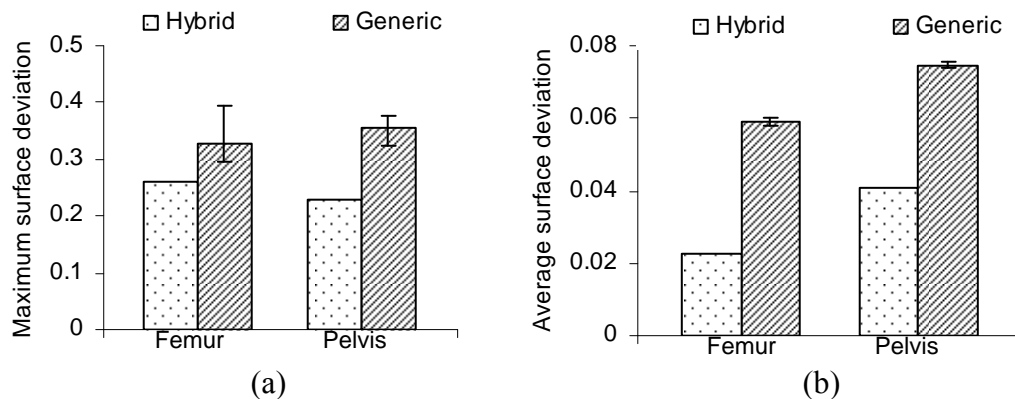Table 5.4. Surface deviation of hybrid model and registered generic models
for weld sections
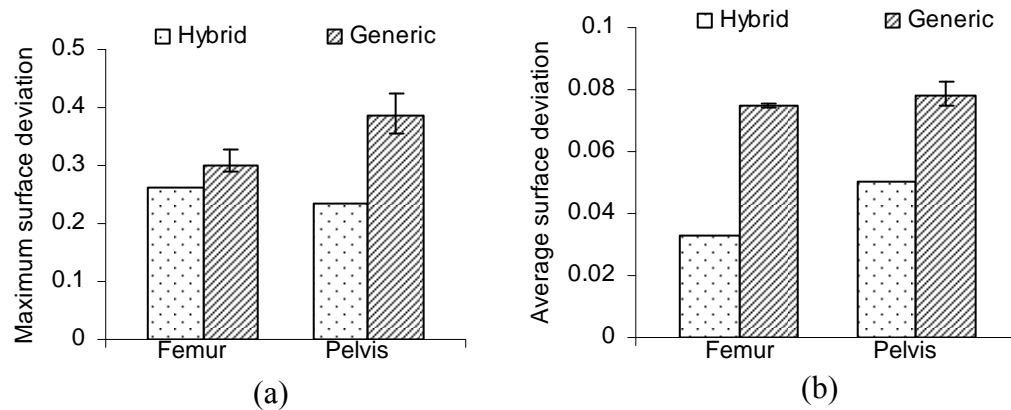
Figure 5.28. (a) Maximum surface deviation and (b) Average surface deviation
of hybrid model and registered generic models for weld sections

Figure 5.28 shows that the maximum and average surface deviation of the hybrid

model is still lower than all registered generic models when considering only the welded

regions.   For the femur model, the maximum surface deviation from hybrid sections is 10-

20% lower than that of generic sections and the average deviation is 55-56% lower. For the pelvis model, the maximum surface deviation of hybrid sections is 34-44% lower than that of generic sections and the average deviation is 33-39% lower. For all cases, the standard deviation and RMS of the hybrid section is lower than those of generic sections.

5.7.3.3. Part III

From the overall results in Part I and II, it is consistently shown that the hybrid model is a better approximation than the generic model. However, it can be observed that the repaired surfaces of hybrid model *look* less appealing to utilize as a finished model. Thus, an attempt to improve the current hybrid model was conducted by using simple global smoothing techniques, in this case a tool available in Rapidform software. Figure 5.29 illustrates the hybrid model before and after the global smoothing tool was applied.

| (a) Non-smooth | (b) Smooth 50% | (c) Smooth 100% |
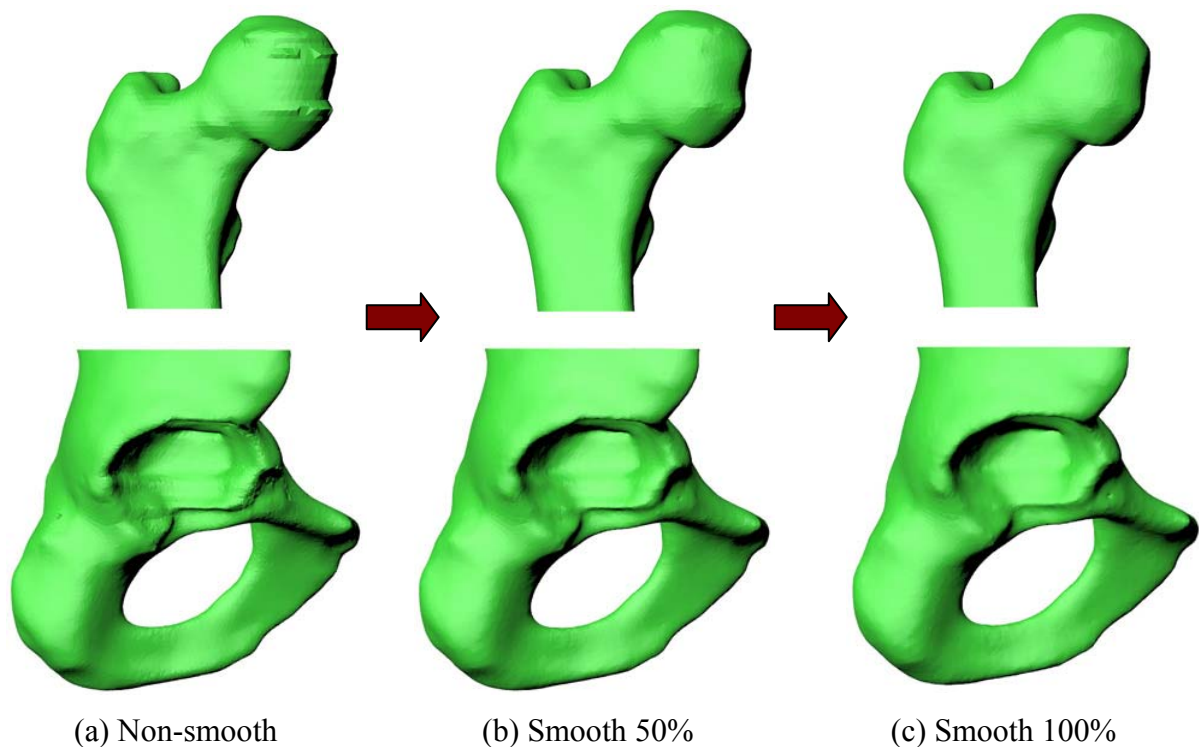
Figure 5.29. Hybrid model with smooth operation: (a) non-smooth, (b) smooth 50% of weight, and (c) smooth 100% of weight

The surface deviation of the smoothed hybrid model and sections was individually computed for the femur and pelvis (Table 5.5).

	Hybrid Femur (Model)			Hybrid Pelvis (Model)		
Type:	Non-smooth	Smooth 50%	Smooth 100%	Non-smooth	Smooth 50%	Smooth 100%
Max:	0.2596	0.2565	0.2504	0.2273	0.2263	0.2067
Average:	0.0225	0.0254	0.0324	0.0408	0.0408	0.0414
Std dev:	0.0242	0.0234	0.0258	0.0278	0.0280	0.0286
RMS:	0.0330	0.0345	0.0414	0.0494	0.0495	0.0503
	Hybrid Femur (Section)			Hybrid Pelvis (Section)		
Type:	Non-smooth	Smooth 50%	Smooth 100%	Non-smooth	Smooth 50%	Smooth 100%
Max:	0.2621	0.2565	0.2504	0.2353	0.2263	0.2297
Average:	0.0330	0.0354	0.0431	0.0501	0.0498	0.0487
Std dev:	0.0368	0.0336	0.0348	0.0352	0.0351	0.0333
RMS:	0.0494	0.0488	0.0554	0.0612	0.0610	0.0590

Unit: inch (x 25.4 millimeter)

Table 5.5. Surface deviation of hybrid model and smooth hybrid model

As shown in Table 5.5, although the smoothed models may be more appealing, it does little to improve the fitting accuracy of the model. The maximum surface deviation may decrease but the average surface deviation actually tended to increase. Over smoothing could actually degrade the model instead of improving it; however, a reduction in maximum deviation could be beneficial to the success of low level segmentation methods and obviously, the models look better.

5.8. Conclusions and Future work

This paper presented a new approach to automated high-level segmentation for medical images of bone joint structures. The method employs a generic CAD model as anatomical knowledge to substitute that of medical experts/technicians. A slice model was utilized to simplify the geometric analysis, and adding to its more robust and reliable natures. The paper focused methods that detects and repair unintended geometry of the object model

caused by virtual welding of bone joints by comparing to a properly segmented generic model. The method provides a set of hybrid slices that contain most of the object model, but also sections cut from the generic model used to repair removed welds. The hybrid results (either 2D or 3D) can be used for direct approximation of separated bone joint models or can also be iterated as a feedback for low-level segmentation to avoid the welding problem in the first place. Utilizing hybrid results for low-level segmentation provides the following advantages: 1) the results are automatically registered to the object in CT images since the hybrid model is grown from the object model, and 2) only repaired regions of the hybrid results are required to find optimal solution in low-level segmentation because other portions were already derived successfully from the object model.

Although the method proved functional and shows significant improvements, there are areas for future research. Future work could include automated smoothing algorithms in specific areas where the welded regions were replaced. In stead of smoothing the entire model surfaces, a method based on the curvature of the good (object) surfaces could be used to further transform the partial generic segments. The current approach could obviously be applied to a variety of bone joints, as one may expect subtle nuances of each joint to dictate at least minor modifications to the strategy. In this paper, we suggest that the hybrid model results can be used as feedback to the initial low-level segmentation; however, we do not propose how this implementation would work. The future work could investigate would need to determine how the hybrid contours are fed to low-level segmentation methods found in the literature on 2D approaches. Similarly, one would need to determine whether to input the hybrid model completely as a 3D shape or if partial sections should be carved from the model that only represent the welded regions.

This work will impact efforts in complete automation of both low and high level segmentation. Granted, when medical experts are available, manual segmentation of these troublesome regions is quite successful, and other nearly automated methods in the literature have been very successful. However, as 3D medical imaging and personalized medicine become ubiquitous, creative new methods that completely automate these processes will be necessary in order to provide both available and low-cost health services.

5.9. References

[1] Bajaj, C.L., Coyle, E.J., and Lin, K.N., "Arbitrary Topology Shape Reconstruction from Planar Cross Sections", Graphical Models and Image Processing, Vol. 58, pp. 310-319, 1996

[2] Bohm, G., Knoll, C., Colomer, V.G., Alcaniz-Raya, M., and Albalat, S., "Three-dimensional segmentation of bone structures in CT images", SPIE Conference on Image Processing, Vol. 3661, pp. 277-286, 1999

[3] Chan, C.F., Kwoh, C.K., Teo, M.Y., and Ng, W. S., "Tessellated Surface Reconstruction from 2D contours", 1999

[4] Cootes, T.F., Hill, A., Taylor, C.J., and Haslam, J., "The Use of Active Shape Models For Locating Structures in Medical Images", Image and Vision Computing, Vol. 12, no. 6, pp. 355-366, 1994

[5] Heo, H., and Chae, O.S., "Segmentation of tooth in CT images for the 3D reconstruction of teeth", Proceeding of SPIE, Vol. 5298, pp. 455-466, 2004

[6] Jeong, J., Kim, K., Park, H., and Jung, M., "A New Method for Solving Branching Problems in Surface Reconstruction", International Journal of Advanced Manufacturing Technology, Vol. 16, pp. 259-264, 2000

[7] Josephson, K., Ericsson, A., and Karlsson, J., "Segmentation of Medical Images Using Three-Dimensional Active Shape Models", Lecture Notes in Computer Science, Vol. 3540, pp. 719-728, 2005

[8] Kass, M., Witkin, A., and Terzopoulos, D., "Snakes: Active contour models", International Journal of Computer Vision, Vol. 1, pp. 321-331, 1988

[9] Liu, J., Udupa, J.K., Saha, P.K., Odhner, D., Hirsch, B.E., Siegler, S., Simon, S., and Winkelstein, B.A., "Model-based 3D segmentation of the bones of joints in medical images", Medical Imaging 2005: Image Processing, Proceeding of SPIE, Vol. 5747, pp. 1793-1803, 2005

[10] McInerney T., and Terzopoulos D., "Deformable Models in Medical Image Analysis", Proceedings of MMBIA'1996, Toronto, Canada, pp. 171-180, 1996

[11] Mimics Medical Imaging Software, Web site: http://www.materialise.com/materialise/view/en/92458-Mimics.html, Retrieved March 23, 2009

[12] OsiriX Imaging Software, Web site: http://www.osirix-viewer.com, Retrieved March 23, 2009

[13] Pardo, X.M., Carreira, M.J., Mosquera, A., and Cabello, D., "A snake for CT image segmentation integrating region and edge information", Image and Vision Computing, Vol. 19, pp. 461-475, 2001

[14] Park, H., and Kim, K., "3-D shape reconstruction from 2-D cross-sections", Journal of Design and Manufacturing, Vol. 5, pp. 171-185, 1995

[15] Parker, J.R., "Algorithms for image processing and computer vision", John Wiley & Sons, Inc., New York, 1997

[16] Pauly, M., Mitra, N., Giesen, J., Gross, M., and Guibas, L.J., "Example-Based 3D Scan Completion", Third Eurographics Symposium on Geometry Processing, pp. 23-32, 2005

[17] Pham, D.T., and Gault, R.S., "A comparison of rapid prototyping technologies", International Journal of Machine Tools & Manufacture, Vol. 38, pp. 1257-1287, 1998

[18] Pitas, I., "Digital Image Processing Algorithms and Applications", John Wiley & Sons, Inc., New York, 2000

[19] Rakshe, T., Fleischmann, D., Rosenberg, J., Roos, J.E., and Napel, S., "Knowledge-based interpolation of curves: Application to femoropopliteal arterial centerline restoration", Medical Image Analysis, Vol. 11, pp. 157-168, 2007

[20] Rapidform Software, Web site: http://www.rapidform.com, Retrieved March 23, 2009

[21] Ryu, J.H., Kim, H.S., and Lee, K.H., "Contour-based algorithms for generating 3D CAD models from medical images", International Journal of Advanced Manufacturing Technology, Vol. 24, pp. 112-119, 2004

[22] Shen, H., Shi, Y., and Peng, Z., "Applying Prior Knowledge in the Segmentation of 3D complex Anatomic Structures, Lectures Notes in Computer Science, Vol. 3765, pp. 189-199, 2005

[23] Starly, B., Fang, Z., Sun, W., Shokoufandeh, A., and Regli, W., "Three-Dimensional Reconstruction for Medical-CAD Modeling", Computer-Aided Design, Vol. 2, pp. 431-438, 2005

[24] Toussaint, G.T., "A Simple Linear Algorithm for Intersecting Convex Polygons", The Visual Computer, Vol. 1, no. 2, pp. 118-123, 1985

[25] Vince, J., "Geometry for Computer Graphics: Fomulae, Examples & Proofs", Springer Verlag, 2004

[26] Westin, C.F., Richolt, J., Moharir, V., and Kikinis, R., "Affine adaptive filtering of CT data", Medical Image Analysis, Vol. 4, pp. 161-177, 2000

[27] Zoroofi, R.A., Sato, Y., Sasama, T., Nishii, T., Sugano, N., Yonenobu, K., Yoshikawa, H., Ochi, T., and Tamura, S., Member, IEEE, "Automated Segmentation of Acetabulum and Femoral Head from 3-D CT Images", IEEE Transactions on Information Technology in Biomedicine, Vol. 7, no. 4, pp. 329-343, 2003

CHAPTER 6. CONCLUSIONS AND FUTURE WORK

Automated high-level segmentation is a desired method for 3D medical imaging and could be a key to develop a fully automatic segmentation and reconstruction system. The method is most valuable for non medical users involved in reconstructing models but generally reduces the amount of time and human intervention required for this task. Some potential uses involve *rapid prototyping* processes intended to provide timely manufacturing of medical implants at lower costs. However, existing approaches for high-level segmentation typically require human intervention. In this research, a new methodology for high-level segmentation is presented. Rather than trying to offer a solution for segmenting medical images, the proposed method first allows errors in the reconstructed model and later removes these errors without the help of a medical expert/technician; allowing for a completely automated approach.

The proposed method employs a *generic* model as prior knowledge for high-level segmentation. As part of automated system, an *object* model is reconstructed from patient's data and accepted errors (*welded regions*) on the model. A *slice model* representation is used to transform welded regions from 3D surfaces to 2D contours. The proposed method covers two major processes for automated high-level segmentation: 1) sliced model registration and 2) weld removal processes. The sliced model registration process analyzes slices of generic and object models and locates corresponding sections of the two models. Next, it identifies the closest match of generic slices to individual object slices. The weld removal process utilizes the matches of generic slices and object slices to remove and repair welded regions. The final results have contours of individual bones successfully separated.

Although a feasible result can be obtained with the current method, several opportunities remain for improvement in future research. One could explore the use of generic slices with smaller thickness to expand the number of slices for matching. This may help capturing variability of shapes of object slices with more example patterns of generic slices. The computational cost can be reduced by only applying the method to sections of generic model that corresponds to welded regions on object model.

Instead of using generic slices for repairing welded regions in weld removal process, a future method may utilize the separated contours of previous object slices. The advantage of using previous object slices is that the continuity of contours can be maintained, especially where the welded regions are repaired. Some additional algorithms would be required including detecting topological changes and recognizing an appearance/disappearance of individual bones. The method could compare object slices to previous fixed object slices and matching generic slices, and then decide if the previous slice or generic slice is better.

The proposed method may also need to be examined with more number of test subjects and expanded for a variety of joints (e.g. knee, ankle, shoulder, or elbow). The method in current research was proved to be feasible with human hip joint; however, additional test samples may be required to investigate the robustness of algorithm among a variation of individuals. In order to utilize the method with different joints, additional algorithms may be required. For example, the object model of a knee joint which consists of femur, patella (knee cap), tibia and fibula may need to be divided into two groups: 1) an upper group consisting of femur and patella, and 2) a lower group consisting of tibia and fibula.

The other improvement can take an advantage of using a CAD model by varying the orientation of the model slicing to maximize the number of landmarks. In the current research, the object and generic models are sliced with the same direction as the direction of medical imaging. This provides a convenience in feeding back the results to segment scan images; however, more effective landmarks may be revealed by slicing the models along other directions.

Utilizing the results of this research in low-level segmentation needs to be further explored. Several techniques in low-level segmentation including *snake*, *deformable contour*, *deformable model*, *active shape contour*, and *active shape model* generally require the initial 2D contour or 3D model to be close to the target objects. The proposed method can be utilized as a preprocessing step to create initial contours or models for these techniques. Since the results of the proposed method have the location of object preserved, the contour or model could automatically align with the object in scan images.

Lastly, future work should explore using the proposed method to separate the joints that are degraded by disease such as degenerative arthritis. The images of these joints usually show weak bone edges or touching of adjacent bones. It is difficult to identify the bone edges even through visual inspection. The method in this research can employ the generic model from patients who have similar degeneration and level of severity. After the joints are separated and repaired using the proposed method, the result should be verified if it is acceptable to employ in general practice.

REFERENCES

Adams, R., and Bischof, L., "Seeded Region Growing", IEEE Transactions on Pattern Analysis and Machine Intelligence, Vol. 16, no. 6, 1994

Andrew, A.M., "Another Efficient Algorithm for Convex Hulls in Two Dimensions", Information Processing Letters, Vol. 9, pp. 216-219, 1979

Attalla, E., and Siy, P., "Robust shape similarity retrieval based on contour segmentation polygonal multiresolution and elastic matching", Pattern Recognition Society, Vol. 38, pp. 2229-2241, 2005

Audette, M.A., Ferrie F.P., and Peters T.M., "An algorithmic overview of surface registration techniques for medical imaging", Medical Image Analysis, Vol. 4, pp. 201-217, 2000

Bajaj, C.L., Coyle, E.J., and Lin, K.N., "Arbitrary Topology Shape Reconstruction from Planar Cross Sections", Graphical Models and Image Processing, Vol. 58, pp. 310-319, 1996

Barnes, J.W., "Statistical Analysis for Engineers and Scientists: A Computer-Based Approach", McGraw-Hill, 1994

Bennamoun, M., Boashash, b., and Koo, J., "Optimal parameters for edge detection", IEEE International Conference on Systems, Man and Cybernetics", Vol. 2, pp. 1482-1488, 1995

Bohm, G., Knoll, C., Colomer, V.G., Alcaniz-Raya, M., and Albalat, S., "Three-dimensional segmentation of bone structures in CT images", SPIE Conference on Image Processing, Vol. 3661, pp. 277-286, 1999

Bourke, P.D., WASP, M024, University of Western Australia, 35 Stirling Hwy, Crawley, WA 6009, Australia, 1988, Available at: http://local.wasp.uwa.edu.au/~pbourke/geometry, Access: November, 2008

Caselles, V., Kimmel, R., and Sapiro, G., "Geodesic Active Contours", International Journal of Computer Vision, Vol. 22, no. 1, pp. 61-79, 1997

Chan, C.F., Kwoh, C.K., Teo, M.Y., and Ng, W. S., "Tessellated Surface Reconstruction from 2D contours", 1999

Chand, B.M., and Kapur, S.S., "An algorithm for convex polytopes, Journal of the ACM, Vol 17, pp. 78-86, 1970

Chang, C.C., Hwang, M.S., and Bueher, D.J., "A Shape Recognition Scheme Based on Relative Distance of Feature Points from the Centroid", Pattern Recognition, Vol. 24, no. 11, pp. 1053-1063, 1991

Cootes, T.F., Hill, A., Taylor, C.J., and Haslam, J., "The Use of Active Shape Models For Locating Structures in Medical Images", Image and Vision Computing, Vol. 12, no. 6, pp. 355-366, 1994

Davis, L. S., "A survey of edge detection techniques", Computer Graphics and Image Processing, Vol. 4, pp. 248-270, 1975

Graham, R.L., "An Efficient Algorithm for Determining the Convex Hull of a Finite Planar Set", Information Processing Letters, Vol. 1, no. 4, pp. 132-133, 1972

Heo, H., and Chae, O.S., "Segmentation of tooth in CT images for the 3D reconstruction of teeth", Proceeding of SPIE, Vol. 5298, pp. 455-466, 2004

Jeong, J., Kim, K., Park, H., and Jung, M., "A New Method for Solving Branching Problems in Surface Reconstruction", International Journal of Advanced Manufacturing Technology, Vol. 16, pp. 259-264, 2000

Jiantao, P., Yi, L., Guyu, X., Hongbin, Z., Weibin, L., and Uehara, Y., "3D Model Retrieval Based on 2D Slice Similarity Measurements", Proceeding of the 2nd International Symposium on 3D Data Processing, Visualization, and Transmission, IEEE, pp. 95-101, 2004

Josephson, K., Ericsson, A., and Karlsson, J., "Segmentation of Medical Images Using Three-Dimensional Active Shape Models", Lecture Notes in Computer Science, Vol. 3540, pp. 719-728, 2005

Kainmueller, D., Lamecker, H., Zachow, S., and Hege, H. C., "Coupling Deformable Models for Multi-object Segmentation", Biomedical Simulation, Vol. 5104, pp. 69-78, 2008

Kang, Y., Engleke, K., and Kalender, W.A., "A New Accurate and Precise 3-D Segmentation Method for Skeletal Structures in Volumetric CT Data", IEEE Transactions on Medical Imaging, Vol. 22, no. 5, pp. 586-598, 2003

Kass, M., Witkin, A., and Terzopoulos, D., "Snakes: Active contour models", International Journal of Computer Vision, Vol. 1, pp. 321-331, 1988

Klinder, T., Wolz, R., Lorenz, C., Franz, A., and Ostermann, J., "Spine Segmentation Using Articulated Shape Models", Medical Image Computing and Computer-Assisted Intervention, Vol. 5241, pp. 227-234, 2008

Liu, J., Udupa, J.K., Saha, P.K., Odhner, D., Hirsch, B.E., Siegler, S., Simon, S., and Winkelstein, B.A., "Model-based 3D segmentation of the bones of joints in medical

images", Medical Imaging 2005: Image Processing, Proceeding of SPIE, Vol. 5747, pp. 1793-1803, 2005

Loncaric, S., "A Survey of Shape Analysis Techniques", Pattern Recognition, Vol. 31, no 8, pp. 983-1001, 1998

Lorigo, L. M., Faugeras, O., Grimson, W.E.L., Keriven, R., and Kikinis, R., "Segmentation of Bone in Clinical Knee MRI Using Texture-Based Geodesic Active Contours", Medical Image Computing and Computer-Assisted Intervention, Vol. 1496, pp. 1195-1204, 1998

Marr, D., and Hildreth, E., "Theory of Edge Dectection", Proceedings of the Royal Society of London, Series B, Biological Sciences, Vol. 207, no. 1167, pp. 187-217, 1980

McInerney T., and Terzopoulos D., "Deformable Models in Medical Image Analysis", Proceedings of MMBIA'1996, Toronto, Canada, pp. 171-180, 1996

Mimics Medical Imaging Software, Web site: http://www.materialise.com/ materialise/view/en/92458-Mimics.html, Retrieved March 23, 2009

Minns, R.J., Bibb, R., Banks, R., and Sutton, R.A., "The use of a reconstructed three-dimensional solid model from CT to aid the surgical management of a total knee arthroplasty: a case study", Medical Engineering & Physics, Vol. 25, pp. 523-526, 2003

Nikolaidis, N., and Pitas, I., "3-D Image Processing Algorithms", John Wiley & Sons, Inc., 2001

OsiriX Imaging Software, Web site: http://www.osirix-viewer.com, Retrieved March 23, 2009

Pal, N.R., and Pal, S.K., "A review on image segmentation technique", Pattern Recognition, Vol.26, no. 9, pp 1277-1294, 1993

Pardo, X.M., Carreira, M.J., Mosquera, A., and Cabello, D., "A snake for CT image segmentation integrating region and edge information", Image and Vision Computing, Vol. 19, pp. 461-475, 2001

Park, H., and Kim, K., "3-D shape reconstruction from 2-D cross-sections", Journal of Design and Manufacturing, Vol. 5, pp. 171-185, 1995

Parker, J.R., "Algorithms for image processing and computer vision", John Wiley & Sons, Inc., New York, 1997

Pauly, M., Mitra, N., Giesen, J., Gross, M., and Guibas, L.J., "Example-Based 3D Scan Completion", Third Eurographics Symposium on Geometry Processing, pp. 23-32, 2005

Pham, D.T., and Gault, R.S., "A comparison of rapid prototyping technologies", International Journal of Machine Tools & Manufacture, Vol. 38, pp. 1257-1287, 1998

Pitas, I., "Digital Image Processing Algorithms and Applications", John Wiley & Sons, Inc., New York, 2000

Preparata, D.F., and Hong, S.J., "Convex Hulls of Finite Sets of Points in Two and Three Dimensions", Comm. ACM, Vol. 20, pp. 87-93, 1977

Preparata, D.F., and Shamos, M., "Computational Geometry: An Introduction", Springer Verlag, New York, 1985

Rakshe, T., Fleischmann, D., Rosenberg, J., Roos, J.E., and Napel, S., "Knowledge-based interpolation of curves: Application to femoropopliteal arterial centerline restoration", Medical Image Analysis, Vol. 11, pp. 157-168, 2007

Ramesh, N., Yoo, J. H., and Sethi, I. K., "Thresholding based on histogram approximation", IEE Proceedings Vision, Image & Signal Processing, Vol. 142, no. 5, pp. 271-279, 1995

Rapidform Software, Web site: http://www.rapidform.com, Retrieved March 23, 2009

Ryu, J.H., Kim, H.S., and Lee, K.H., "Contour-based algorithms for generating 3D CAD models from medical images", International Journal of Advanced Manufacturing Technology, Vol. 24, pp. 112-119, 2004

Sahoo, P. K., Soltani, S., Wong, A. K.C., and Chen, Y. C., "A Survey of Thresholding Techniques", Computer Vision, Graphics, and Image Processing, Vol. 41, no. 2, pp. 233-260, 1988

Shen, H., Shi, Y., and Peng, Z., "Applying Prior Knowledge in the Segmentation of 3D complex Anatomic Structures, Lectures Notes in Computer Science, Vol. 3765, pp. 189-199, 2005

Starly, B., Fang, Z., Sun, W., Shokoufandeh, A., and Regli, W., "Three-Dimensional Reconstruction for Medical-CAD Modeling", Computer-Aided Design, Vol. 2, pp. 431-438, 2005

Sun, W., Starly, B., Nam, J. and Darling, A., "Bio-CAD Modeling and Its Applications in Computer-Aided Tissue Engineering", Computer-Aided Design, Vol. 37, pp. 1097-1114, 2005

Suzuki, M.T., Kato, T., and Otsu, K., "A Similarity Retrieval of 3D Polygonal Models Using Rotation Invariant Shape Descriptors", Proceedings of the IEEE International Conference on Systems, Man and Cybernetics, Vol. 4, pp. 2946-2952, 2000

Suzuki, M.T., "A Web-based Retrieval System for 3D Polygonal Models", Annual Conference of the North American Fuzzy Information Processing Society, Vol. 4, pp. 2271-2276, 2001

Tan, K.L., OOI, B.C., and Thiand, L.F., "Retrieving Similar Shapes Effectively and Efficiently", Multimedia Tools and Applications, Vol. 19, pp. 111-134, 2003

Toussaint, G.T., "A Simple Linear Algorithm for Intersecting Convex Polygons", The Visual Computer, Vol. 1, no. 2, pp. 118-123, 1985

Vince, J., "Geometry for Computer Graphics: Fomulae, Examples & Proofs", Springer Verlag, 2004

Westin, C.F., Richolt, J., Moharir, V., and Kikinis, R., "Affine adaptive filtering of CT data", Medical Image Analysis, Vol. 4, pp. 161-177, 2000

Yen, J. C., Chang, F. J., and Chang, S., "A new criterion for automatic multilevel thresholding", IEEE Transaction on Image Processing, Vol. 4, no. 3, pp. 370-378, 1995

Yao, W., Abolmaesumi, P., Greenspan, M., and Ellis, R.E., " An Estimation/Correction Algorithm for Detecting Bone Edges in CT images", IEEE Transactions on Medical Imaging, Vol. 24, no. 8, pp. 997-1010, 2005

Zhang, C., and Chen, T., "Indexing and Retrieval of 3D models Aided by Active Learning", Proceedings of ACM Multimedia 2001, pp. 615-616 Ottawa, Ontario, Canada, 2001

Zhang, D., and Lu, G., "Review of shape representation and description techniques", Pattern Recognition, Vol. 37, pp. 1-19, 2004

Zoroofi, R.A., Sato, Y., Sasama, T., Nishii, T., Sugano, N., Yonenobu, K., Yoshikawa, H., Ochi, T., and Tamura, S., Member, IEEE, "Automated Segmentation of Acetabulum and Femoral Head from 3-D CT Images", IEEE Transactions on Information Technology in Biomedicine, Vol. 7, no. 4, pp. 329-343, 2003

Zucker, S. W., "Region growing: Childhood and adolescence", Computer Graphics and Image Processing, Vol. 5, no. 3, pp. 382-399, 1976

ACKNOWLEDGEMENT

I would like to express my sincerest gratitude to my major professor, Dr. Matthew C. Frank, whose expert guidance, mentorship, and encouragement have provided all the support that I needed to complete my degree.

My deepest appreciation also goes to Drs. Douglas D. Gemmill, James H. Oliver, Frank E. Peters, and Eliot H. Winer, who have given valuable time, knowledge, and assistance for serving on my program of study committee.

I wish to thank my friends in Ames and abroad for their wonderful friendship and would like to extend my special thanks to my parents, brother, and sisters for always giving me love and support. Finally, none of these would have been possible without the love, patient, understanding and constant encouragement from my wife, Florensia F. Surjadi, through the duration of my study.